



Universität für Bodenkultur Wien

Interuniversitäres Department für Agrarbiotechnologie

Institut für Umweltbiotechnologie

Betreuer: Prof. Dr. Georg M. Gübitz

ENZYME-SUBSTRATE INTERACTIONS IN BIOACTIVE
MATERIALS

Dissertation
zur Erlangung des Doktorgrades
an der Universität für Bodenkultur Wien

Eingereicht von
DI Gregor Tegl

Wien, Juli 2016

Preamble	I
Abstract	II
Kurzfassung	III
1 Aim of the Thesis	1
2 Introduction	2
2.1. Biomaterials for medical applications	2
2.1.1. Polysaccharides (PS)	4
2.2. Glycoside hydrolases	6
2.3. Cellobiose dehydrogenase and Myeloperoxidase	8
2.4. The wound	9
2.5. Direct detection of bacterial wound contaminants	18
2.5.1. Near real-time detection methods	19
2.5.2. Analytical methods for infection detection	21
2.6. Indirect detection methods for the determination of wound infection	22
2.6.1. Enzyme biomarkers for infection detection	22
2.6.2. Metabolites and sensing molecules for infection detection	24
2.7. References	26
3 Chitosan based substrates for wound infection detection based on increased lysozyme activity	33
3.1. Introduction	33
3.2. Material and Methods	35
3.2.1. Materials	35
3.2.2. Purification of chitosan	35
3.2.3. Preparation and characterization of N-acetylated chitosan	35
3.2.4. N-acetylation of chitosan	35
3.2.5. Determination of the degree of acetylation (DA)	35
3.2.6. Hydrolysis of N-acetylated chitosan by lysozyme	36
3.2.7. Preparation of chitosan substrates	37
3.2.8. Enzyme activity assays	37
3.2.9. Determination of the swelling properties	38
3.2.10. Lysozyme degradation of chitosan-based substrates	38
3.2.11. Dye release of chitosan based substrates upon lysozyme degradation	38

3.3.	Results and Discussion	39
3.3.1.	N-acetylation of chitosan	39
3.3.2.	Functionalization of N-acetyl chitosan	41
3.3.3.	Reactive Black 5-functionalised N-acetyl chitosan [CTS 200 RB5]	41
3.3.4.	Evans Blue-functionalized N-acetyl chitosan/starch substrate [CTS 200 ST EB]	42
3.3.5.	Substrate testing in human wound fluid from infected wounds	45
3.4.	Conclusion	46
3.5.	References	47
4	Myeloperoxidase responsive materials for infection detection based on immobilized aminomethoxyphenol	49
4.1.	Introduction	49
4.2.	Material and Methods	50
4.2.1.	Functionalization of 5-Amino-2-Methoxyphenol	50
4.2.2.	Immobilization of Functionalized Aminomethoxyphenol	51
4.2.3.	Visual Detection of MPO Activity Using Immobilized Aminomethoxyphenol	51
4.2.4.	Enzymatic Conversion of Functionalized Aminomethoxyphenol Analyzed by HPLC and LC ESI-TOF	52
4.2.5.	NMR Measurements of MPO-Mediated Aminomethoxyphenol Oxidation	53
4.3.	Results and Discussion	53
4.3.1.	Reaction Mechanism of 5-Amino-2-Methoxyphenol Oxidation by MPO	56
4.4.	Conclusion	61
4.5.	References	62
5	Antimicrobial cellobiose dehydrogenase-chitosan particles	64
5.1.	Introduction	64
5.2.	Material and Methods	66
5.2.1.	Materials and Microorganisms	66
5.2.2.	Purification of Chitosan	66
5.2.3.	Immobilization of CDH on Chitosan	66
5.2.4.	Analyses of Enzyme Immobilized on Chitosan	67
5.2.5.	Antimicrobial activity	68
5.3.	Results and Discussion	69
5.3.1.	Antimicrobial activity and leaching behavior of CDH-chitosan particles	74

5.4.	Conclusion	78
5.5.	References	79
6	Cellobiohydrolases Produce Different Oligosaccharides from Chitosan	82
6.1.	Introduction	82
6.2.	Materials and Methods	83
6.2.1.	Materials	83
6.2.2.	Purifications of Chitosan	84
6.2.3.	Characterization of enzyme activities on chitosan	84
6.2.4.	Characterization of oligomeric hydrolysis products	85
6.3.	Results and Discussion	87
6.3.1.	Temperature and pH Optima of the Enzymes with Chitosan as Substrate	87
6.3.2.	Analysis of Produced Chito-oligosaccharides	88
6.3.3.	Characterization of the Preferred Enzyme Cleavage Sites	92
6.4.	Conclusion	98
6.5.	References	99
7	General Conclusion	103
8	Appendix	107
8.1.	Scientific publications	107
8.2.	Oral presentations	107
8.3.	Acknowledgements	109
8.4.	Statutory declaration	111

Preamble

This thesis is divided into four main sections.

The first section (Chapter 1 and 2) presents the aim of the work and provides the reader with an introduction to the topic of the thesis. General information about the properties and applicability of biomaterials and of the most relevant enzymes used within this thesis is given. Further insight is provided into the biology of wounds as well as the importance of alternative wound treatment strategies and the role of wound infection detection is discussed also within the framework of publication 1.

The second section (Chapter 3 and 4) covers two publications on novel strategies for timely detection of wound infection based on the assessment of elevated enzymes activities in wound fluids. Publication 2 discusses infection detection based on elevated activities of lysozyme in wound fluids by the aid of modified chitosans. Publication 3 within this section describes the functionalization of a carrier for infection detection based on myeloperoxidase in wound fluids.

The third section (Chapter 5 and 6) includes two publications discussing applications of enzymes for alternative antimicrobial systems and the production of bioactive substances. Publication 4 deals with an antimicrobial system for *in-situ* hydrogen peroxide production based on cellobiose dehydrogenase immobilized on chitosan. Publication 5 describes the use of commercial cellobiohydrolases for the production of versatile fractions of chito-oligosaccharides.

Section four concludes the findings in the thesis with a general conclusion and list scientific publications and conference contributions resulting from this thesis.

Abstract

This thesis was conducted in the context of the INFACCT project of the seventh framework program of the European Union, which aimed at the development of functional materials for fast diagnosis of wound infection. The target of the project was the production of diagnostic materials for the three immune system-derived infection biomarkers namely lysozyme (LYS) myeloperoxidase (MPO) and elastase, which show highly elevated activities in infected wounds. As the development stage is progressed, these materials should be incorporated in diagnostic wound dressings, which inform the therapist and the patient about the wound status and allow a timely initiation of treatment.

Consequently, the focus of this thesis was the development of infection responsive materials based on the detection of lysozyme and myeloperoxidase, and of the utilization of enzymes for the production of antimicrobial and bioactive compounds.

Enzymes responsive materials that allow a visual detection of wound infection were developed. Lysozyme mediated infection detection was realized by the synthesis of N-acetyl chitosan and further covalent modification with Reactive Black 5. The lysozyme substrate insoluble under physiological conditions released colored hydrolysis fragments in response to lysozyme in infected wound fluids. The time of detection could be improved by the co-precipitation of N-acetyl chitosan with starch and Evans Blue, and led to a clear color response after short time incubation. MPO mediated infection detection was achieved by covalent immobilization of the MPO substrate aminomethoxyphenol onto silica plates via an alkoxyloxane spacer. Upon incubation of the functionalized white test plates with wound fluids from infected wounds, a red colored spot occurred after few minutes of incubation. Using comprehensive MS and NMR analysis, a dimeric reaction product was identified and the reaction mechanism for MPO mediated aminomethoxyphenol oxidation elucidated.

Besides the early detection of infection, the prevention of wound infection via topical antimicrobial treatments gains in importance considering emerging resistances. This led to the development of a system generating an *in-situ* hydrogen peroxide (H_2O_2) by cellobiose dehydrogenase (CDH). CDH immobilized on chitosan produced H_2O_2 in response to cellobiose as substrate and completely inhibited growth of *E. coli* and *S. aureus* over 24 h. Different immobilization methods were tested and covalent immobilized CDH turned out the most efficient candidate for the antimicrobial system for the potential application in wound infection prevention.

Another bioactive substance class with reported antimicrobial activity are chito-oligosaccharides (COSs), but the exploitation of their various bioactivities is still impeded by the limited amounts of poorly characterized mixtures available to date. Within this thesis the ability of commercial cellobiohydrolases (CBHs) for COS production was investigated and superior potential of these enzymes was found. NMR and MS analyses of the reaction

products could unveil different mode-of-actions among different CBHs, which lead to the production of COSs with different structural properties.

The interactions of enzymes with bioactive materials investigated in this thesis opened up a broad field of applications comprising infection detection and prevention as well as the exploitation of novel antimicrobial strategies and bioactive compounds.

Kurzfassung

Diese Dissertation wurde im Rahmen des INFACT Projektes im EU-7th Framework Programme for Research and Technological Development durchgeführt, das die Entwicklung funktionalisierter Materialien für die schnelle Diagnose von Wundinfektion zum Ziel hat. Dafür sollen bioresponsive Materialien zum Nachweis spezifische Enzyme mit erhöhter Aktivität in Wundflüssigkeiten entwickelt werden. Bei diesen Enzymen handelt es sich um Lysozym, Myeloperoxidase und Elastase, welche als Reaktion auf bakterielle Wundkontamination in verstärktem Ausmaß vom Immunsystem produziert werden. Im weiteren Verlauf des Projektes werden die entwickelten Detektionssysteme in Wundverbänden eingebaut, um aufgrund einer schnellen Infektionsdiagnose geeignete Maßnahmen treffen zu können.

Der Fokus dieser Dissertation liegt in der Entwicklung Infektions-responsiver Materialien basierend auf Lysozym und Myeloperoxidase, sowie in der Verwendung von Enzymen für die Entwicklung neuer antimikrobieller Strategien und zu Herstellung bioaktiver Substanzen.

Es wurden Enzym-responsive Materialien entwickelt, die eine visuelle Detektion von Wundinfektion ermöglichen. So wurde die Detektion von Infektion durch die Synthese von N-acetyl chitosan als Substrat für Lysozym und weitere Modifikation mit dem Farbstoff Reactive Black 5 realisiert. Nach Inkubation dieses unlöslichen Substrats mit infizierten Wundflüssigkeiten werden gefärbte Hydrolysefragmente freigesetzt was zu einem deutlichen Farbumschlag führt. Die Detektionzeit konnte durch die Herstellung eines Präzipitates von N-acetyl chitosan mit Stärke und dem Farbstoff Evans Blue noch weiter verkürzt werden.

Wundinfektionsdetektion basierend auf Myeloperoxidase wurde durch die kovalente Immobilisierung von Aminomethoxyphenol auf Silicagelplatten realisiert. Die funktionalisierten farblosen Platten wurden bei Inkubation mit infizierten Wundflüssigkeiten innerhalb weniger Minuten rötlich. Durch detaillierte MS and NMR Analysen konnte ein Dimer als farbgebendes Reaktionsprodukt identifiziert werden und weiters der Mechanismus für diese Reaktion aufgeklärt werden.

Neben Infektionsdetektion spielen auch alternative Wundbehandlungsmethoden aufgrund vermehrter Resistenzbildung eine immer wichtigere Rolle. Im Rahmen dieser Dissertation wurde ein antimikrobielles System mithilfe von Cellobiose Dehydrogenase (CDH) entwickelt, das eine kontinuierliche Produktion von Wasserstoffperoxid (H_2O_2) gewährleistet. CDH wurde auf Chitosan immobilisiert und produzierte durch Oxidation von Cellobiose H_2O_2 in ausreichenden Mengen, um das Wachstum von *E. coli* und *S. aureus* über 24 h vollständig zu inhibieren. Die kovalente Immobilisierung von CDH stellte sich dabei für eine potentielle Anwendung zur Infektionsprevention als die effektivste Methode heraus.

Chitooligosaccharide (COSs) sind bioaktive Substanzen mit antimikrobieller Aktivität, jedoch ist eine genauere Untersuchung dieser Substanzklasse aufgrund limitiert erhältlichen Mengen und unzureichend analysierten Proben nicht möglich. In dieser Arbeit wurden

Cellobiohydrolasen (CBHs) erfolgreich für die Produktion von COSs eingesetzt, wobei mittels NMR und MS Analysen der oligomeren Reaktionsprodukte unterschiedliche Wirkungsmechanismen für verschiedenen CBHs nachgewiesen wurden. Dies ermöglicht die gezielte Produktion von COSs mit unterschiedlichen strukturellen Eigenschaften.

Die Erforschung der Interaktion von Enzymen mit bioaktiven Materialien öffnet ein breites Anwendungsgebiet dieser Systeme, das Infektionsdetektion und - prevention umfasst, genauso wie die Entwicklung und Herstellung neuer antimikrobieller Systeme und bioaktiver Substanzen.

1 Aim of the Thesis

The work of this thesis was conducted within the INFACT project of the seventh framework program of the European Union, which aimed at the development of functional materials for fast diagnosis of wound infection. Early detection of an emerging infection enables the timely initiation of treatment and consequently lowers the severity of the disease. The goal of the project was the production of diagnostic materials for the three immune system-derived infection biomarkers lysozyme (LYS), myeloperoxidase (MPO) and elastase (ELA), which show highly elevated activities in infected wounds. In order to realize an easily assessable infection detection system, materials that allow a visual detection of infection in response to elevated enzymes activities in wound fluids should be developed. Later, these materials should be incorporated in diagnostic wound dressings, which inform the therapist and the patient about the wound status. Project partners from university and industry are involved in this project comprising the development of the substrates, their efficient incorporation into diagnostic wound dressings and the final production and sales.

The aim of the thesis was to make use of specific enzyme-substrate interactions for their realization in medical applications and the production of bioactive compounds. Representatives of oxidative and hydrolytic enzymes were utilized and interactions with biomaterials were investigated to achieve following aims:

- 1 The development of materials for early detection of wound infection based on lysozyme and myeloperoxidase as infection biomarkers.
- 2 The investigation of an alternative antimicrobial system based on cellobiose dehydrogenase and chitosan to achieve a continuous *in-situ* production of hydrogen peroxide
- 3 Utilization of chitosan-unspecific, commercial enzymes for the production of chito-oligosaccharides

2 Introduction

2.1. Biomaterials for medical applications

The term biomaterial comprises a vast amount of substances, which resulted in multiple definitions over time depending on the substance's application. Most abundant definitions refer to its broad use in all areas of medicine, which defines biomaterials as substances that are applied in therapeutic and diagnostic systems. The engineering of a substance enables a material to interfere with a biological system via specific interactions, thereby inducing a certain therapeutic or diagnostic response [1]. Humans have been using biomaterials for thousands of years to treat diseases, however increased use for medical applications was only achieved with the emergence of synthetic polymers and biopolymer modifications [2]. From that perspective biopolymers can to date be classified into naturally derived, synthetic and semi-synthetic/hybrid materials [3]. Significant developments in biomaterial research led scientist to discover new materials and to modify naturally occurring materials to improve properties like biocompatibility and responsiveness.

The constant improvement and development of biomaterials is illustrated and structured in three generations of biomaterials. The early intention was the use of materials with suitable physical properties *in vivo*, thereby not being toxic for the host [4]. Initial applications were based on already existing materials that were biologically inert and were thus used in high purity as implants. These co-called first-generation biomaterials were long time improved with the emphasis to reduce their toxicity, but less attention was drawn to the interaction with the host tissue. Time lapsed and finally led to the invention of biocomposite materials, which facilitated a tailored engineering of mechanical properties and also introduced the concept of bioactivities. Biomaterials could be designed to interact with the host tissue and thus initiated the era of second-generation biomaterials [5]. Glass composites were the first representatives of biomaterials that were designed to evoke distinct reactions with the tissue environment, mainly the colonization by cells, and were predominantly used for orthopedic and dental applications. Soon composites of synthetic polymers expanded the range of applications because of their resolvability, which enabled a successive replacement of these implants by regenerating tissue once implanted. This strategy paved the way for various applications involving controlled drug delivery [6].

While this generation of biomaterials plays the active part in the diverse medical applications as bone grafts and others, third-generation biomaterials comprise biological approaches that initiate specific molecular responses. These materials are able to stimulate cell proliferation via gene activation and thus induce a host mediated tissue repair [7]. This innovative strategy is divided in two general approaches, namely tissue engineering and tissue regeneration. The tissue engineering approach is based on the *ex vivo* cell seeding on a biomaterial scaffold and subsequent implantation in the body. A produced functional tissue then overtakes the physiological role of formerly destroyed/non-functional matter. Tissue regeneration aims at a directed tissue repair *in vivo* induced by the controlled release of cell activating substances on site. The respective drug should initiate growth factor production in the targeted cells and further lead to the *in situ* tissue assembling. In comparison to the tissue engineering method, cells are stimulated to proliferate to a tissue in the host, which circumvents the adaption to a physiological environment that is necessary in tissue engineering [8].

The rapid development of biomaterial applications in the past decades does not find an end due to the emergence of new and modified biomaterials, which broaden the scope dramatically. Steady progress is reported in healthcare using gene-activating biomaterials including soft tissue engineering and stem cell engineering.

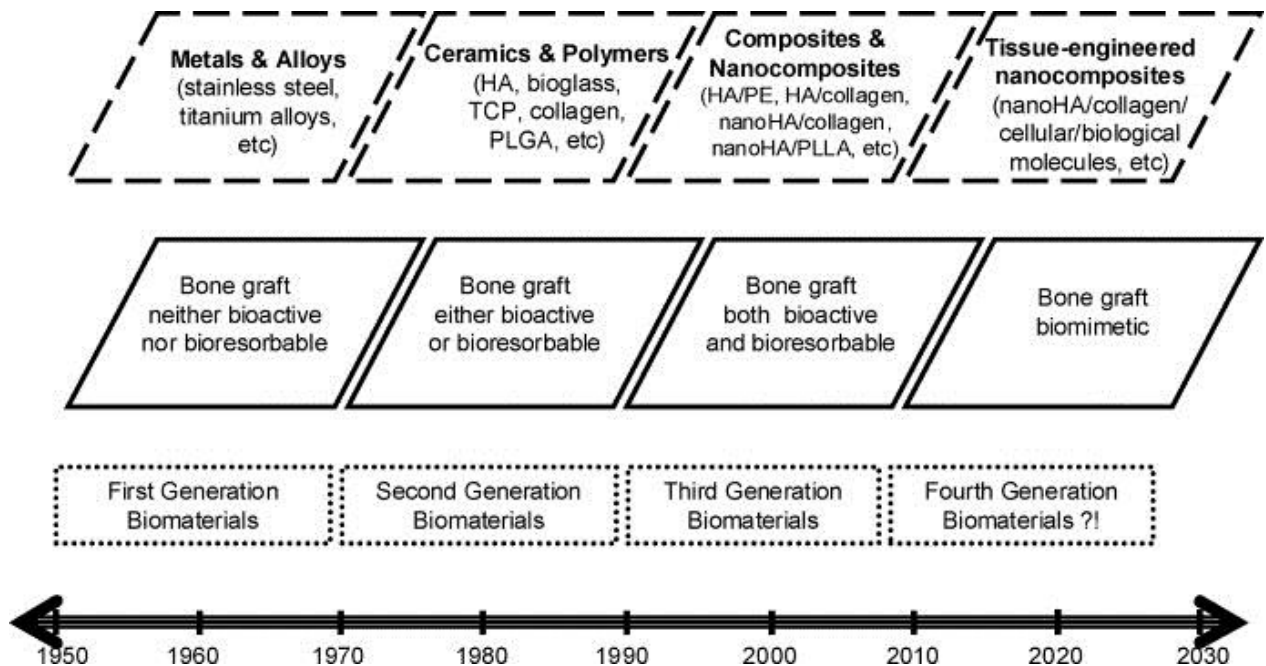


Figure 1: The evolution of biomaterials illustrated on the example of bone grafting (Permission obtained by Elsevier) [9].

2.1.1. Polysaccharides (PS)

Complex carbohydrates are ubiquitous in nature and thereby fulfill various functions. Polysaccharides are chain-shaped biomaterials composed of one or of several different monosaccharides connected via glycosidic linkages. They are key players in many biological processes including energy storage, providing mechanical strength and protective properties. A variety of parameters determine the overall structural properties and functions of PS, which enables multiple applications of these substances. Monosaccharide composition, chain length, branching and anomeric configuration are only some parameters, which strongly influence the quaternary structure and functions of PS [10]. PS can be classified in many ways like chemical composition and structure, mostly depending on the parameter of interest. Generally these biomaterials can be categorized in homo- and hetero glycans. Homoglycans are PS, which exclusively consist of only one type of sugar whereas heteroglycans contain also other sugar constituents [11].

PS can be obtained from various resources including plant origin, algal origin, microbial origin and animal origin [12]. Many of these resources are abundant enough and the respective carbohydrates are easily extractable thus low cost production of various natural PS is to date possible. For medical applications, particularly charged PS are of high interest because of their bioadhesive properties [13]. In this regard frequently mentioned PS are alginate and chitosan due to their anionic and cationic nature, respectively.

Alginate is an abundant structural polysaccharide component in marine brown algae, which consists of guluronic acid (G) and mannuronic acid (M) in varying composition. The anionic character and monomer composition allows alginate to form gels at neutral pH by the aid of divalent cations and is frequently used for the microencapsulation of drugs. High bioavailability and biodegradability promote the controlled oral delivery of drugs and the reduction of systemic side effects [14,15]. A major drawback of alginate is the moderate solubility in water and consequently low stability under physiological conditions, which renders this biomaterial impractical for many medical applications. Chemical modifications and copolymer grafting of the alginate are two examples, which greatly improve erosion time and other biological properties [16–18].

Chitosan is one of few cationic polysaccharides known, a copolymer consisting of glucosamine and N-acetyl glucosamine. It is the second most abundant polysaccharide in its native form chitin (poly-N-acetyl glucosamine) and commonly found in exoskeletons of crustaceans, insects but also in algae and fungi [19]. Chitin is hydrophobic and insoluble in water, which greatly narrows the range of applications. A harsh N-deacetylation process converts chitin into chitosan and the unprotected primary amines give this biomaterial superior property, which enable a broad set of applications [20]. Chitosan is soluble in dilute

acidic solutions and can thus be processed into many different fabrics by the aid of chemical/enzymatic network formation. The physicochemical properties of chitosan strongly depend on the various parameters like the molecular weight, degree of N-acetylation and the pattern of N-acetylation [21,22] and were found to alter various biological properties including biocompatibility, biodegradability and antimicrobial activity. Chemical and enzymatic modifications of chitosan are widely explored and led to a broad scope of chitosan-based materials in medicine, which is facilitated by the good processability of the chitosan derivatives.

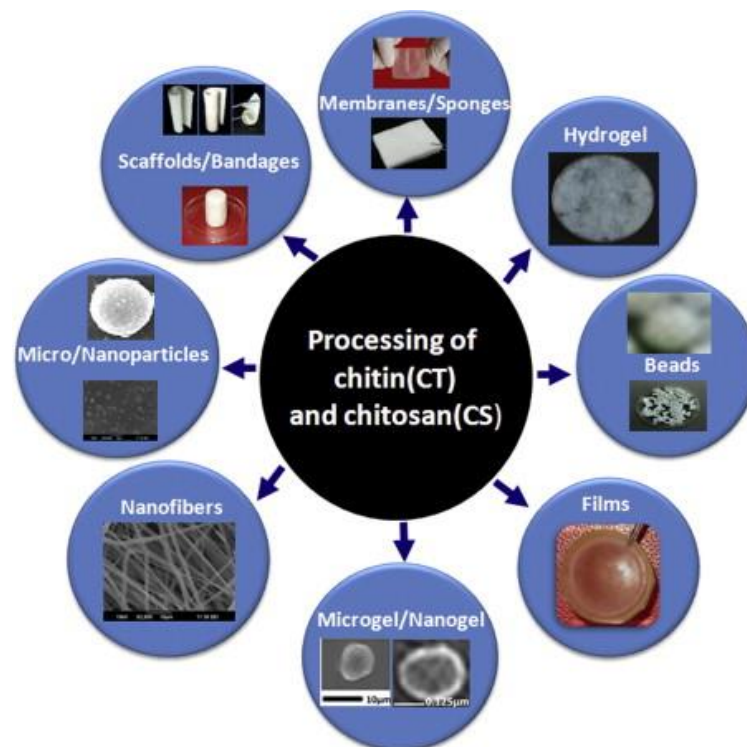


Figure 2: The possibilities fabricating different functional materials from chitin and chitosan (Permission obtained by Elsevier) [23].

A special interest emerged on the hydrolysis products of chitosan, in particular on chito-oligosaccharides (COSs). Various bioactivities were reported for COSs, but the application of poorly characterized COS mixtures in biological studies complicated secured conclusions on structure-property relationships. It is assumed that distinct degrees of polymerization, the degree of N-acetylation and the pattern of N-acetylation have a great impact on the biological activities of COSs [24]. Depolymerization of chitin and chitosan can be achieved by a high number of chemical and enzymatic methods. Chemical hydrolysis is commonly performed using sodium hydroxide and often leads to an undefined mixture of short and long chain COSs [25]. The enzymatic production of COSs is the key to obtain well-defined fractions of

oligomers for further studies to improve the understanding of the underlying mechanisms at the interface of COSs and biological matter. Various glycoside hydrolases are currently studied regarding their ability of hydrolyzing chitin and chitosan. However major attention is drawn to chitinases and chitosanases, whereby special emphasis is laid to the analysis of enzyme binding sites and cleavage sites [26]. Chitosan-specific enzymes like chitosanases show a great potential for the production of defined COSs but the progress of eventual large-scale productions suffers from the poor availability of these enzymes. A great potential relies in the utilization of commercial chitosan-unspecific enzymes, which are already produced in large scale and are thus unconditionally withdrawable. Lysozyme is a well-known representative, whose chitosan hydrolyzing activity is already well studied and found to mainly result in COSs with high degree of N-acetylation [27]. Recent studies also revealed cellulases to be potential candidates for the production of COSs with varying physicochemical properties [28].

2.2. Glycoside hydrolases

In nature a large variety of enzymes have evolved those are specific to cleave glycosidic bonds. These enzymes are commonly termed glycoside hydrolases (GH; EC 3.2.1.) and categorized in over 130 different families based on sequence and folding similarities [29,30]. The enzymatic hydrolysis of glycosidic bonds is well conserved among the different GHs and involves a proton donor (acid) and a nucleophile (base) residue. Two catalytic mechanisms can occur, defined by the anomeric configuration, whereby the stereochemistry can be retained or inverted upon enzyme hydrolysis. The different mode-of-action is mainly determined by the relative position of the nucleophilic base to the anomeric carbon, whereby the proton donor holds the same distance to the sugar. Inverting enzymes have an average distance of 11 Å between the two catalytic residues whereas a distance of 5 Å in retaining enzymes. The additional space of inverting enzymes is stuffed by a water molecule and results in a direct displacement mechanism. The nucleophilic residue thereby activates the water and the proton donor promotes the cleavage of the glycosidic bond. Retaining enzymes proceed with a double displacement mechanism via an glycosyl-enzyme intermediate (figure 3) [31]. The catalytic amino acids commonly found in GHs are aspartate and glutamate, however also some diversity is observed among the GH family including additional residues like tyrosine and cofactor dependent GHs [32].

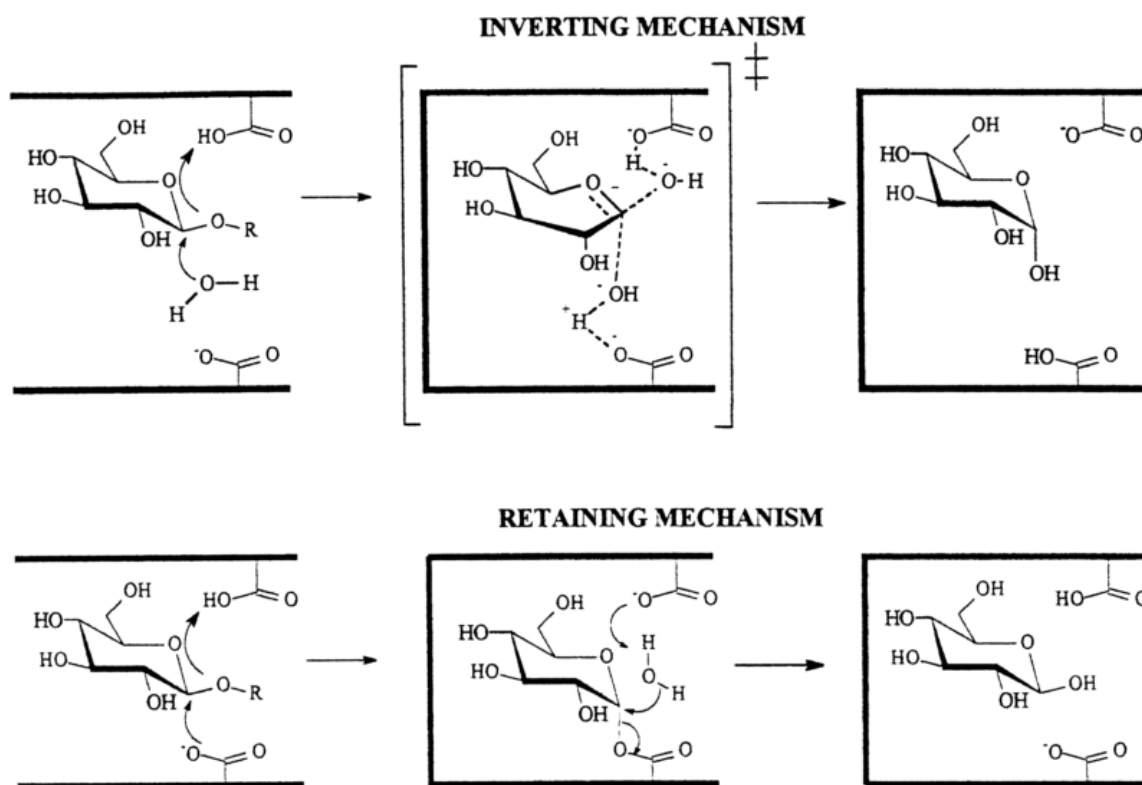


Figure 3: Catalytic mechanism of inverting and retaining glycoside hydrolases. (Permission obtained by Elsevier) [33]

The 3D structure of proteins is highly conserved in comparison to their sequences, which even more holds true for the active site topology. Amongst the GH family, only three topologies are known, which are independent of the enzyme mechanism and the involved catalytic residues. The pocket topology is mainly found in exopolysaccharidases and favors the recognition of non-reducing ends, which occur in high numbers in polysaccharide granules. Endo-acting glycosidases commonly have a cleft conformation, which enables efficient binding of polymeric substrates and is often expanded by a tunnel like topology where the cleft is covered by loops. Tunnel conformations are mainly found in cellobiohydrolases and are connected with the increased processivity of these enzymes [34]. Chitosanases are found in various GH families including chitosan specific and unspecific representatives. They use both, the inverting and retaining mechanism, whereby especially chitosanases from GH families 46, 75 and 80 predominantly use the inverting mechanism. Due to the sequence based classification in GH families, chitosanases are further subdivided in three classes (I, II and III), based on their preferred cleavage sites in chitosan [35]. Subclass I chitosanases hydrolyze GlcNAc-GlcN and GlcN-GlcN linkages, subclass II exclusively GlcN-GlcN linkages and subclass III GlcN-GlcNAc linkages. Amongst the spectrum of chitosanases, different mode of actions can be observed regarding exo/endo-activity and processivity, which illustrates the great diversity of this enzyme class [26].

Besides chitosanases, many unspecific enzymes were found to have chitosan hydrolyzing activity. Special emphasis was thereby laid to cellulases because of their high availability and use in various biotechnological areas. The substantial chitosan hydrolyzing activity of cellulases can be explained by the structural similarity of cellulose to chitosan, which only differs in the C-2 hydroxyl group that is replaced in chitosan by an amine group. The majority of cellulases degrading chitosan was found in fungi of the genus *Trichoderma* and comprises endo-glucanases, cellobiohydrolases and glycosidases [36]. Although chitosan-hydrolyzing activity is described for a variety of cellulases, the evidence was often provided just by the analysis of the viscosity, which does not give information about the reaction products. Consequently, less conclusions can be drawn on the exact mode-of-action of these unspecific enzymes on chitosan, despite studies revealing the impact of molecular weight and degree of N-acetylation on the hydrolysis efficiency [37,38].

The probably best-studied unspecific enzyme able to hydrolyze chitosan is lysozyme, which is mainly active on N-acetylated chitosan. In contrast to the most of the cellulases, the exact mode-of-action of lysozyme on chitosan is already explored and involves a preferred binding site on N-acetyl chitosan, which consists of a hexamer region with mixed monomer composition [39]. The cleavage of the glycosidic bond involves aspartate and glutamate in the common manner of GHs, however participating effects of the C-2 acetamido groups of GlcNAc units at subsite -1 were observed in the cleavage mechanism. This additional substrate mediated catalysis is supposed to overcome the lack of a suitable catalytic base in the active site and was found to dramatically increase the reaction rate [40].

2.3. Cellobiose dehydrogenase and Myeloperoxidase

Oxidoreductases are ubiquitous enzymes catalyzing the electron transfer from an electron donor to an electron acceptor, thereby usually involving cofactors. They are classified in 22 subclasses, which reveals the wide distribution of these enzymes in nature [41]. This chapter concentrates on two well-known representatives of this class, namely cellobiose dehydrogenase and myeloperoxidase.

Cellobiose dehydrogenase (CDH) is an important participant in the multi enzymatic cellulose degradation machinery of various fungi. This enzyme gained attention in biofuel science, which aims an efficient saccharification of cellulose to produce biofuel from plant material, which was long assumed to be the business exclusively of hydrolytic enzymes [42]. CDH is an extracellular flavocytochrome consisting of a haem-binding cytochrome domain (CYT) and a FAD-binding dehydrogenase domain (DH), which are connected via a flexible peptide linker. CDHs are classified into class-I CDHs and class-II CDHs, whereby class-II CDHs frequently bear a carbohydrate-binding module [43]. The native substrate of CDH is

cellobiose, however also other oligosaccharides can be metabolized by CDH. Thereby the DH domain oxidizes C-1 of the respective sugar to a lactone with parallel reduction of FAD. The withdrawn electron is directly transferred from the reduced FAD to the haem group of the CYT domain via an inter-domain electron transfer (IET) and subsequently to an external electron acceptor [44]. The proposed electron acceptor within the cellulose degradation process is the lytic polysaccharide monooxygenase (LPMO), but CDH also accepts other compounds including molecular oxygen (O_2). Recent studies revealed a rapid single electron transfer from the CYT domain to LPMO [45]. Despite the potential of CDH for improved cellulose processing, its ability to generate hydrogen peroxide (H_2O_2) via the electron transfer to O_2 broadens the scope of this enzyme. This property can be utilized for medical applications like antimicrobial systems and antioxidant regenerating systems [46,47].

Myeloperoxidase (MPO) is the major protein part in neutrophils and plays a key role in the human defense system. It is synthesized in the bone marrow, which ends up in a large homodimer consisting of a heavy and a light subunit which are linked by a disulphide bond [48]. MPO was initially classified as peroxidase but also has chlorination activity. This versatility renders this enzyme an important antimicrobial compound in the body combating bacterial contamination. The range of substrates for MPO is broad and includes H_2O_2 , chloride and thiocyanate which are quite abundant in physiological fluids [49]. The predominantly produced antimicrobial compound is hypochlorous acid (HOCl), which is produced by MPO via a two-electron transfer from H_2O_2 to chloride. Besides the antimicrobial property, MPO was also found to detoxify microbial toxins [50]. Due to the high concentration in neutrophils, which occur in wound environments in the stage of inflammation, MPO acts as an efficient biomarker for the detection of wound infection [51].

2.4. The wound

The skin serves as a protective barrier against the outer environment and consists of two layers called the epidermis and dermis. It is one part of the innate immune system impeding microorganisms from colonization not least by unfavorably low pH values. Invading organisms are further confronted with a defense cascade consisting of mono- and granulocytes, macrophages and natural killer cells that result from the activated innate immune response [52].

A destruction of the protective skin layers results in a wound and in the loss of the initial defense function. Acute wounds are either superficial or full thickness depending on the compromised skin layers [53]. The emergence of a wound initiates a well-defined wound management process, which involves four stages: hemostasis, inflammation, proliferation and remodeling. Hemostasis constitutes the first step of wound healing whereby coagulation

factors are activated to initiate blood clotting accompanied by the release of various growth factors, which are required for the subsequent stages. Phagocytic neutrophils predominate the inflammation phase and play an important role in the destruction of invading bacteria and necrotic cell components, which is performed by excreted enzymes and radicals. Monocytes are attracted on site by the neutrophils in the wound bed and differentiate to macrophages, which prepare the wound for the following stages. Triggered by macrophages, fibroblasts appear in the wound and start to proliferate by the aid of various growth factors. A complex interplay of tissue generation and the destruction of existing matrix started, mainly regulated by enzymes such as matrix metalloproteinases (MMPs) and finally results in highly vascularized granulation tissue. The remodeling started and lasts several weeks to months whereby scar tissue is formed, matures and new formed tissue is cross-linked with collagen to obtain the required tensile strength [54,55].

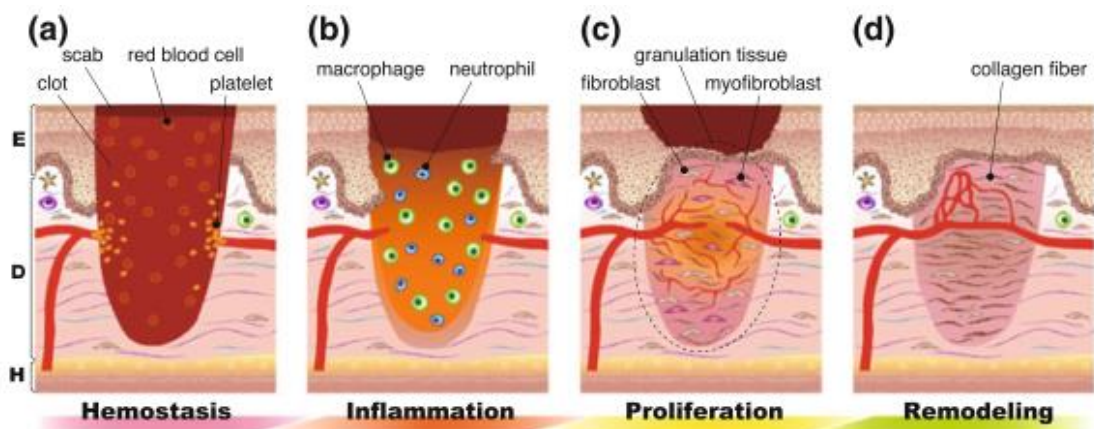


Figure 4: The wound healing process in mammals. (Permission obtained by Springer) [55]

The success of a wound to heal strongly depends on the proper course of the four previously described stages. Many factors are known, which interfere with cellular processes in one of these stages, including diabetes and obesity [56]. Another critical cause of a retarded wound healing is infection, which accompanies with the expression of virulence factors by microorganisms that interfere with the biological processes of inflammation [57]. Infection is the result of microbial contamination, which is a special risk for wounds because of the lack of an intact skin surface protecting underlying tissue. Bacterial invasion of the wound bed is classified in contamination, critical contamination and invasive infection [58]. At the stage of critical colonization, replicating bacteria trigger local tissue responses subsequently causing systemic host responses. Ineffective decontamination of the wound with progressed infection results in a prolonged inflammation stage due to elevated pro-inflammatory cytokines. The consequence of this process is chronic wounds, which are defined as wounds that fail to

heal. The extent of the infection thereby depends on the composition of the microbial flora as well as its pathogenicity and invasiveness. A variety of microorganisms is described to date that were found in infected wounds, including aerobic and anaerobic bacteria [57].

Chronic wounds are a major threat affecting 1-2% of the population in developed countries. There is a high estimated number of unknown cases mainly caused by overshadowing the significance of wound infection by diseases like diabetes [59]. Because of the difficulty in their treatment, chronic wounds have a substantial impact on the total health care expenses with increasing numbers, driven by an aging population and the increase of associated diseases. The economic and social impact of wound infection and chronic wounds is the driving force for the intense research and investment in alternative wound care strategies to combat the practical challenges in wound management [60].

Common wound care procedures comprise infection monitoring and wound treatment by the aid of cleaning, wound dressings and antimicrobial compounds [61]. The applied antimicrobial methods formerly concentrated on the systemic treatment with antibiotics. The past decades evoked a broad range of antibiotic substances for an effective treatment of polymicrobial infections and the type of administered antibiotics was adjusted according the possible bacterial contaminations in the respective wounds [62]. The emerging and to date omnipresent issue of bacterial resistances strengthen the need for new antimicrobial drugs and alternative treatment strategies. Several strategies are followed including the development of new drugs as well as the reemergence of therapies, which were used centuries ago. All policies thereby follow the same credo, which is the development of therapies that are safe, effective and reduce the likelihood of emerging resistances [57]. The prerequisite to choose the best wound treatment modality accompanies with an accurate wound monitoring, which requires reliable detection systems for the fast infection assessment.

References

- [1] Peppas NA, Langer R. New challenges in biomaterials. *Science* 1994;263:1715–20.
- [2] Langer R, Tirrell D a. Designing materials for biology and medicine. *Nature* 2004;428:487–92.
- [3] Bhat S, Kumar A. Biomaterials and bioengineering tomorrow's healthcare. *Biomatter* 3.
- [4] Hench L. Biomaterials. *Science* (80-) 1980;208:826–31.
- [5] Hench L, Wilson J. Surface-active biomaterials. *Science* (80-) 1984;226:630–6.

- [6] Gajjar CR, King MW. Resorbable Fiber-Forming Polymers for Biotextile Applications. Cham: Springer International Publishing; 2014.
- [7] Hench LL, Thompson I. Twenty-first century challenges for biomaterials. *J R Soc Interface* 2010;7 Suppl 4:S379–91.
- [8] Hench LL, Polak JM. Third-generation biomedical materials. *Science* 2002;295:1014–7.
- [9] Murugan R, Ramakrishna S. Development of nanocomposites for bone grafting. *Compos Sci Technol* 2005;65:2385–406.
- [10] Lapasin R. Rheology of Industrial Polysaccharides: Theory and Applications. 2012.
- [11] Aspinall GO. The Polysaccharides. Elsevier Science; 2014.
- [12] Sinha VR, Kumria R. Polysaccharides in colon-specific drug delivery. *Int J Pharm* 2001;224:19–38.
- [13] Lee JW, Park JH, Robinson JR. Bioadhesive-based dosage forms: the next generation. *J Pharm Sci* 2000;89:850–66.
- [14] Russo R, Malinconico M, Santagata G. Effect of cross-linking with calcium ions on the physical properties of alginate films. *Biomacromolecules* 2007;8:3193–7.
- [15] Tønnesen HH, Karlsen J. Alginate in drug delivery systems. *Drug Dev Ind Pharm* 2002;28:621–30.
- [16] Kang H-A, Shin MS, Yang J-W. Preparation and characterization of hydrophobically modified alginate. *Polym Bull* 2002;47:429–35.
- [17] Laurienzo P, Malinconico M, Mattia G, Russo R, La Rotonda MI, Quaglia F, et al. Novel alginate-acrylic polymers as a platform for drug delivery. *J Biomed Mater Res A* 2006;78:523–31.
- [18] Lee KY, Mooney DJ. Alginate : properties and biomedical applications. *Prog Polym Sci* 2012;37:106–26.
- [19] Zargar V, Asghari M, Dashti A. A Review on Chitin and Chitosan Polymers: Structure, Chemistry, Solubility, Derivatives, and Applications. *ChemBioEng Rev* 2015;2:204–26.
- [20] Lamarque G, Chaussard G, Domard A. Thermodynamic aspects of the heterogeneous deacetylation of beta-chitin: reaction mechanisms. *Biomacromolecules* 2007;8:1942–

50.

- [21] Lamarque G, Lucas JM, Viton C, Domard A. Physicochemical behavior of homogeneous series of acetylated chitosans in aqueous solution: Role of various structural parameters. *Biomacromolecules* 2005;6:131–42.
- [22] Pillai CKS, Paul W, Sharma CP. Chitin and chitosan polymers: Chemistry, solubility and fiber formation. *Prog Polym Sci* 2009;34:641–78.
- [23] Anitha a., Sowmya S, Kumar PTS, Deepthi S, Chennazhi KP, Ehrlich H, et al. Chitin and chitosan in selected biomedical applications. *Prog Polym Sci* 2014;39:1644–67.
- [24] Dumitriu S. *Polysaccharides : structural diversity and functional versatility*. Marcel Dekker; 2005.
- [25] Weinhold MX, Sauvageau JCM, Kumirska J, Thöming J. Studies on acetylation patterns of different chitosan preparations. *Carbohydr Polym* 2009;78:678–84.
- [26] Aam BB, Heggset EB, Norberg AL, Sørli M, Vårum KM, Eijsink VGH. Production of chitooligosaccharides and their potential applications in medicine. *Mar Drugs* 2010;8:1482–517.
- [27] Nordtveit RJ, Varum KM, Smidsrod O. Degradation of partially N-acetylated chitosans with hen egg white and human lysozyme. *Carbohydr Polym* 1996;29:163–7.
- [28] Tegl G, Öhlknecht C, Vielnascher R, Rollett A, Hofinger-Horvath A, Kosma P, et al. Cellobiohydrolases Produce Different Oligosaccharides from Chitosan. *Biomacromolecules* 2016;17:2284–92.
- [29] Laine RA. A calculation of all possible oligosaccharide isomers both branched and linear yields 1.05×10^{12} structures for a reducing hexasaccharide: the Isomer Barrier to development of single-method saccharide sequencing or synthesis systems. *Glycobiology* 1994;4:759–67.
- [30] Henrissat B, Bairoch a. New families in the classification of glycosyl hydrolases based on amino acid sequence similarities. *Biochem J* 1993;293 3:781–8.
- [31] Davies G, Henrissat B. Structures and mechanisms of glycosyl hydrolases. *Structure* 1995;3:853–9.
- [32] Vuong T V., Wilson DB. Glycoside hydrolases: Catalytic base/nucleophile diversity. *Biotechnol Bioeng* 2010;107:195–205.

- [33] Withers SG. Mechanisms of glycosyl transferases and hydrolases. *Carbohydr Polym* 2001;44:325–37.
- [34] Divne C, Ståhlberg J, Reinikainen T, Ruohonen L, Pettersson G, Knowles JK, et al. The three-dimensional crystal structure of the catalytic core of cellobiohydrolase I from *Trichoderma reesei*. *Science* (80-) 1994;265:524–8.
- [35] Fukamizo T, Ohkawa T, Ikeda Y, Goto S. Specificity of chitosanase from *Bacillus pumilus*. *Biochim Biophys Acta* 1994;1205:183–8.
- [36] Xia W, Liu P, Liu J. Advance in chitosan hydrolysis by non-specific cellulases. *Bioresour Technol* 2008;99:6751–62.
- [37] Liu J, Xia W. Purification and characterization of a bifunctional enzyme with chitosanase and cellulase activity from commercial cellulase. *Biochem Eng J* 2006;30:82–7.
- [38] Ike M, Ko Y, Yokoyama K, Sumitani JI, Kawaguchi T, Ogasawara W, et al. Cellobiohydrolase I (Cel7A) from *Trichoderma reesei* has chitosanase activity. *J Mol Catal B Enzym* 2007;47:159–63.
- [39] Stokke BT, Varum KM, Holme HK, Hjerde RJN, Smidsrsd O. Sequence specificities for lysozyme depolymerization of partially N-acetylated chitosans. *Can J Chem* 1995;1981:1972–81.
- [40] Lowe G, Sheppard G. Acetamido-group participation in lysozyme catalysis. *Chem Commun* 1968;949:529.
- [41] Toone EJ, Wiley InterScience (Online service). *Advances in enzymology and related areas of molecular biology*. Volume 77. Wiley-Blackwell; 2011.
- [42] Gelfand I, Sahajpal R, Zhang X, Izaurralde RC, Gross KL, Robertson GP. Sustainable bioenergy production from marginal lands in the US Midwest. *Nature* 2013;493:514–7.
- [43] Zamocky M, Ludwig R, Peterbauer C, Hallberg B, Divne C, Nicholls P, et al. Cellobiose Dehydrogenase – A Flavocytochrome from Wood-Degrading, Phytopathogenic and Saprotrophic Fungi. *Curr Protein Pept Sci* 2006;7:255–80.
- [44] Pricelius S, Ludwig R, Lant N, Haltrich D, Guebitz GM. Substrate specificity of *Myriococcum thermophilum* cellobiose dehydrogenase on mono-, oligo-, and polysaccharides related to in situ production of H₂O₂. *Appl Microbiol Biotechnol* 2009;85:75–83.

- [45] Tan T-C, Kracher D, Gandini R, Sygmund C, Kittl R, Haltrich D, et al. Structural basis for cellobiose dehydrogenase action during oxidative cellulose degradation. *Nat Commun* 2015;6:7542.
- [46] Thallinger B, Prasetyo EN, Nyanhongo GS, Guebitz GM. Antimicrobial enzymes: an emerging strategy to fight microbes and microbial biofilms. *Biotechnol J* 2013;8:97–109.
- [47] Nyanhongo GS, Sygmund C, Ludwig R, Prasetyo EN, Guebitz GM. Synthesis of multifunctional bioresponsive polymers for the management of chronic wounds. *J Biomed Mater Res - Part B Appl Biomater* 2013;101 B:882–91.
- [48] SCHULTZ J, KAMINKER K. Myeloperoxidase of the leucocyte of normal human blood. I. Content and localization. *Arch Biochem Biophys* 1962;96:465–7.
- [49] Klebanoff SJ. Myeloperoxidase-halide-hydrogen peroxide antibacterial system. *J Bacteriol* 1968;95:2131–8.
- [50] Winterbourn CC. Comparative reactivities of various biological compounds with myeloperoxidase-hydrogen peroxide-chloride, and similarity of the oxidant to hypochlorite. *Biochim Biophys Acta* 1985;840:204–10.
- [51] Tegl G, Schiffer D, Sigl E, Heinzle A, Guebitz GM. Biomarkers for infection: enzymes, microbes, and metabolites. *Appl Microbiol Biotechnol* 2015;99:4595–614.
- [52] Fearon DT, Locksley RM. The instructive role of innate immunity in the acquired immune response. *Science* (80-) 1996;272:50–3.
- [53] Korting HC, Schöllmann C, White RJ. Management of minor acute cutaneous wounds: importance of wound healing in a moist environment. *J Eur Acad Dermatology Venereol* 2011;25:130–7.
- [54] Schultz GS, Sibbald RG, Falanga V, Ayello E a., Dowsett C, Harding K, et al. Wound bed preparation: a systematic approach to wound management. *Wound Repair Regen* 2003;11:S1–28.
- [55] Kawasumi A, Sagawa N, Hayashi S, Yokoyama H, Tamura K. Wound Healing in Mammals and Amphibians: Towards Limb Regeneration in Mammals. *Curr Top Microbiol Immunol* 2013;367:33–49.
- [56] Guo S, Dipietro LA. Factors affecting wound healing. *J Dent Res* 2010;89:219–29.

- [57] Bowler PG, Duerden BI, Armstrong DG. Wound microbiology and associated approaches to wound management. *Clin Microbiol Rev* 2001;14:244–69.
- [58] Williams DT, Hilton JR, Harding KG. Diagnosing foot infection in diabetes. *Clin Infect Dis* 2004;39:S83–6.
- [59] Gottrup F. A specialized wound-healing center concept: importance of a multidisciplinary department structure and surgical treatment facilities in the treatment of chronic wounds. *Am J Surg* 2004;187:38 – 43.
- [60] Sen CK, Gordillo GM, Roy S, Kirsner R, Lambert L, Hunt TK, et al. Human Skin Wounds: A Major and Snowballing Threat to Public Health and the Economy. *Wound Repair Regen* 2009;17:763–71.
- [61] Dreifke MB, Jayasuriya A a., Jayasuriya AC. Current wound healing procedures and potential care. *Mater Sci Eng C* 2015;48:651–62.
- [62] Murphy PS, Evans GRD. Advances in Wound Healing: A Review of Current Wound Healing Products. *Plast Surg Int* 2012;2012:1–8.
- [63] Schiffer D, Tegl G, Vielnascher R, Weber H, Schoeftner R, Wiesbauer H, et al. Fast Blue RR—Siloxane Derivatized Materials Indicate Wound Infection Due to a Deep Blue Color Development. *Materials* 2015;8:6633–9.

In vitro diagnostics for early detection of bacterial wound infection

Published in: Handbook of Online and Near-Real-Time Methods in Microorganism Detection, CRC Press, in press

Gregor Tegl, Andrea Heinzle, Eva Sigl, Georg M. Guebitz

Introduction

Bacterial contamination is the basis of wound infection and still constitutes a threat in health care. Despite the significant developments of aseptic methods in the past century, a residual risk of bacterial contamination remained that pictures in about 10% postoperative wound infections [1]. A high risk of infection is also reported for chronic wounds [2], an issue predominantly affecting immune suppressed people [3]. As a consequence of manifestation of wound infection wounds fail to heal. This greatly complicates the treatment modalities and life quality of the patients.

The infection progress strongly correlates with the interaction of invading bacteria with the wound environment. This process is divided into four sections, namely contamination, colonization, critical colonization and infection, whereby impaired wound healing is considered to start at stage of critical bacterial colonization [4]. To date applied detection methods are still based on the assessment of clinical signs such as redness (rubor), heat (calor), swelling (tumor), pain (dolor) and impairment of function (functiolaesa) which are strongly influenced by parameters like impaired leukocyte functions of patients [5,6]. These classical signs turn obvious at a progressed stage of infection and when microorganisms have already established a stable community increasing resistance towards a variety of treatment strategies. Timely interference in the infection progression is of great importance and requires an effective online detection system indicating an infection at an early stage.

A variety of infection biomarkers is known based on microbes and their metabolites as well as based on intrinsic signal molecules secreted by the host immune system [7]. Since bacteria are the key players of infection, their early recognition is a reliable sign predicting an emerging infection. Several strategies are followed and described in the literature directly assessing bacteria concentrations in wounds but also indirectly detecting bacterial contamination by the aid of signal molecules. Available techniques in diagnostics enabled a substantial set of tools to be investigated for early stage detection of wound infection including synthetic materials, polysaccharides and proteins, amongst others (figure 1) [8].

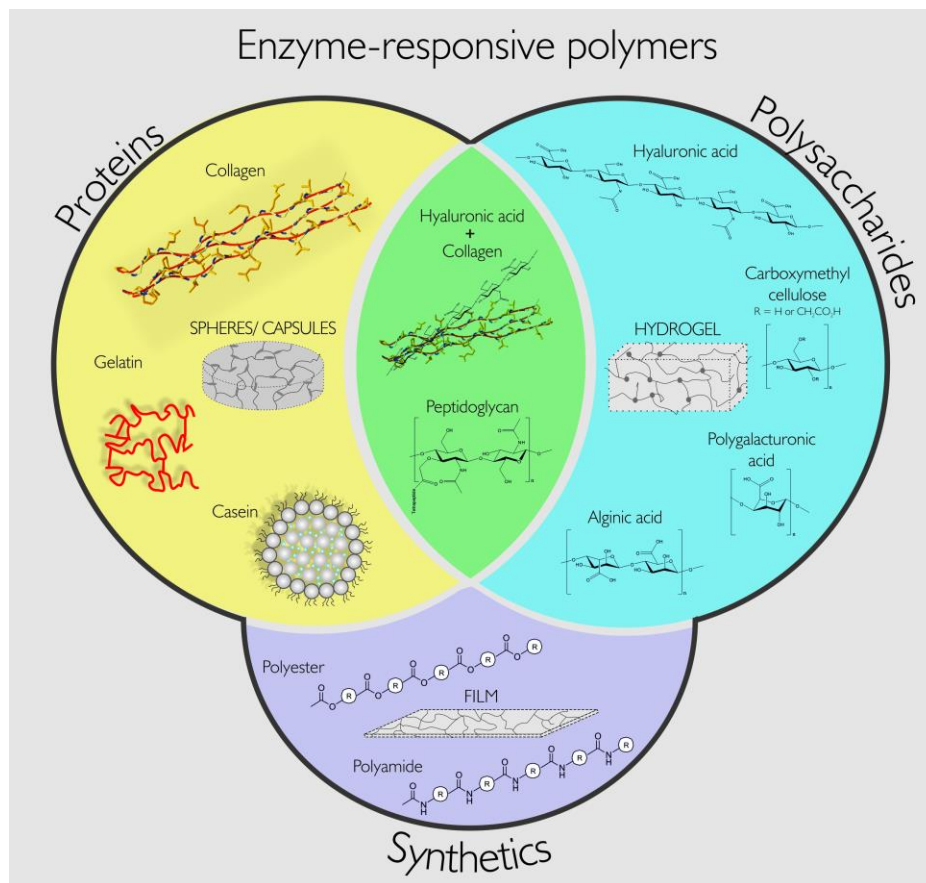


Figure 1: Enzyme-responsive polymers suitable for modification to detect wound infection. The different polymers are grouped into biopolymers (protein and polysaccharides) and synthetic polymers.

This chapter discusses the promising methods available for microbial infection detection divided in direct bacterial detection and indirect infection detection. The advantages and disadvantages of the available detection systems are elucidated and future perspectives in early detection of bacterial wound infection are discussed.

2.5. Direct detection of bacterial wound contaminants

The assessment of the bacterial load in a wound represents a meaningful strategy since microbe concentration in a wound strongly correlates with the infection status [9]. Early research on microbes in wounds targeted an estimation of bacteria concentration that evokes wound infection and numbers always varied with the sampling technique chosen [10]. It is still questioned whether distinct bacterial species are responsible for an infection or if the emergence of a polymicrobial consortium is the crucial etiology [11]. However, bacteria are the key players in wound infection and thus constitute suitable biomarkers for infection

detection. Initial detection methods were based on long lasting analytical methods but substantial progress was made resulting in novel strategies for a fast assessment of bacterial wound contamination [7]. The investigated methods thereby target either single bacterial species but also consider the wound microbiome.

2.5.1. Near real-time detection methods

Amongst the available detection systems, stimuli responsive systems cover a broad pool of materials that change physical properties upon interaction with an external stimulus. Targeted modification of these materials can lead to real-time detection systems enabling an application as point-of-care (PoC) diagnostics. An effective strategy was chosen by Zhou et al. producing lipid vesicles that were responsive towards virulence factors of pathogenic bacteria like *S. aureus* and *P. aeruginosa* [12]. The working mechanism is based on bacteria excreted toxins and lipases that also destruct human cell membranes and thus are capable of cleaving lipid based vesicles. The respective vesicles, loaded with fluorescein or/and antimicrobial compounds, resulted in detection of pathogenic bacteria as well as in growth inhibition. The choice of lipids as responsive material further enabled a discrimination between pathogenic and non-pathogenic bacteria, which commonly do not produce biological weapons against membranes. Subsequent refinements of the developed system could enhance stability of the lipid vesicles and functionalization on fabrics led to a responsive system that proved effective for detecting pathogenic bacteria while not responding to *E.coli* [13]. In 2015, the vesicles were incorporated in a wound dressing prototype and applied towards an ex vivo porcine skin burn wound model finally proving the detection of pathogenic bacteria in a biofilm consortium (figure 2) [14]. Detection of the pathogens *Enterococcus faecalis*, *P. aeruginosa* and *S. aureus* was realized after 6 hr incubation time and thus counts as a suitable system for fast detection of wound infection. This system renders of particular interest considering the bifunctional character of the vesicles as detection system as well as for antimicrobial treatment. Whether non-pathogenic bacteria have to be excluded or also contribute to an emerging infection remains part of discussion.

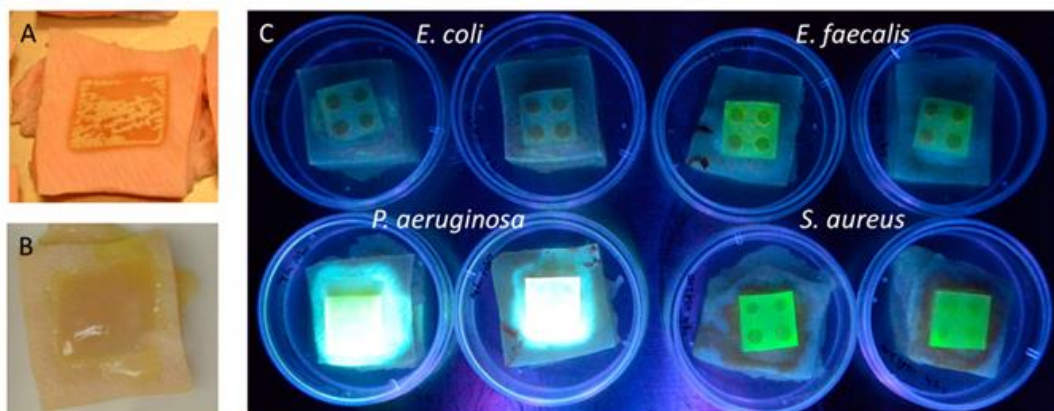


Figure 2: A wound dressing prototype based on bacteria responsive fluorescent vesicles, applied on an infected porcine skin wound model. (A) a second degree partial thickness burn wound with blisters, (B) the burn wound 24 hr after infection with *P. aeruginosa*, and (C) the fluorescence response of prototype dressings on infected wounds of SPE (*Staphylococcus-Pseudomonas- Enterococcus*) group pathogens 24 hr later. The pathogenic bacteria *Enterococcus faecalis*, *P. aeruginosa* and *S. aureus* showed a fluorescence response from the dressing, while the non-pathogenic reference *E. coli* did not show any signal. Reproduced with permission from ACS Publications [14].

Infection detection based on fluorescence and/or color signals depicts an efficient and easily assessable method, however it requires the formulation of complex systems enabling a visualization process. Bioluminescence by contrast is a widely observed phenomenon induced by endogenous fluorescing molecules [15]. Tissue components as well as a bunch of pathogenic bacteria such as *S. aureus* are auto-fluorescent and can thus be visualized. The spectral range of the respective fluorescence signals differ enabling a distinction of connective tissue of a wound and contaminating bacteria [16].

Wu et al. utilized the auto-fluorescence of both cell types detecting wound infection by the aid of auto fluorescent (AF) imaging [17]. White light (WL) and AF images were acquired using a charge-coupled device (CCD) camera whereby *S. aureus* could be detected via the red bioluminescence of endogenous porphyrins. Experiments were conducted assessing mouse skin wound models inoculated with *S. aureus* whereby a clear increase of bacteria concentration was visualized and also quantified assessing the spread area over time. Microbiological tests compared to AF imaging on chronic wounds of patients proved the suitability of the imaging system to detect multi-resistant *S. aureus* (MRSA). However simultaneous detection of different strains is not possible with that system but of great importance due to significant variations in the polymicrobial flora within wounds that renders single bacteria detection invalid [18].

2.5.2. Analytical methods for infection detection

The need of PoC diagnostics for infection detection drives research to innovation of online measurement tools providing fast information on the infection status. However, various methods were developed for bacteria detection in wounds that are based on analytical techniques like mass spectrometry (MS) and microscopy [7]. The major disadvantage does not only arise from the duration of measurement and analysis but much more from the withdrawal of wound samples and further preparation for analytics. Withdrawals of wound samples via swabbing are less reliable depending on the location of withdrawal, whereas quantitative biopsy constitutes the most accurate technique but is invasive [19]. Consequently, techniques relying on sample withdrawal are from many perspectives not favorable, but possess analytical value and are thus considered in this chapter.

Capillary zone electrophoresis (CZE) could be utilized for the selective detection of *E. coli* in wound fluids of infected wounds [20]. Although a method not intended for whole cell analysis, a single peak was elucidated reliably detecting *E. coli* in wound samples in good sensitivity within a 30 min measurement. The advantage of the CZE method is the possibility to apply directly diluted wound fluid, which avoids complex sample preparation. *E. coli* can act as pathogen in wound beds thus its detection is meaningful, nevertheless the assessment of a single microbial species in a wound does not reliably indicate the infection status. Progress in microbe detection using CZE techniques could enable simultaneous detection of multiple cell types and was proposed by Rodriguez et al [21].

Beside capillary electrophoresis, mass spectrometry (MS) is another powerful tool that finds multiple applications in various research areas and routine analytics. Matrix-assisted laser desorption ionization time-of-flight (MALDI-TOF) mass spectrometry constitutes an efficient method for the analysis of complex biological samples and has gained considerable attention for the identification of bacteria [22]. A standard procedure using *Leuconostoc*, *Fructobacillus* and *Lactobacillus* as reference species was implemented by De Bruyne et al. that was based on the comprehensive analysis using MS and machine learning [23]. This combination led to high accuracies for the identification of the investigated bacteria, however the approach was not applied on wound samples. Biswas and Rolain reviewed the capabilities and frontiers of MALDI-TOF MS for the detection of aerobic and anaerobic bacteria, amongst others, and illustrated the advantages of MS. The crucial aspect in bacteria identification with MS is the restricted amount of reference spectra to date available but required for bacteria detection. Expanding databases would enable MALDI-TOF to act as fast and less expensive first-line identification system circumventing the immediate use of complex techniques like gene sequencing. Antibiotics treatment strategies could be fairly improved if knowledge is gained from MS reference databases including multi resistant bacteria. Despite the great potential of

MS in infection detection, wound sample withdrawal and sample preparation still constitute a major burden.

Modern PCR and sequencing methods are without any doubt the most accurate analytical techniques detecting multiple bacteria in complex samples [24,25]. Simultaneous assessment of the entire wound microbiome could result in personalized treatment strategies. However, high instrumental costs and required sample withdrawals render these sophisticated approaches not profitable for fast infection detection.

2.6. Indirect detection methods for the determination of wound infection

The core concept of online monitoring outlines an early detection of an emerging infection and thus concentrates rather on infection prevention than on infection treatment. Assessment of the microbiome can unveil the pathogenomic picture of a wound but constitutes an extrinsic biomarker not fully reflecting the activity of the host immune system. A variety of other infection biomarkers was found in infected wound beds that give detailed information on bacteria concentration at an early phase of contamination. A substantial fraction of known biomarkers have also direct impact on the wound healing process like the pH, which makes its detection particularly interesting. Biomolecules secreted in the wound environment either derive from bacterial metabolism but can also be part of the human immune response.

2.6.1. Enzyme biomarkers for infection detection

The immune system tends to control biological processes by the aid of enzymes as it holds true for bacterial contamination of wounds. Activities of various enzymes like myeloperoxidase and lysozyme are down and up regulated in response to the bacterial count and support the destruction of bacteria as well as damaged tissue [26,27]. The infection status can thus be expressed as function of enzyme activity and just requires transformation into a visual signal.

The so far most intense elaboration detecting wound enzymes is based on modified polymer systems [8]. The occurrence of distinct stimuli can be well visualized due to the change of physicochemical properties in response to external stimuli like enzymes. Amongst the variety of assays available detecting enzymes, color formation in response to enzyme activities is of particular interest considering the application in PoC diagnostics due to the ease of interpretation. Enzymes indicating wound infection include myeloperoxidase (MPO), lysozyme, human neutrophil elastase (HNE), cathepsin G and matrix metalloproteases (MMP). Their catalytic activity determines the polymer to be modified for the detection of the

respective enzyme, whereby infection indicating enzymes are classified as hydrolases and oxidoreductases.

Proteolytic enzymes are excreted into the wound to destruct damaged tissue. The respective responsive materials are thus mainly based on protein substrates [28]. HNE was detected using a peptide sequence (MeOSuc-AAPV) that was tagged with para-nitroaniline (pNA) and HNE mediated hydrolysis led to release of yellow colored pNA. The system was successfully tested discriminating between infected and non-infected wound fluids with the free peptide as well as with immobilized derivatives on polyamides, polyester and protein-based polymers [29–31]. Non colorimetric detection methods are based on quartz crystal microbalance (QCM) measurements [32] and DNA aptamer sensors [33] but show restricted applicability for PoC devices compared to color changing detection systems.

Other elevated protease activities like cathepsin G and MMPs were successfully detected based on their ability to hydrolyze gelatin. Heinzle et al. produced gelatin beads that were loaded with Reactive Blue leading to color release after incubation with gelatinolytic enzymes²⁸. This detection system exhibited optimal reaction kinetics for ex-vivo diagnostics visually discriminating infected wounds from non-infected wounds within 30 min. Direct detection of Cathepsin G was also proved via plasmon resonance imaging (SPRI) whereby a peptidyl inhibitor was immobilized on a gold chip and enabled quantification in high sensitivity and selectivity [34–36]. The SPRI detection system further proved effective measuring cathepsin G in complex samples like white blood cells, saliva samples and endometrial tissue.

Lysozyme is another important indicator of wound infection responsible for the cell wall degradation of wound invading bacteria. It specifically attacks the peptidoglycan (PG) of cell walls hydrolyzing glycosidic linkages between N-acetylmuramic acid and N-acetylglucosamine residues that further results in cell destruction [37,38]. Hydrolysis of PG dispersed in wound fluid leads to increasing transparency and visual detection was achieved by covalently attached Remazol Brilliant Blue. Colored oligosaccharides were released and led to significant absorbance differences detecting elevated lysozyme activities in wound fluids [39]. The lysozyme detection concept was extended and incorporated in a lateral flow system for the assessment of wound infection. The system is based on a size exclusion membrane only allowing migration of cleaved colored oligosaccharides, which are subsequently captured on a membrane [40]. Intentions to increase signal intensity led to the invention of enhanzymes that should multiply lysozyme mediated PG hydrolysis by the aid of laccases [41]. Such a system could be incorporated in a lateral flow device that enables a fast and real-time assessment of the wound status. Alternative strategies for lysozyme detection are based on aptamer sensors and nanosensors. Both sensor systems show superior selectivity and sensitivity, but their application for complex samples like wound fluids is still restricted [42]. Aptamer based systems were successfully tested for lysozyme

detection including sensors using electrochemical impedance spectroscopy [43], fluorescent aptasensors [44] [45] and piezoelectric sensors [46]. Nanosensors share advantages with aptamer sensors, like high sensitivity, but have also proven to work in complex media such as in the case of a fluorescence nanosensor based on CdTe quantum dots (QDs) and carboxymethyl chitosan (CMCS) incorporating Zn^{2+} [47]. Lysozyme mediated hydrolysis of CMCS resulted the release of Zn^{2+} that led to quenching of photoluminescence and enabled quantitative lysozyme detection in human serum. A QCM nanosensor proved same capability but no information about measurements in human fluids is available yet [48].

MPO is another important biomarker not only for wound infection but also for several more disorders like cardiovascular diseases. In case of bacterial wound contamination, MPO activity is highly elevated based on the increased production of the neutrophils by the immune system [49]. It exhibits chlorination activity and thus produces hypochloric acid (HOCl), which is a bactericidal oxidative agent. Hasmann et al. could determine elevated MPO activity in wound fluids of infected wounds using guaiacol as substrate and MPO detection systems were rapidly extended to non-natural phenolic substrates [50]. The phenol Fast Blue RR turned out MPO responsive and was functionalized with a siloxane spacer enabling covalent immobilization on silica based materials. Wound infection was determined comparing MPO activity in infected and non-infected wound fluids and interference tests with hemoglobin could further reveal the sensitivity of the detection system [51]. The chlorination activity of MPO was utilized detecting wound infection by the aid of an electrochemical sensor system [52]. A correlation of MPO oxidation and chlorination activity was visualized using a hydrogen peroxide (H_2O_2) sensor that detected H_2O_2 consumption, which was supplied using glucose oxidase, as function of MPO activity. The produced biosensor could thereby clearly distinguish between wound samples from infected and non-infected wounds.

2.6.2. Metabolites and sensing molecules for infection detection

The variety of compounds contributing to the complexity of wound fluids is either secreted by the invading microflora or part of the human immune response [53], their concentrations nevertheless reflects the wound infection status. A majority of the biomarkers discussed in this subchapter are bacteria derived and also have impact on the wound healing process.

An electrochemical impedance immune sensor was developed that combined the detection of both, immune system derived receptor-1 and MMP as well as N-3-oxo-dodecanoyl-1-homoserine lactone (HSL) that was unveiled as a quorum sensing molecule of *P. aeruginosa* [54]. Specific antibodies were immobilized on a gold solid phase electrolyte (SPE) and binding of the respective biomarkers resulted in an increase of electron transfer resistance.

The applicability of the detection system was confirmed measuring the mentioned analytes in mock wound fluids in good sensitivity.

Dealing with microbial infections, latest research focuses on quorum sensing molecules of bacteria due to their crucial role in biofilm formation. Gene expression is up and down regulated by the aid of sensing molecules and strongly effects bacterial virulence and thus the infection progress [55]. *P. aeruginosa* is a representative frequently found in infected wounds and known to produce the redox active quorum sensor pyocyanin, whose concentration correlates with the bacterial load. Sharp et al invented a sensor based on a carbon fiber tow electrode consisting of sandwiched carbon fibres electrically connected by a copper shielding tape that monitored pyocyanin via square wave voltammetry [56]. The sensor turned out selective also detecting *P. aeruginosa* in mixed bacteria populations. However, the proof of concept on wound fluid samples was not published yet.

Another powerful wound infection indicator is the change of pH in the wound environment. The pH of an intact epidermis ranges from 4 to 6, a triggered immune response was found to increase the pH, which also influences the wound healing process [57]. Simple sensor systems for pH detection were prepared based on common pH indicators like bromocresol green and bromocresol purple that were immobilized on tetraethoxysilane films [58]. Chip-LED mediated illumination of bromocresol green resulted in successful indication of pH changes of buffer solutions, the system was however inaccurate in artificial wound fluid. A pH detection system that proved its applicability in complex media was achieved utilizing 2D luminescence imaging [59]. The use of fluorescein isothiocyanate (FITC) in combination with ruthenium (II)tris-(4,7-diphenyl-1,10-phenanthroline) (Ru(dpp)_3) and a time-gated CCD camera detected pH dependent luminescence. The pH responsive system was incorporated into microparticles that were further immobilized on polyurethane hydrogels to improve applicability.

A pH changing compound accumulated in response to the host immune response is uric acid, which is produced by xanthine oxidase (XO) from purine derivatives [60]. Disposable pH sensors for urate detection were produced by Phair et al. that were based on SPEs and could successfully detect urate in buffer and blood samples [61]. Further developments of carbon fiber sensors and pad-imprinted carbon-uric acid composite electrodes proved a sensitive detection of pH changes caused by uric acid in complex media like artificial wound fluid, serum and blister fluid. However these systems are lacking of a definite proof on human wound fluids samples of infected wounds.

The majority of bacterial metabolites are small molecules like ethanol, acetic acid and butyric acid [62]. A substantial percentage of these molecules are volatile (organic volatile compounds, VOC), thus detectable in the wound headspace, which circumvents sample withdrawals. Initial attempts to assess VOCs in the bacterial headspace were undertaken by

Setkus et al. developing an SnO₂ gas sensor that was tested on cultures of *E. coli*, *P. aeruginosa* and *S. aureus* [63]. Investigated compounds could be detected and were observed to vary with the growth stage of the bacteria. The great number of molecules to be considered led to the investigation of conducting organic polymer sensor arrays that were combined with neural network techniques [64], but important parameter like resistance and conductivity did not fulfill the requirements. Further improvements finally led to the invention of the e-nose consisting of a gas sensor array combined with a feature extraction method and a neural network classifier [65] [66]. The complex setup including sampling unit, conditioning unit and processing unit was proven successful on single bacteria populations and VOCs could also be detected in infected wounds of mice. Methods for background elimination and improvement of the feature extraction render this approach powerful for infection detection by the aid of an intelligent sensor system [33,67,68]

2.7. References

- [1] Petherick ES, Dalton JE, Moore PJ, Cullum N. Methods for identifying surgical wound infection after discharge from hospital: a systematic review. *BMC Infect Dis* 2006;6:170.
- [2] Sen CK, Gordillo GM, Roy S, Kirsner R, Lambert L, Hunt TK, et al. Human Skin Wounds: A Major and Snowballing Threat to Public Health and the Economy. *Wound Repair Regen* 2009;17:763–71.
- [3] Siddiqui AR, Bernstein JM. Chronic wound infection: facts and controversies. *Clin Dermatol* 2010;28:519–26.
- [4] Schultz GS, Sibbald RG, Falanga V, Ayello E a., Dowsett C, Harding K, et al. Wound bed preparation: a systematic approach to wound management. *Wound Repair Regen* 2003;11:S1–28.
- [5] Cutting KF, White RJ. Criteria for identifying wound infection--revisited. *Ostomy Wound Manage* 2005;51:28–34.
- [6] Howell-Jones RS, Wilson MJ, Hill KE, Howard a J, Price PE, Thomas DW. A review of the microbiology, antibiotic usage and resistance in chronic skin wounds. *J Antimicrob Chemother* 2005;55:143–9.
- [7] Tegl G, Schiffer D, Sigl E, Heinzle A, Guebitz GM. Biomarkers for infection: enzymes, microbes, and metabolites. *Appl Microbiol Biotechnol* 2015;99:4595–614.

- [8] Schiffer D, Tegl G, Heinzle A, Sigl E, Metcalf D, Bowler P, et al. Enzyme-responsive polymers for microbial infection detection. *Expert Rev Mol Diagn* 2015;15:1–7.
- [9] Bendy RH, Nuccio PA, Wolfe E, Collings B, Tamburro C, Glass W, et al. Relationship of quantitative wound bacterial counts to healing of decubiti: Effect of Topical gentamicin. *Antimicrob Agents Chemother* 1964;10:147–55.
- [10] Gardner SE, Frantz R a, Saltzman CL, Hillis SL, Park H, Scherubel M. Diagnostic validity of three swab techniques for identifying chronic wound infection. *Wound Repair Regen* 2006;14:548–57.
- [11] Bowler PG, Duerden BI, Armstrong DG. Wound microbiology and associated approaches to wound management. *Clin Microbiol Rev* 2001;14:244–69.
- [12] Zhou J, Loftus AL, Mulley G, Jenkins a T a. A thin film detection/response system for pathogenic bacteria. *J Am Chem Soc* 2010;132:6566–70.
- [13] Zhou J, Tun TN, Hong S, Mercer-Chalmers JD, Laabei M, Young AER, et al. Development of a prototype wound dressing technology which can detect and report colonization by pathogenic bacteria. *Biosens Bioelectron* 2011;30:67–72.
- [14] Thet NT, Alves DR, Bean JE, Booth S, Nzakizwanayo J, Young a. ER, et al. Prototype Development of the Intelligent Hydrogel Wound Dressing and Its Efficacy in the Detection of Model Pathogenic Wound Biofilms. *ACS Appl Mater Interfaces* 2015
- [15] Lee S, Camilli A. Novel approaches to monitor bacterial gene expression in infected tissue and host. *Curr Opin Microbiol* 2000;3:97–101.
- [16] Moriwaki Y, Caaveiro JMM, Tanaka Y, Tsutsumi H, Hamachi I, Tsumoto K. Molecular Basis of Recognition of Antibacterial Porphyrins by Heme- Transporter IsdH-NEAT3 of *Staphylococcus aureus*. *Biochemistry* 2011;50:7311–20.
- [17] Wu YC, Kulbatski I, Medeiros PJ, Maeda A, Bu J, Xu L, et al. Autofluorescence imaging device for real-time detection and tracking of pathogenic bacteria in a mouse skin wound model: preclinical feasibility studies. *J Biomed Opt* 2014;19:085002.
- [18] Gardner SUEE, Frantz RA, Doebbeling BN. The validity of the clinical signs and symptoms used to identify localized chronic wound infection. *Wound Repair Regen* 2001;9:178–86.
- [19] Bill TJ, Ratliff CR, Donovan AM, Knox LK, Morgan RF, Rodeheaver GT. Quantitative swab culture versus tissue biopsy: a comparison in chronic wounds. *Ostomy Wound*

Manage 2001;47:34–7.

- [20] Szeliga J, Kłodzińska E, Jackowski M. The clinical use of a fast screening test based on technology of capillary zone electrophoresis (CZE) for identification of *Escherichia coli* infection in biological material. *Med Sci Monit* 2011;17:91–6.
- [21] Rodriguez MA, Lantz AW, Armstrong DW. Capillary electrophoretic method for the detection of bacterial contamination. *Anal Chem* 2006;78:4759–67.
- [22] Biswas S, Rolain JM. Use of MALDI-TOF mass spectrometry for identification of bacteria that are difficult to culture. *J Microbiol Methods* 2013;92:14–24.
- [23] De Bruyne K, Slabbinck B, Waegeman W, Vauterin P, De Baets B, Vandamme P. Bacterial species identification from MALDI-TOF mass spectra through data analysis and machine learning. *Syst Appl Microbiol* 2011;34:20–9.
- [24] Melendez JH, Frankel YM, An AT, Williams L, Price LB, Wang N-Y, et al. Real-time PCR assays compared to culture-based approaches for identification of aerobic bacteria in chronic wounds. *Clin Microbiol Infect* 2010;16:1762–9.
- [25] Mazumdar RM, Chowdhury A, Hossain N, Mahajan S, Islam S. Pyrosequencing-A Next Generation Sequencing Technology. *World Appl Sci J* 24 2013;24:1558–71.
- [26] Schiffer D, Blokhuis-Arkes M, van der Palen J, Sigl E, Heinzle A, Guebitz GM. Assessment of infection in chronic wounds based on the monitoring of elastase, lysozyme and myeloperoxidase activities. *Br J Dermatol* 2015.
- [27] Sinclair RD, Ryan TJ. Proteolytic enzymes in wound healing: the role of enzymatic debridement. *Australas J Dermatol* 1994;35:35–41.
- [28] Heinzle A, Papen-Botterhuis NE, Schiffer D, Schneider KP, Binder B, Schintler M, et al. Novel protease-based diagnostic devices for detection of wound infection. *Wound Repair Regen* 2013;21:482–9.
- [29] Hasmann A, Gewessler U, Hulla E, Schneider KP, Binder B, Francesko A, et al. Sensor materials for the detection of human neutrophil elastase and cathepsin G activity in wound fluid. *Exp Dermatol* 2011;20:508–13.
- [30] Heumann S, Eberl A, Fischer-Colbrie G, Pobeheim H, Kaufmann F, Ribitsch D, et al. A novel aryl acylamidase from *nocardia farcinica* hydrolyses polyamide. *Biotechnol Bioeng* 2009;102:1003–11.

- [31] Fleck CA, Simman R. Modern Collagen Wound Dressings: Function and Purpose. *J Am Col Certif Wound Spec* 2010;2:50–4.
- [32] Stair JL, Watkinson M, Krause S. Sensor materials for the detection of proteases. *Biosens Bioelectron* 2009;24:2113–8.
- [33] He Q, Yan J, Shen Y, Bi Y, Ye G, Tian F, et al. Classification of Electronic Nose Data in Wound Infection Detection Based on PSO-SVM Combined with Wavelet Transform. *Intell Autom Soft Comput* 2012;18:967–79.
- [34] Gorodkiewicz E, Sieńczyk M, Regulaska E, Grzywa R, Pietruszewicz E, Lesner A, et al. Surface plasmon resonance imaging biosensor for cathepsin G based on a potent inhibitor: development and applications. *Anal Biochem* 2012;423:218–23.
- [35] Grzywa R, Gorodkiewicz E, Burchacka E, Lesner A, Laudański P, Lukaszewski Z, et al. Determination of cathepsin G in endometrial tissue using a surface plasmon resonance imaging biosensor with tailored phosphonic inhibitor. *Eur J Obstet Gynecol Reprod Biol* 2014;182C:38–42.
- [36] Zou F, Schmon M, Sienczyk M, Grzywa R, Palesch D, Boehm BO, et al. Application of a novel highly sensitive activity-based probe for detection of cathepsin G. *Anal Biochem* 2012;421:667–72.
- [37] Torsteinsdóttir I, Håkansson L, Hällgren R, Gudbjörnsson B, Arvidson NG, Venge P. Serum lysozyme: a potential marker of monocyte/macrophage activity in rheumatoid arthritis. *Rheumatology (Oxford)* 1999;38:1249–54.
- [38] Salton MR. The properties of lysozyme and its action on microorganisms. *Bacteriol Rev* 1957;21:82–100.
- [39] Hasmann A, Wehrsuetz-Sigl E, Kanzler G, Gewessler U, Hulla E, Schneider KP, et al. Novel peptidoglycan-based diagnostic devices for detection of wound infection. *Diagn Microbiol Infect Dis* 2011;71:12–23.
- [40] Schiffer D, Verient V, Luschig D, Blokhuis-Arkes MHE, Palen J v. d., Gamerith C, et al. Lysozyme-Responsive Polymer Systems for Detection of Infection. *Eng Life Sci* 2015;15:368–75.
- [41] Schneider KP, Gewessler U, Flock T, Heinzle A, Schenk V, Kaufmann F, et al. Signal enhancement in polysaccharide based sensors for infections by incorporation of chemically modified laccase. *N Biotechnol* 2012;29:502–9.

- [42] Yoshida W, Abe K, Ikebukuro K. Emerging techniques employed in aptamer-based diagnostic tests. *Expert Rev Mol Diagn* 2014;14:143–51.
- [43] Erdem A, Eksin E, Muti M. Chitosan-graphene oxide based aptasensor for the impedimetric detection of lysozyme. *Colloids Surf B Biointerfaces* 2014;115:205–11.
- [44] Chen C, Zhao J, Jiang J, Yu R. A novel exonuclease III-aided amplification assay for lysozyme based on graphene oxide platform. *Talanta* 2012;101:357–61.
- [45] Rodríguez MC, Rivas G a. Label-free electrochemical aptasensor for the detection of lysozyme. *Talanta* 2009;78:212–6.
- [46] Lian Y, He F, Mi X, Tong F, Shi X. Lysozyme aptamer biosensor based on electron transfer from SWCNTs to SPQC-IDE. *Sensors Actuators B Chem* 2014;199:377–83.
- [47] Song Y, Li Y, Liu Z, Liu L, Wang X, Su X, et al. A novel ultrasensitive carboxymethyl chitosan-quantum dot-based fluorescence “turn on-off” nanosensor for lysozyme detection. *Biosens Bioelectron* 2014;61:9–13.
- [48] Sener G, Ozgur E, Yilmaz E, Uzun L, Say R, Denizli A. Quartz crystal microbalance based nanosensor for lysozyme detection with lysozyme imprinted nanoparticles. *Biosens Bioelectron* 2010;26:815–21.
- [49] Hansson M, Olsson I, Nauseef WM. Biosynthesis, processing, and sorting of human myeloperoxidase. *Arch Biochem Biophys* 2006;445:214–24.
- [50] Hasmann A, Wehrsuetz-Sigl E, Marold A, Wiesbauer H, Schoeftner R, Gewessler U, et al. Analysis of myeloperoxidase activity in wound fluids as a marker of infection. *Ann Clin Biochem* 2013;50:245–54.
- [51] Schiffer D, Tegl G, Vielnascher R, Weber H, Schoeftner R, Wiesbauer H, et al. Fast Blue RR—Siloxane Derivatized Materials Indicate Wound Infection Due to a Deep Blue Color Development. *Materials (Basel)* 2015;8:6633–9.
- [52] Hajsek M, Schiffer D, Harrich D, Koller D, Verient V, Palen J V.D., et al. An electrochemical sensor for fast detection of wound infection based on myeloperoxidase activity. *Sensors Actuators B Chem* 2015;209:265–74.
- [53] Gethin G. Understanding the inflammatory process in wound healing. *Br J Community Nurs* 2012;Suppl:S17–8, S20, S22.
- [54] Ciani I, Schulze H, Corrigan DK, Henihan G, Giraud G, Terry JG, et al. Development

- of immunosensors for direct detection of three wound infection biomarkers at point of care using electrochemical impedance spectroscopy. *Biosens Bioelectron* 2012;31:413–8.
- [55] Van Delden C, Iglewski BH. Cell-to-cell signaling and *Pseudomonas aeruginosa* infections. *Emerg Infect Dis* 1998;4:551–60.
- [56] Sharp D, Gladstone P, Smith RB, Forsythe S, Davis J. Approaching intelligent infection diagnostics: Carbon fibre sensor for electrochemical pyocyanin detection. *Bioelectrochemistry* 2010;77:114–9.
- [57] Lars Schneider, Andreas Korber, Stephan Grabbe JD. Influence of pH on wound-healing: a new perspective for wound-therapy? *Arch Dermatol Res* 2007;298:413–20.
- [58] Puchberger-Enengl D, Krutzler C, Vellekoop MJ, Gusshausstrasse E. Organically modified silicate film pH sensor for continuous wound monitoring. *Sensors* 2011, IEEE, vol. 11679,682, 2011, p. 679–82.
- [59] Schreml S, Meier RJ, Wolfbeis OS, Landthaler M, Szeimies R. 2D luminescence imaging of pH in vivo. *PNAS* 2010.
- [60] Fernandez ML, Upton Z, Edwards H, Finlayson K, Shooter GK. Elevated uric acid correlates with wound severity. *Int Wound J* 2012;9:139–49.
- [61] Phair J, Newton L, McCormac C, Cardosi MF, Leslie R, Davis J. A disposable sensor for point of care wound pH monitoring. *Analyst* 2011;136:4692–5.
- [62] Bailey A, Pisanelli AM, Persaud KC. Development of conducting polymer sensor arrays for wound monitoring. *Sensors Actuators B Chem* 2008;131:5–9.
- [63] Šetkus A, Galdikas A-J, Kancleris Ž-A, Olekas A, Senulienė D, Strazdienė V, et al. Featuring of bacterial contamination of wounds by dynamic response of SnO₂ gas sensor array. *Sensors Actuators B Chem* 2006;115:412–20.
- [64] Bailey ALPS, Pisanelli AM, Persaud KC. Development of conducting polymer sensor arrays for wound monitoring. *Sensors Actuators B Chem* 2008;131:5–9.
- [65] Feng J, Tian F, Yan J, He Q, Shen Y, Pan L. A background elimination method based on wavelet transform in wound infection detection by electronic nose. *Sensors Actuators B Chem* 2011;157:395–400.
- [66] Yan J, Tian F, He Q, Shen Y. Feature Extraction from Sensor Data for Detection of

Wound Pathogen Based on Electronic Nose. *Sensors Mater* 2012;24:57–73.

[67] Feng J, Tian F, Jia P, He Q, Shen Y, Liu T. Feature Selection Using Support Vector Machines and Independent Component Analysis for Wound Infection Detection by Electronic Nose. *Sensors Mater* 2013;25:527–38.

[68] Jia P, Tian F, He Q, Fan S, Liu J, Yang SX. Feature extraction of wound infection data for electronic nose based on a novel weighted KPCA. *Sensors Actuators B Chem* 2014;201:555–66.

3 Chitosan based substrates for wound infection detection based on increased lysozyme activity

Published in: Carbohydrate Polymers 151 (2016) 260–267

Gregor Tegl, Alexandra Rollett, Jasmin Dopplinger, Clemens Gamerith, Georg M. Guebitz

Abstract

There is a strong need of point-of-care diagnostics for early detection of wound infection. In this study, substrates based on functionalized chitosan were developed for visual detection of elevated lysozyme activity, an infection biomarker in wound fluids. For efficient hydrolysis by lysozyme, N-acetyl chitosan with a final degree of acetylation of around 50% was synthesized. N-acetylated chitosan and a chitosan-starch composite were labeled with structurally different dyes resulting in lysozyme-responsive biomaterials. Incubation with lysozyme in buffer and artificial wound fluid lead to a release of colored hydrolysis products already after 2 h incubation. Tests in human wound fluid from infected wounds indicated a clear visual color change after 2.5 h compared to control samples. A higher degree of swelling of the chitosan/starch containing substrate led to faster hydrolysis by lysozyme. This study demonstrates the potential of the lysozyme-responsive materials for diagnosis of wound infection and provides different diagnostic substrates for potential incorporation in point-of-care devices.

3.1. Introduction

Infections are a major health issue. Traumatic, surgical wounds and accompanying healthcare-associated infections are a major cause of retarded wound healing and of the development of chronic wounds. Life-endangering consequences like sepsis illustrate the importance of effective prevention and treatment strategies. The number of patients suffering from wound infections is going to increase significantly due to an aging population and accompanying diseases [1-2].

Wound infection is a consequence of bacterial contamination, often by poly-microbial microflora whose complex networks favor their proliferation and complicate treatment. The variety of microorganisms encompasses aerobic and anaerobic bacteria including *Staphylococcus aureus* and *Pseudomonas aeruginosa* as the most frequently found representatives [3]. Their interaction with the wound environment can be separated into four phases: contamination, colonization, critical colonization and infection. Despite the still unclear role of individual bacterial species on wound infection, this division allows an

assessment whether the wound healing process is impaired or not and if an infection becomes evident. A disruption of the wound healing process is characterized by the interruption of the cell signaling cascade involving growth factors and the extracellular matrix (ECM). Non-healing leads the wound to remain in the inflammation phase and consequently triggers infection. [4,5]

To date, clinicians still diagnose wound infection using classical signs like redness, heat, swelling and pain. In many cases, like chronic wounds, these indicators are not obvious and consequently lead to false negatives impeding the wound treatment. [6,7]. To date, no point-of-care (Poc) testing device is available providing an online monitoring of the wound infection status. Nevertheless, the high demand reflects the need for PoC testing devices to facilitate the choice of an appropriate therapy. [8]

More reliable information on infection can be deduced from biomarkers in wound fluids like enzymes or metabolites [9,3]. Elevated activities of certain enzymes in wound fluids directly depict the immune response and consequently give a direct view into the current wound status. Frequently mentioned representatives of enzyme biomarkers are lysozyme, myeloperoxidase and human neutrophil elastase. [10]. Among these, lysozyme takes a special position since it is exclusively produced by the human immune system and thus only reflects the host immune response [11]. Its antimicrobial activity was known before the 3-dimensional structure was elucidated. Classified as a glycosidase, the native substrate of lysozyme is the peptidoglycan of bacterial cell walls. It cleaves the glycosidic linkage between units of N-acetyl glucosamine and N-acetylmuramic acid and thus promotes lysis of the bacterial cell. However lysozyme was found also hydrolyzing chitosan, a biopolymer consisting of $\beta(1,4)$ -linked units of N-acetyl glucosamine and glucosamine [12]. Due to the different composition compared to peptidoglycan a decreased hydrolysis rate towards chitosan is observed that can be increased via chemical modification of chitosan. Several effects of physico-chemical properties of chitosan have been described to influence its susceptibility towards lysozyme hydrolysis, including the degree of acetylation (DA) and the distribution of acetyl groups along the polymer chain [13].

The objective of this work was the synthesis of substrates for fast and visual lysozyme detection in wound fluids. Chitosan was chemically modified ensuring high susceptibility towards lysozyme degradation. Previously processed chitosan was further modified with copolymers and dyes applying two different strategies that resulted in efficient substrates for the visual detection of elevated lysozyme activities in infected wounds. The chitosan based enzyme substrates circumvent the use of bacterial peptidoglycan potentially causing immune reactions and the substrates, differing in chemistry and composition, can be further evaluated for incorporation into diagnostic devices.

3.2. Material and Methods

3.2.1. Materials

For all experiments, chitosan from shrimp shells was used with a number average molecular weight of 200 kDa (Sigma-Aldrich, Steinheim, Germany) and was purified as described below. All chemicals were from Sigma-Aldrich and used without further purification.

3.2.2. Purification of chitosan

The commercial chitosan was purified to remove residual proteins and glucans prior to all further modifications. Therefore, 20 g chitosan were dispersed in double distilled water (ddH₂O) prior to acidification with acetic acid to obtain a 1% w/v chitosan solution in 0.05% acetic acid. The solution was stirred overnight and thereafter insoluble material was removed via vacuum filtration using a 30 µm filter. Subsequently, the pH was adjusted to 8 for precipitation of the chitosan. The precipitate was washed with ddH₂O and ethanol until the pH reached 7. The resulting pure chitosan was lyophilized for further use.

3.2.3. Preparation and characterization of N-acetylated chitosan

The DA of the purified chitosan was adjusted by selective N-acetylation ensuring high susceptibility towards lysozyme. The DA was analyzed by ¹H NMR spectroscopy and FTIR.

3.2.4. N-acetylation of chitosan

Purified chitosan was dissolved in 10% acetic acid to obtain a 1% w/v chitosan solution which was then diluted 1:1 with ethanol and stirred for several minutes. Afterwards, 1 mole equivalent of acetic anhydride was added (calculated on the glucosamine units in the polymer) and the mixture was further stirred for 1 h. The pH was adjusted to 8, which led to gel formation which was lyophilized. After subsequent washing with ddH₂O to remove salts, the N-acetylated chitosan was lyophilized again.

3.2.5. Determination of the degree of acetylation (DA)

NMR

Nuclear magnetic resonance ¹H and ¹³C measurements were performed on a Bruker Avance II 400 spectrometer (resonance frequencies 400.13 MHz for ¹H and 100.63 MHz for

13C) equipped with a 5 mm observe broadband probe head with z-gradients. D₂O with a drop of 37% DCI was used as NMR solvent if not otherwise specified. The DA was calculated using the integrals of the proton peaks H2 of the deacetylated monomer and the three proton peaks of the acetyl groups:

$$DA (\%) = \left(100 - \left(\frac{H2D}{H2D + \frac{HAc}{3}} \right) \right) * 100$$

where H2D is the integral of H2 proton and HAc is the summation of integrals of the N-acetyl group.

FTIR

The degree of acetylation was further confirmed by Fourier transform infrared spectroscopy in attenuated reflection mode (ATR – FTIR) using a Spectrum 100 Perkin Elmer FT-IR spectrometer (Massachusetts, USA). The amide I band at 1640 cm⁻¹ and the amide II band at 1560 cm⁻¹ were considered and compared with native chitosan. Spectra were normalized considering the peak at 1025 cm⁻¹ (C-O stretching vibration) and spectra have been stacked afterwards for better illustration.

3.2.6. Hydrolysis of N-acetylated chitosan by lysozyme

N-acetylated chitosan (25 mg) was dissolved in 0.1 M sodium acetate buffer (pH 5) or 0.1 M sodium phosphate buffer (pH 6.2) yielding 5 mg/mL chitosan solution. Afterwards lysozyme dissolved in the respective buffer was added resulting in a total concentration of 2 mg/mL (70 000 U/mg) and the samples were incubated at 37 °C and 150 rpm. The progress of hydrolysis was monitored using the DNS method detecting the reducing sugar content in sample withdrawals. Reducing sugars are generated during the hydrolysis of chitosan by lysozyme.

Determination of the reducing sugar content

The amount of reducing sugars present was assessed using the 3,5-dinitrosalicylic acid (DNS) method [14]. A standard curve was plotted determining the absorbance of different concentrations of N-acetyl glucosamine at 540 nm. The relative sugar content is given as mg/mL glucosamine equivalents.

Determination of the degree of polymerization by SEC

The number average molecular mass (M_n) was determined by analytical size exclusion chromatography composed of an Agilent 1100 Series Chromatography system equipped with an Agilent 1200 G1362A refractive index detector. A TSKgel G5000PW_{XL} column was used

for analysis (Tosoh Bioscience, Montgomeryville, PA, USA). Calibration was performed using a pullulan standard set (Fluka, Buchs, Switzerland). As mobile phase an acetate buffer was used consisting of 0.15 M acetic acid, 0.1 M sodium acetate, 0.4 mM sodium azide in ddH₂O, previously filtered through an Express™Plus filter with 0.22 µm pore size (47 mm diameter, Millipore).

3.2.7. Preparation of chitosan substrates

Two different substrates based on N-acetyl chitosan were developed that differ in the methods for dye incorporation. Substrate 1 is based on the covalent conjugation of Reactive Black 5 whereas substrate 2 includes non-covalent incorporation of Evans Blue triggered by a co-precipitation process with starch.

3.2.8. Enzyme activity assays

Lysozyme activity was determined by a method of Shugar [15] based on the lysis of *Micrococcus lysodeikticus* cells, suspended in potassium 66 mM phosphate buffer (pH 6.2) to obtain a 0.01% (w/v) solution. 290 µL of bacteria solution were mixed with 10 µL of a lysozyme solution of varying concentrations and an increase in transparency was recorded over 15 min at 450 nm and 25°C. One unit of lysozyme was defined as the amount of enzyme that decreases the absorbance at 450 nm by 0.001 per minute at pH 7.0 and 25°C. Chitosanase activity was determined using the method of Osswald et al [16]. One unit of chitosanase was defined as 1 µmol of glucosamine being released from chitosan per minute at pH 5.0 and 37°C.

Substrate 1: Conjugation of Reactive Black 5 to N-acetylated chitosan

N-acetylated chitosan (100 mg) was suspended in distilled water before a solution of Reactive Black 5 (0.05%-0.4% w/w) was added (0.5 mL). A solution consisting of 2.5% (w/v) Na₂SO₄ and 1% (w/v) Na₂CO₃ in ddH₂O was added and the mixture was incubated at 25°C for 10 min. After a subsequent incubation step at 65°C, the solid was isolated by centrifugation (7800 rpm, 5 min). The precipitate was washed with distilled water until the washing solution remained colorless and subsequently lyophilized. In the following this substrate is referred to as [CTS 200_RB5].

Substrate 2: Preparation of a stained chitosan-starch precipitate

A 1% chitosan solution in 1% acetic acid was mixed with a 5% starch solution in ddH₂O in a ratio of 40:60 (w/w, chitosan: starch). Staining and concomitantly co-precipitation was induced by the addition of Evans Blue dissolved in 10% sodium hydroxide (0.1 M). The

morphology of the chitosan/starch co-precipitate was observed using a tabletop scanning electron microscope (SEM) (Hitachi, Model: TM3030). Therefore, a particle of the freeze dried sample was taped onto the SEM stub and the pictures were acquired under vacuum at an acceleration voltage of 15 kV without prior sample preparation. In the following this substrate is referred to as [CTS 200 ST_EB].

3.2.9. Determination of the swelling properties

The swelling properties of the prepared substrates were determined by immersing a known amount in 66 mM potassium phosphate buffer (pH 6.2) for a definite time period. The weight of the soaked particle was determined after carefully drying its surface with a filter paper and the degree of swelling was calculated using following formula:

$$S = \frac{W_t - W_0}{W_0}$$

where W_0 is the weight of the dry samples applied and W_t is the weight of the swollen sample after a defined time.

3.2.10. Lysozyme degradation of chitosan-based substrates

The prepared substrates were tested using buffered lysozyme solutions and with artificial wound fluid containing lysozyme. Selected substrates were tested using human wound fluid of infected wounds. All experiments were performed in triplicate.

3.2.11. Dye release of chitosan based substrates upon lysozyme degradation

The synthesized substrates were investigated in different media: potassium phosphate buffer (66 mM, pH 6.2) as well as artificial wound fluid (Table 1) containing 5000 U of lysozyme from hen egg white, and human wound fluid from infected wounds. Two milligrams of the lysozyme substrates were suspended in the respective test medium and incubated at 35°C. For time measurements, the sample was briefly centrifuged, then 200 μ L of the supernatant was transferred to a 96 well plate and photometrically analyzed at the absorption maximum of the respective dye. After the analysis, the withdrawn sample was returned in the reaction vial and further incubated.

Artificial wound fluid was used in the following composition: 2% human serum albumin, 0,36% NaCl, 0,05% NaHCO₃, 0,02% sodium citrate, 0,1% sodium lactate, 0,1% glucose, 0,01% CaCl₂*2H₂O, 0,02% MgCl₂, 0,01% urea.

Human wound fluids from infected wounds were obtained and characterized as described in the work of Hasmann et al [17]. Briefly, the substrates were tested using a wound fluid

sample, which was described being clinically infected by the attending doctors. Artificial wound fluid was used as blank medium.

3.3. Results and Discussion

The potential of lysozyme as biomarker for wound infection has recently been demonstrated [17]. However, detection based on the hydrolysis of peptidoglycan (PG) from bacterial cells limits the diagnosis to non-patient contacting systems since contacting PG with the wound may cause immune responses towards the diagnostic material. Lysozyme also exhibits hydrolytic activity towards chitosan. This polysaccharide is already used for medical applications and is thus a good alternative for the detection of lysozyme. However, lysozyme activity towards chitosan with a high DA is low, and the same holds true for highly N-deacetylated chitosan. Consequently, the production of N-acetyl chitosan exhibiting an appropriate DA can enhance the susceptibility towards lysozyme hydrolysis.

3.3.1. N-acetylation of chitosan

N-acetylation of chitosan was carried out using acetic anhydride as acetylating agent. The DA of chitosan was determined by ^1H NMR spectroscopy considering the H2 proton instead of the commonly used H1, which enables the DA determination by NMR at room temperature, yet gives the same results. A doubtless interpretation of the H1 signal would only be possible shifting the overlaying water signal by raising the temperature, which takes time and analytical effort [18]. The resulting DAs were further confirmed by ATR-FTIR, mainly based on the amide carbonyl stretching band at 1640 cm^{-1} and the amide N-H stretching band at 1540 cm^{-1} (Fig. 1) [19]. These characteristic IR bands showed an increased intensity in several N-acetyl chitosan formulations compared to native chitosan.

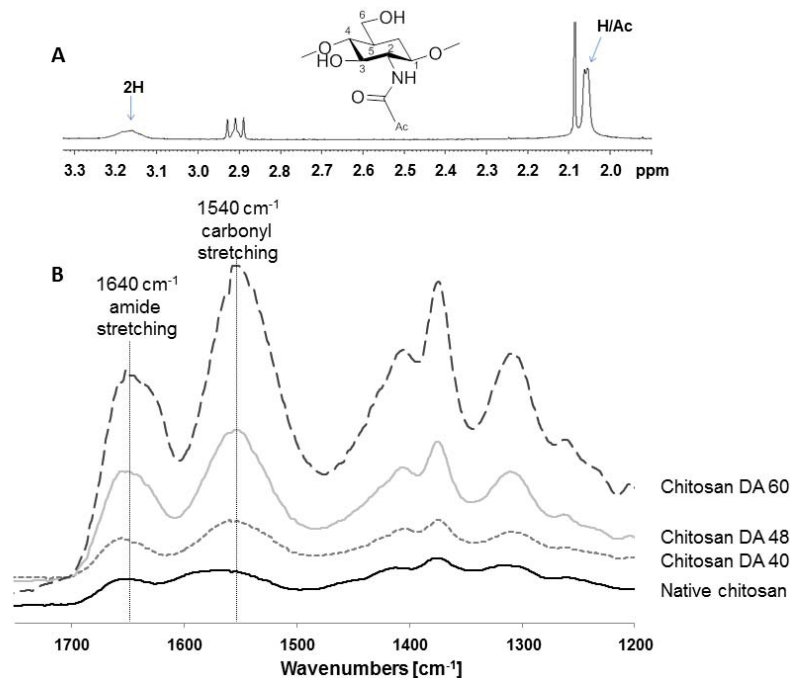


Fig. 1. (A) ¹H NMR spectrum of N-acetylated chitosan indicating a DA of 48% (A). The DA was determined considering the proton signal of H2 and the proton signals of the acetyl group. **(B)** ATR-FTIR spectrum of N-acetyl chitosan with varying DA as measured by using NMR; the bands at 1540 cm⁻¹ and 1640 cm⁻¹ refer to amide stretching and carbonyl stretching and reveal the difference in the DA applying different amounts of acetic anhydride.

Several studies on the hydrolysis efficiency of lysozyme towards chitosan describe partially N-acetylated chitosan to be most susceptible [20]. Consequently, in preliminary studies we have assessed the effect of DA in the range of 40% to 60% on lysozyme hydrolysis at two different pH values. At pH 5.0 and pH 6.2, N-acetylated chitosan was provided in solubilized and solid state, respectively, Hydrolysis rates were found to be about 20% higher at pH 5 for all N-acetyl chitosans (Fig. 2A and 2B). Slightly faster hydrolysis at pH 5 was most likely due to complete dissolution of chitosan at this pH in contrast to pH 6.2, where a heterogeneous reaction system was obtained. However, chitosan with a DA of 48% appeared to be most susceptible to lysozyme hydrolysis and was thus used for further studies. The random distribution of acetyl groups along the polymer chain is reported to provide a substantial amount of lysozyme-binding sites consisting of hexameric sequences with a distinct acetylation pattern as described by Stokke et al. [21].

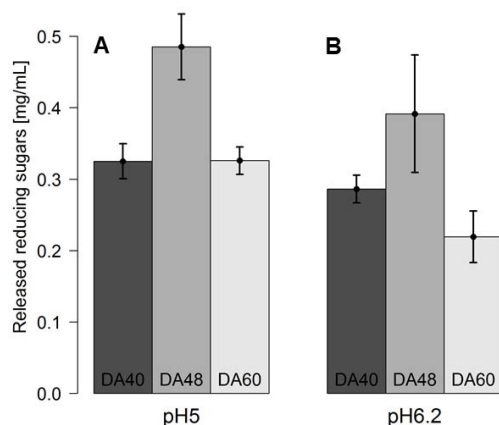


Fig. 2. Hydrolysis of N-acetyl chitosan with different DAs by lysozyme at pH 5 (**A**) and at pH 6.2 (**B**) measured based on the amount of reducing sugars released. Slightly higher degradation rates were observed at pH 5 where N-acetyl chitosan was completely soluble; for both pH values N-acetyl chitosan with a DA of 48% showed highest susceptibility towards lysozyme hydrolysis.

3.3.2. Functionalization of N-acetyl chitosan

N-acetyl chitosan with a DA of around 50% turned out to be most susceptible towards lysozyme hydrolysis and was thus used for further modification. To allow visible detection of lysozyme activity, chitosan was labeled with specific dyes resulting in colored enzyme substrates. Two strategies were followed covering a covalent attachment of a dye on N-acetyl chitosan as well as a non-covalent incorporation of a dye into a co-polymer system. Both processes elude the use of cross-linking chemicals and the experimental design kept the reactions straightforward to facilitate later implementation in industrial production processes.

3.3.3. Reactive Black 5-functionalised N-acetyl chitosan [CTS 200 RB5]

Reactive dyes are an alternative to dye attachment with cross-linkers. Among the large family of reactive dyes, vinylsulfone dyes represent a reactive system forming a vinyl intermediate under basic conditions that consequently reacts with a given nucleophile. Within this work, the azo reactive dye Reactive Black 5 (RB5) was used.

N-acetyl chitosan with a DA of 48% was stained with RB5 in a heterogeneous reaction using varying concentrations of RB5. A stepwise change in signal intensity was observed proportional to the concentration of dye applied, which confirmed the reliability of this staining method (Fig. 4A). No leaching was observed in the absence of lysozyme (Fig. 4) When lysozyme hydrolysis of the CTS 200_RB5 substrate was carried out in the matrix of artificial

wound fluids (AWF), the signal was roughly reduced by half (Fig 4.). The AWF applied within this work consisted of several compounds known to interact with enzymes and/or respective substrates like albumin, urea, metal ions and various salts. Moreover, it is likely that confounding factors present in AWF interact with the chitosan-based substrate owing to its good chelating properties towards metal ions. However, the obtained signals were clearly visible by the naked eye after only 2 h. This makes this substrate an attractive candidate for infection detection.

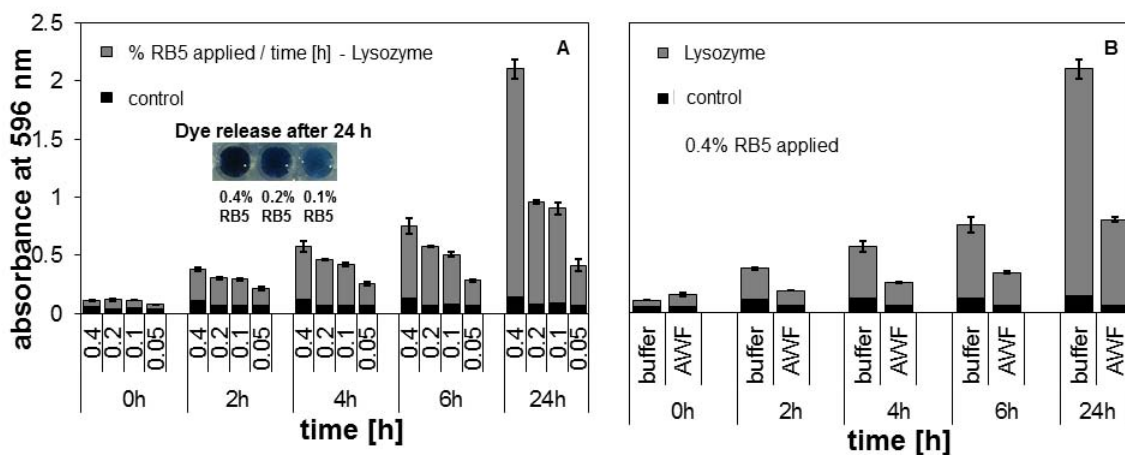


Fig. 4. Release of colored oligomers from CTS 200_RB5 upon incubation with lysozyme. **(A)** Incubation of CTS 200_RB5 with varying content of RB5 **(B)** Comparison of absorbance values of CTS 200_RB5 (0.4% w/w RB5) upon incubation with lysozyme in buffer medium and artificial wound fluid (AWF).

3.3.4. Evans Blue-functionalized N-acetyl chitosan/starch substrate [CTS 200 ST EB]

The covalent attachment of dyes onto enzyme-responsive materials has several advantages like a decreased risk of leaching. However, these modifications can also alter the susceptibility of the substrate to enzymatic hydrolysis. Here, a method for a non-covalent incorporation of the azo dye Evans Blue into a mixture of N-acetyl chitosan and starch was developed. Chitosan and starch are frequently used for the preparation of films and particles with the aid of co-agents [22]. Co-precipitation of these polysaccharides forms stable networks that are suitable for the trapping of charged molecules like most dyes. At the precipitation process starch is responsible for the formation of a highly porous network. [23]. The precipitation of N-acetyl chitosan in the presence of solubilized starch and Evans Blue led to the formation of a porous mesh. With other dyes like RB5 no efficient incorporation of the respective dye was observed. Presumably the anionic sulfate groups of Evans Blue lead to strong electrostatic interactions with chitosan and consequently promote effective dye

incorporation. Best results were obtained with a 40:60 mixture of a 1% N-acetyl chitosan solution (DA 48) and a starch solution. The precipitation of chitosan dissolved in acetic acid was triggered by the addition of sodium hydroxide. The resulting deep blue colored precipitate was investigated by SEM indicating a sponge-like structure of the substrate in its freeze dried state (Fig 5B).

A strong color formation was observed after only 2 h of lysozyme hydrolysis with increasing signal intensity until 6 h (Fig. 5A). Interestingly, only very low leaching of the dye was observed in the absence of the enzyme when compared to the substrate with covalently bound RB5. The low leaching is most likely due to the stable network formed by chitosan and starch efficiently trapping the dye in its micro-cavities. After 6 h of incubation nearly all substrate was hydrolyzed. The fast hydrolysis of the chitosan / starch substrate by lysozyme when compared to the other lysozyme responsive materials could be explained by the high degree of swelling of 71.8%, which is due to the porous structure of the substrate as well as the presence of starch.

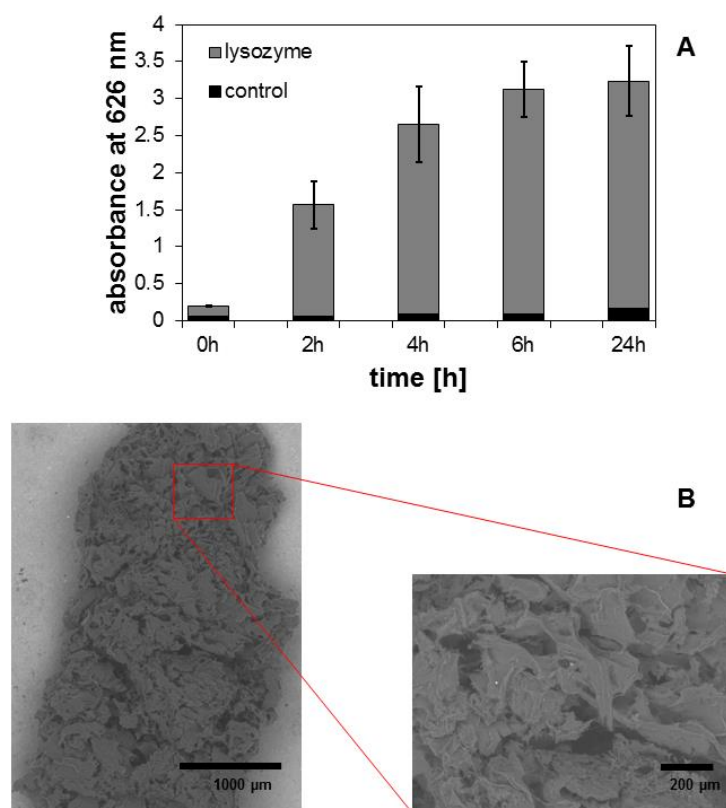


Fig. 5. (A) Color formation from CTS 200 ST_EB upon incubation with lysozyme. High signal intensity was observed after only 2 h and the substrate applied was completely digested after 6 h incubation. No significant leaching was detected visually even after 24 h incubation time. **(B)** The SEM picture shows the porous structure of the N-acetyl chitosan/starch/Evans Blue lysozyme substrate at 200-fold magnification.

The substrate based on the non-covalent incorporation of a dye constitutes an efficient extension to the lysozyme substrates with covalently attached RB5 for the detection of wound infection developed in this study. The presented substrates differ in several parameters including their composition and way the respective dye is attached, as illustrated in figure 6. The derivatization of the N-acetyl chitosan backbone has a strong influence on the susceptibility towards lysozyme. The presented results suggest that a conjugation of the primary hydroxide even by a complex anionic dye like RB5 apparently does not hamper the enzyme-substrate interaction.

Another factor playing a major role influencing the hydrolysis kinetics is the degree of swelling, which depends on the composition of the respective substrate. Expectedly, a higher degree of swelling lead to faster hydrolysis and consequently faster color formation most likely due to an increased accessibility of substrate for lysozyme. Table 1 indicates a correlation of swelling properties with the percent of dye that was released from the substrate.

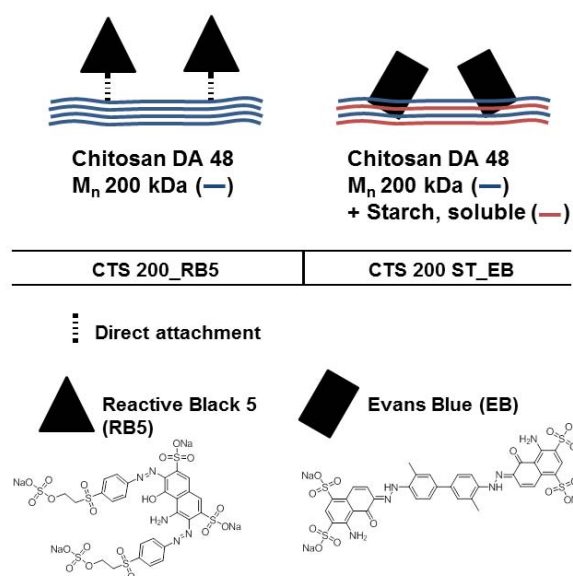


Fig. 6. A scheme of the lysozyme responsive materials based on chitosan including the applied dye incorporation methods and the compositions of the substrates.

Table 1

Influence of the degree of swelling of different stained N-acetyl chitosan materials on color formation after 24 h due to lysozyme hydrolysis.

Polysaccharide	Dye	Molecular weight of	Degree of swelling	Lysozyme response after 24 h (% dye released from
----------------	-----	---------------------	--------------------	---

		chitosan (kDa)	(%)	substrate)
N-acetyl chitosan DA 48	Reactive Black 5	200	41.1	38.0 ± 1.67
N-acetyl chitosan DA 48; Soluble starch	Evans Blue	200	71.8	47.5 ± 7.83

3.3.5. Substrate testing in human wound fluid from infected wounds

In a next step, the potential of lysozyme responsive materials was assessed in human wound fluid. A major factor impeding substrate-enzyme interactions is known to be human serum albumin (HSA), which interacts with a variety of natural compounds and thus can prevent enzyme docking [24]. Considering human wound fluid, especially from infected wounds, its complexity highly exceeds that of AWF due to the presence of a variety of active biomolecules that are excreted into the wound fluid by the immune system upon infection. Proving the selectivity of the prepared substrates towards lysozyme under realistic conditions, the presented lysozyme substrates were tested in human wound fluid from infected wounds. All samples were analyzed at an absorbance of 597 nm enabling the parallel assessment of all three different materials. The absorbance spectra of the used dyes do not show a sharp absorbance maximum, which enables the parallel measurement at 597 nm without obtaining significant differences in the absorbance intensities. Figure 8 shows color formation from the two prepared lysozyme substrates. Differences in the absorbance intensities could be observed compared to the tests in buffer. The CTS 200 ST_EB (Fig. 8C) showed the highest signal intensity with no leaching of the blank and thus confirmed its suitability for the detection of lysozyme activities. The fast response with high signal intensity already after 1 h incubation time could still be observed upon incubation with human wound fluid.

The release of soluble and stained oligomers from the CTS 200_RB5 substrate resulted in only 20% of absorbance compared to CTS 200 ST_EB. Again no leaching was observed in the control samples of the RB5 substrate, which constitutes an important prerequisite for the application in a PoC testing device.

Although the comparison of the signal intensities favors CTS 200 ST_EB being the best candidate, its incorporation in a PoC testing device could be more difficult due to the non-covalent attachment of the dye. The covalent modification with RB5 enables further

processing of the substrate, like printing on carriers that is required for an effective incorporation into diagnostics. However, the fast reaction kinetics of the CTS 200 ST_EB substrate enable its application in *ex-vivo* rapid test systems that do not require extensive additional processing. Consequently, high signal intensities are not the only criterion for selection and strengthens the impact of the physicochemical properties on future applications.

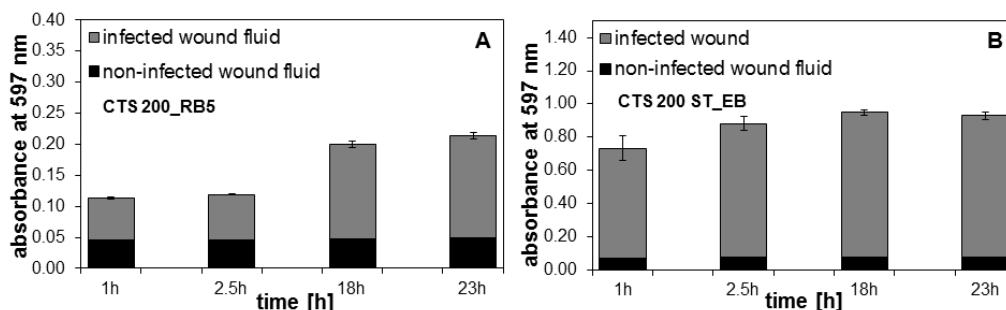


Fig. 7. Dye release from the prepared substrates in the presence of human wound fluid from infected wounds. **(A)** Dye release of N-acetyl chitosan stained with RB5 indicating a continuous dye release. **(B)** Dye release upon incubation of the N-acetyl chitosan/starch precipitate stained with Evans Blue, indicating a high dye release after short time.

3.4. Conclusion

The potential of chitosan for the preparation of lysozyme-responsive materials was demonstrated for the first time. Chitosan based materials circumvent the use of bacterial-derived materials such as peptidoglycan which may cause immune reactions if in direct contact with wounds. Different strategies were applied for the formation of efficient substrates for lysozyme mediated infection detection, all based on previously produced N-acetyl chitosan. As a result, two lysozyme-responsive chitosan derivatives were obtained that possess different physicochemical properties, including swelling properties and composition of the substrates, due to the co-agents used in their preparation. Tests in human wound fluid from infected wounds revealed their suitability for the use in diagnostics. Not least their properties, whereby insolubility is the most important one, will facilitate an effective incorporation into respective testing systems.

Acknowledgements

This study was performed within the European Project Infact. Financial support from the European FP7-programme under grant agreement no. 604278 and the Austrian Centre of Industrial Biotechnology (ACIB) is gratefully acknowledged. All authors declare no potential conflicts of interest.

3.5. References

- [1] F. Gottrup, A. Melling DAH. An overview of surgical site infections: aetiology, incidence and risk factors 2005.
<http://www.worldwidewounds.com/2005/september/Gottrup/Surgical-Site-Infections-Overview.html> (accessed May 26, 2015).
- [2] Sen CK, Gordillo GM, Roy S, Kirsner R, Lambert L, Hunt TK, et al. Human Skin Wounds: A Major and Snowballing Threat to Public Health and the Economy. *Wound Repair Regen* 2009;17:763–71. doi:10.1111/j.1524-475X.2009.00543.x.Human.
- [3] Tegl G, Schiffer D, Sigl E, Heinzle A, Guebitz GM. Biomarkers for infection: enzymes, microbes, and metabolites. *Appl Microbiol Biotechnol* 2015;99:4595–614. doi:10.1007/s00253-015-6637-7.
- [4] Howell-Jones RS, Wilson MJ, Hill KE, Howard a J, Price PE, Thomas DW. A review of the microbiology, antibiotic usage and resistance in chronic skin wounds. *J Antimicrob Chemother* 2005;55:143–9. doi:10.1093/jac/dkh513.
- [5] Schultz GS, Wysocki A. Interactions between extracellular matrix and growth factors in wound healing. *Wound Repair Regen* 2009;17:153–62. doi:10.1111/j.1524-475X.2009.00466.x.
- [6] Gardner SE, Frantz R a, Doebbeling BN. The validity of the clinical signs and symptoms used to identify localized chronic wound infection. *Wound Repair Regen* 2001;9:178–86. doi:10.1046/j.1524-475x.2001.00178.x.
- [7] Gardner, S, S.L. Hillis RAF. Clinical Signs of Infection in Diabetic Foot Ulcers with High Microbial Load. *Biol Res Nurs* 2009;11:119–28. doi:10.1177/1099800408326169.Clinical.
- [8] Cutting KF, White RJ. Criteria for identifying wound infection--revisited. *Ostomy Wound Manage* 2005;51:28–34.
- [9] Yager DR, Kulina RA, Gilman LA. Wound fluids: a window into the wound environment? *Int J Low Extrem Wounds* 2007;6:262–72. doi:10.1177/1534734607307035.
- [10] World Union of Wound Healing Societies (WUWHS). Principles of best practice: Diagnostics and wounds. A consensus document. 2008.
- [11] Torsteinsdóttir I, Håkansson L, Hällgren R, Gudbjörnsson B, Arvidson NG, Venge P. Serum lysozyme: a potential marker of monocyte/macrophage activity in rheumatoid arthritis. *Rheumatology (Oxford)* 1999;38:1249–54. doi:10.1093/rheumatology/38.12.1249.
- [12] Stokke BT, Varum KM, Holme HK, Hjerde RJN, Smidsrod O. Sequence specificities for lysozyme depolymerization of partially N-acetylated chitosans. *Can J Chem Can*

- Chim 1995;73:1972–81. doi:10.1139/v95-244.
- [13] Han T, Nwe N, Furuike T, Tokura S, Tamura H. Methods of N -acetylated chitosan scaffolds and its in vitro biodegradation by lysozyme. *J Biomed Sci Eng* 2012;5:15–23.
- [14] Miller GL. Use of Dinitrosalicylic Acid Reagent for Determination of Reducing Sugar. *Anal Biochem* 1959;31:426–8.
- [15] Shugar D. The measurement of lysozyme activity and the ultra-violet inactivation of lysozyme. *Biochim Biophys Acta* 1952;8:302–9. doi:10.1016/0006-3002(52)90045-0.
- [16] Osswald WF, McDonald RE, Niedz RP, Shapiro JP, Mayer RT. Quantitative fluorometric analysis of plant and microbial chitosanases. *Anal Biochem* 1992;204:40–6. doi:10.1016/0003-2697(92)90136-U.
- [17] Hasmann A, Wehrsuetz-Sigl E, Kanzler G, Gewessler U, Hulla E, Schneider KP, et al. Novel peptidoglycan-based diagnostic devices for detection of wound infection. *Diagn Microbiol Infect Dis* 2011;71:12–23. doi:10.1016/j.diagmicrobio.2010.09.009.
- [18] Lavertu M, Xia Z, Serreqi a. N, Berrada M, Rodrigues a., Wang D, et al. A validated ¹H NMR method for the determination of the degree of deacetylation of chitosan. *J Pharm Biomed Anal* 2003;32:1149–58. doi:10.1016/S0731-7085(03)00155-9.
- [19] Duarte ML, Ferreira MC, Mar MR. An optimised method to determine the degree of acetylation of chitin and chitosan by FTIR spectroscopy 2002;31.
- [20] Zhang Y, Wang Z, Zhang J, Chen C, Wu Q, Zhang L, et al. Quantitative determination of chitinolytic activity of lysozyme using half-deacetylated chitosan as a substrate. *Carbohydr Polym* 2011;85:554–9. doi:10.1016/j.carbpol.2011.03.009.
- [21] Stokke BT, Varum KM, Holme HK, Hjerde RJN, Smidsrsd O. Sequence specificities for lysozyme depolymerization of partially N-acetylated chitosans. *Can J Chem* 1995;1981:1972–81.
- [22] Tuhin MO, Rahman N, Haque ME, Khan R a., Dafader NC, Islam R, et al. Modification of mechanical and thermal property of chitosan–starch blend films. *Radiat Phys Chem* 2012;81:1659–68. doi:10.1016/j.radphyschem.2012.04.015.
- [23] Hamer PW, McGeachie JM, Davies MJ, Grounds MD. Evans Blue Dye as an in vivo marker of myofibre damage: optimising parameters for detecting initial myofibre membrane permeability. *J Anat* 2002;200:69–79.
- [24] Fasano M, Curry S, Terreno E, Galliano M, Fanali G, Narciso P, et al. The extraordinary ligand binding properties of human serum albumin. *IUBMB Life* 2005;57:787–96.

4 Myeloperoxidase responsive materials for infection detection based on immobilized aminomethoxyphenol

Published in: *Biotechnology and Bioengineering* (2016), 9999, 1-8

Doris Schiffer, Gregor Tegl, Robert Vielnascher, Hansjoerg Weber, Alexandra Herrero-Rollett, Eva Sigl, Andrea Heinzle, Georg M. Guebitz

Abstract

There is a strong need for simple and fast diagnostic tools for the detection of wound infection. Immune system-derived enzymes like myeloperoxidase are efficient biomarkers for wound infection that emerge in the early stage infection process. In this study, 5-amino-2-methoxyphenol was functionalized with alkoxy silane to allow visual detection of MPO on carrier materials e.g. in test strips. Indeed, MPO activity was visually detectable in short time in wound background. Oxidation of the substrate was followed spectrophotometrically and proved via HPLC. LC-ESI TOF and NMR analyses unveiled the reaction mechanism and a dimeric reaction product responsible for the visualization of MPO activity. The substrate specificity and sensitivity towards MPO detection was proved and tests with infected wound fluids were successfully performed. The study demonstrates the suitability of the novel MPO substrate for the detection of wound infection and the covalent immobilization on diagnostic carrier materials.

4.1. Introduction

A timely detection of wound infection is crucial for the choice of appropriate treatment to prevent the development of chronic wounds that constitute a rising health issue amongst an ageing population. To date, no reliable and yet simple point-of-care testing device is available to detect emerging wound infection at an early stage. So far implemented standard procedures rely on clinical signs like redness, swelling and pain indicating an already advanced stage of infection that requires extensive antibiotic wound treatment. Detailed investigations of the wound biology unveiled various constituents like microbes, metabolites and enzymes that act as biomarkers for infection detection [1]. Especially enzymes that are excreted by the host immune response at an early stage of bacterial contamination show a great potential as biomarkers [2]. Myeloperoxidase (MPO) is a well-known enzyme taking part in various biological processes in mammals including the detoxification of bacterial toxins [3]. Recently, its role in wound infection processes was described, highly elevated MPO activities identified in infected wounds compared to non-infected wounds revealed its

suitability as infection biomarker [4]. Current strategies for the visual detection of wound infection based on MPO rely on a color change upon MPO oxidation of phenolic enzyme substrates. Enzymatic phenol oxidation is mediated by the reactive oxidant hypochlorous acid (HOCl), which is produced by MPO upon conversion of hydrogen peroxide (H₂O₂). Recently new methods for detection of elevated MPO activity in wound fluids were developed that can visually detect an emerging infection [4–6]. Applying substituted phenols like Fast Blue RR, fast reaction kinetics were obtained enabling rapid detection of wound infections [5]. The efficient immobilization of phenols renders them applicable for incorporation into diagnostic devices to detect wound infection. In particular, siloxane-mediated functionalization recently gained attention for many applications due to the variety of available carrier systems [7]. Despite the frequent application of phenols for MPO detection, little information is available regarding the reaction mechanism and the reaction products resulting from enzymatic conversion.

In this study, the 5-amino-2-methoxyphenol was functionalized for immobilization and successfully tested for its ability to detect wound infection in course of elevated MPO activities in wound fluids. LC ESI-TOF measurements combined with online NMR measurements elucidated the structure of the main reaction products to get detailed insight into the reaction mechanism of MPO-mediated phenol oxidation.

4.2. Material and Methods

4.2.1. Functionalization of 5-Amino-2-Methoxyphenol

5-amino-2-methoxyphenol was coupled to alkoxysilanes for further immobilization according to the procedure of Hasmann et al [4]. The structure of the reaction product was analyzed by ¹H and ¹³C nuclear magnetic resonance (NMR) using a Varian (Agilent) INOVA 500-MHz NMR spectrometer (Agilent Technologies, Santa Clara, California, USA). Proton spectra were acquired at 300 MHz and carbon spectra at 75 MHz. DMSO-d₆ was used as solvent.

¹H-NMR (300 MHz, Bruker Avance III, DMSO-d₆): δ 8.05 ppm (bs, 1H, NH), 6.85 ppm (s, 1H, H-6), 6.75 ppm (d, 1H, H-3), 6.61 ppm (s, 1H, H-4), 6.06 ppm (bt, 1H, NH), 3.65 ppm (q, 6H, H-12), 3.61 ppm (s, 3H, H-1), 2.98 ppm (m, 2H, H-9), 1.42 ppm (m, 2H, H-10), 1.12 ppm (t, 9H, H-13), 0.52 ppm (t, 2H, H-11).

¹³C-NMR (125 MHz, Agilent Inova, DMSO-d₆): δ 156.06 ppm (C-8), 146.83 ppm (C-7), 142.99 ppm (C-2), 134.45 ppm (C-5), 113.36 ppm (C-4), 109.41 ppm (C-3), 107.41 ppm (C-6), 58.25 ppm (C-12), 56.56 ppm (C-1), 40.04 ppm (C-9), 23.48 ppm (C-10), 18.58 ppm (C-13), 7.60 ppm (C-11).

4.2.2. Immobilization of Functionalized Aminomethoxyphenol

The alkoxy silane-functionalized aminomethoxyphenol was immobilized on silica thin layer chromatography (TLC) plates (Merck, Darmstadt, Germany). Briefly, 1x1 cm squares were cut and spotted with 50 mM derivatized aminomethoxyphenol dissolved in EtOH. Subsequent covalent immobilization was performed at 105°C for 24 h.

4.2.3. Visual Detection of MPO Activity Using Immobilized Aminomethoxyphenol

The conversion of immobilized aminomethoxyphenol to its colored reaction product was performed using purified myeloperoxidase (MPO, planta, Austria) in presence of different concentrations of hemoglobin (Sigma, St. Louis, MO, USA). MPO was diluted in potassium phosphate buffer (100 mM; pH 7) to final concentrations of 20 U/mL; 10 U/mL; 5 U/mL. Hemoglobin was used in end concentrations of 0.1 mM, 0.05 mM, 0.01 mM, 0.005 mM and 0.001 mM. Dilutions from 1:100 to 1:1000 were used. Sodium chloride was used in end concentrations of 50 mM. The respective solutions (10 µL) were mixed with a 39.2 mM H₂O₂ solution (10 µL) and the mixture was pipetted on the silica plates with the immobilized substrate. Solutions lacking H₂O₂ were used as blanks. The plates were incubated at room temperature. Color changes on the functionalized TLC plates after incubation with MPO were measured with a ColorLite sph 850 spectrophotometer (ColorLite GmbH, Katlenburg-Lindau, Germany) according to the CIELab concept. As a reference, a wetted silica plate with immobilized substrate, but without enzyme was used. The sensitivity of the detection system was determined using the previously described procedure and applying different MPO activities that ranged 0.5 U/mL to 20 U/mL. Substrate specificity for MPO-mediated infection detection was proved by applying the infection biomarker lysozyme (5000 U/mL) and elastase (20 U/mL) on immobilized aminomethoxyphenol. Possible cross reactions of the substrate with other peroxidases were investigated using horse radish peroxidase (HRP) in different activities ranging from 5 to 10 U/mL.

Tests using artificial wound fluid spiked with different MPO activities were conducted and analyzed the same way. The composition of the artificial wound fluid was as stated in Table I. The suitability of this system for detecting wound infection was tested on human wound fluids from infected wounds that were obtained and characterized as described in the work of Hasmann et al. (2011). The experimental setup was the same as previously described and used a wound fluid sample from a wound, which was described as being clinically infected by the attending doctors. A control reaction was performed with a wound fluid sample from a wound described as clinically non-infected.

Table I: Composition of artificial wound fluid.

Component	Concentration
Human Serum Albumin	2 %
NaCl	0,36 %
NaHCO ₃	0,05 %
Sodium citrate	0,02 %
Sodium lactate	0,1 %
Glucose	0,1 %
Ca (Calciumchloride dihydrate)	0,01 %
Mg (Magnesiumchloride)	0,02 %
Urea	0,01 %

4.2.4. Enzymatic Conversion of Functionalized Aminomethoxyphenol Analyzed by HPLC and LC ESI-TOF

HPLC was performed using a LC coupled with DAD monitoring at 254 nm (Agilent G4212B, Palo Alto, CA, USA). For LC ESI-TOF experiments, the LC system was coupled to a Dual ESI G6230B TOF (Agilent, Palo Alto, CA, USA). For the electrospray ionization (operating in positive ion mode), a nebulizer was used, the dry gas flow was set to 8 L/min and a pressure of 40 psi at 250°C was chosen. The fragmenter voltage was set to 200 V, the skimmer at 65 V, the octopole to a voltage of 750 V and the reference masses were 121.0509 m/z and 922.0098 m/z. Ions from 50 m/z to 1000 m/z were acquired with the Agilent MassHunterWorkstation (Version B06.01, Palo Alto, CA, USA). A statistical calculation in accordance to German industrial standard 32645 for the detection limit, detectability limit, and limit of determination was performed. Significance was tested with p-values less than 0.05.

Functionalized aminomethoxyphenol was used for both HPLC and LC-ESI TOF. The working solutions (1 ml) contained 10 mM of the derivatized Aminomethoxyphenol, 1.5 U/ml MPO, 39.2 mM H₂O₂, 50 mM NaCl in 100 mM potassium phosphate buffer (pH 7) or sodium

acetate buffer (pH 4). As negative controls, all samples were also prepared without MPO. The samples were incubated for 0, 15, 30, 45, 60, 90, 180, 360 minutes. After these time points, 1 ml absolute EtOH was added and the acidic samples were adjusted to a pH of 7. Carrez precipitation was performed and resulting solutions were further diluted with EtOH prior to HPLC measurements.

4.2.5. NMR Measurements of MPO-Mediated Aminomethoxyphenol Oxidation

A Varian (Agilent) INOVA 500-MHz NMR spectrometer (Agilent Technologies, Santa Clara, California, USA) and the VNMRJ 2.2D software were used for all measurements. ^1H NMR spectra (499.98 MHz) were measured on a 5 mm indirect detection PFG-probe, while a 5 mm dual direct detection probe with z-gradients was used for ^{13}C NMR spectra (125.71 MHz).

Non-derivatized 5-amino-2-methoxyphenol was used for NMR measurements under equal condition described above. Measurements were conducted before addition of MPO, after 10 min, 30 min, 60 min and 6 h of enzyme reaction.

4.3. Results and Discussion

The potential of several enzymes from the human immune system as biomarkers for wound infection was recently demonstrated, including that for MPO [8]. MPO can be detected upon oxidation of distinct phenolic compounds in the presence of hydrogen peroxide as co-substrate [9]. However, for integration into diagnostic systems (e.g. test strips) immobilization of MPO substrates is necessary, which often prevents enzymatic oxidation. Here, 5-amino-2-methoxyphenol was found to be suitable for immobilization without losing its susceptibility to MPO-mediated oxidation.

In a first step, AMP was functionalized with alkoxy silane to allow simple immobilization upon hydrolysis (Fig. 1). Successful functionalization was confirmed by NMR and subsequently the functionalized AMP was hydrolytically polymerized onto silica plates as solid model carrier (iAMP).

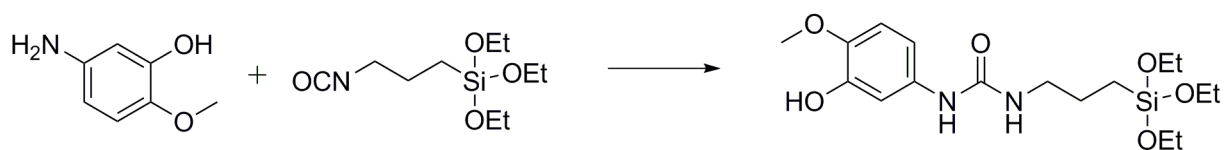


Figure 1: Coupling of 5-amino-2-methoxyphenol on the alkoxy silane spacer

Visual detection of MPO activity was performed by incubating the functionalized silica plates, iAMP, with buffer solutions containing varying activities of MPO and H_2O_2 as co-substrate

(Fig 2A). A color change towards red appeared within the first minutes indicating successful oxidation of iAMP by MPO. After 30 min the maximum color intensity was reached. Control samples were incubated in the same solutions but without MPO and did not lead to any color change. The visual detection was quantified using color light spectrophotometer. Considering the red part of the color space according to the CIELab concept, a significant color change was detected proving an efficient conversion of the immobilized aminomethoxyphenol. A slight signal of the control was also observed, which resulted from evaporation of the spotted liquid and did not yield in visible color change. Once the proof of concept was successfully conducted using buffered MPO solutions, iAMP oxidation was performed by incubating with artificial wound fluid (AWF) that was spiked with MPO concentrations that equal to slightly elevated MPO activities in critical wounds [6]. Results shown in figure 2B indicated a clear color change towards red after 60min incubation with 10 and 20 units MPO, whereas no appearance of color could be detected in the control sample consisting of AWF without MPO. Using artificial wound fluid resulted in a significant difference in color intensity between the MPO activities applied. Increased a values were obtained for the samples and the control measured with AWF, which was caused by the complex composition of the fluid consisting of high concentration of protein and various trace elements. The obtained results clearly indicate the suitability of the iAMP system for MPO detection in buffer as well as in complex media like wound fluids.

Since hemoglobin obviously present in wound fluids is also known to exhibit peroxidase activity [10], interferences in iAMP oxidation and color development were investigated. No color change was observed at heme concentrations up to 10 μ M. Heme concentrations in wound fluids were previously reported to be around 7 μ M, [5], thus cross reactions in iAMP based MPO can be excluded.

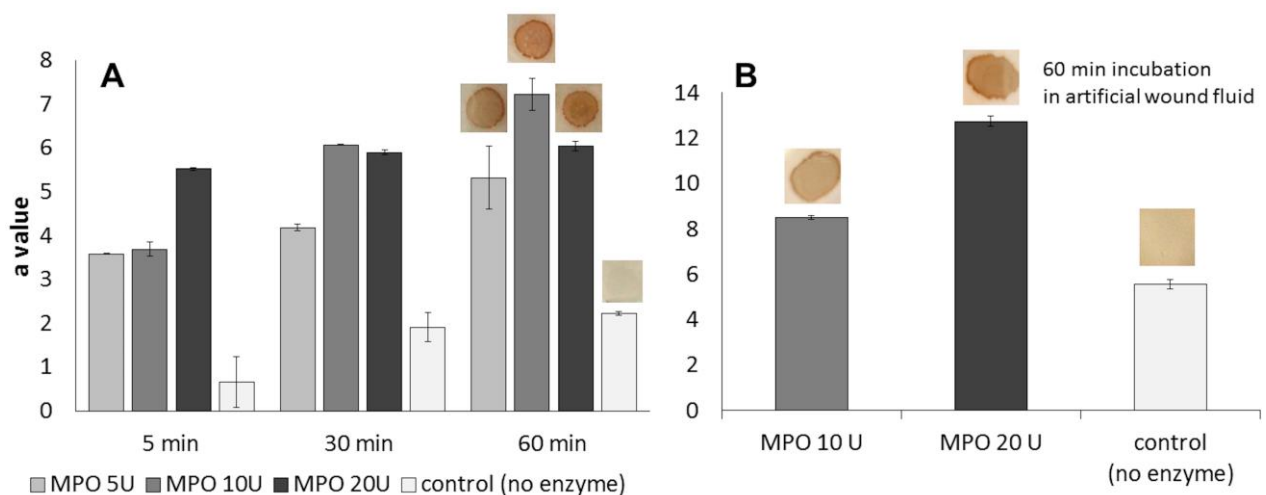


Figure 2: Visual and spectrophotometric detection of oxidation of immobilized aminomethoxyphenol by MPO detected by color light spectrophotometer. (A) Color formation

using MPO in buffer was observed already after 5 min incubation while the maximum of color intensity was detected after 60 min. (B) Color formation after 60 min incubation applying artificial wound fluid with different concentrations of MPO.

The sensitivity and specificity of the prepared infection diagnostic based on MPO detection is crucial, considering the complexity of biological samples like wound fluids. MPO activity of 92.2 ± 45 U/ml was determined in infected wounds compared to 1.9 ± 1.8 U/ml in non-infected wounds in previous studies [8]. As there was a residual MPO activity in the non-infected wounds, a diagnostics methods based on this assay should not detect MPO activities around 1 U/ml. The suitability of the described diagnostic was tested applying different concentrations of MPO on the iAMP. After incubation for 5 min, clear color changes were observed down to 10 U. Only a slight color change was observed applying 5 U MPO and no MPO activities below 5 U could be detected, which indicates a detection limit of 5 U (Fig 3A). The obtained result fits with the requirements for infection detection based on MPO since the detection limit is above the MPO activities observed for non-infected wounds.

Specificity towards MPO recognition is important to avoid false positive results with the prepared diagnostic. The iAMP was incubated with other infection biomarkers like lysozyme and elastase as well as with horse radish peroxidase (HRP) to investigate the interference with other peroxidases. Lysozyme and elastase (Fig 3B) did not show any signal whereas HRP (10 U) resulted in slight color change after 5 min incubation. However, 8 U of HRP did not result in a visible color change, suggesting a decreased affinity of the iAMP towards other peroxidases (Fig 3C).

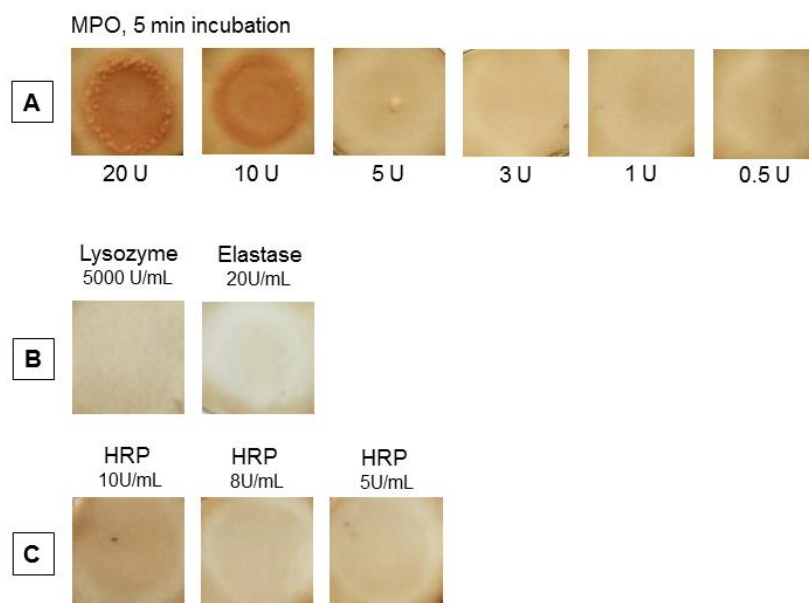


Figure 3: Investigation of the visual detection limit of MPO (A) and the specificity of iAMP towards MPO by applying the substrate on the infection biomarker lysozyme and elastase

(B) and horse radish peroxidase (C). Activities of lysozyme and elastase were used that are commonly found in infected wounds.

The MPO-responsive material was subsequently tested with human wound fluid samples: fluids from non-infected wounds were compared to infected wound fluids. A clear color change was detected after incubation of the iAMP substrate for 5 min with infected wound fluid (Fig 4C), whereas non-infected wound fluid did not result in a visible color change (Fig 4B). The complex composition of human wound fluids leads to a yellowish color of the fluid, which results in a slight coloring of the iAMP plate incubated with non-infected wound fluid. A plate soaked with buffer (Fig 4A) was compared to figure 4B and reveals the initiated color deriving from wound fluid. The positive results obtained with human wound fluid samples further revealed the potential of the carrier immobilized aminomethoxyphenol for infection detection based on MPO. The fast reaction rates were retained when biological samples were compared to buffered MPO solutions, which indicates that possible reaction inhibitors in biological samples do not interfere with the presented diagnostic material.

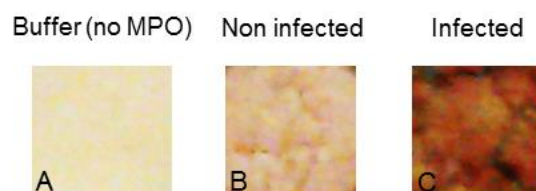


Figure 4: Visual detection of wound infection based on the MPO-responsive iAMP. The functionalized plates were incubated for 2 min with wound fluids from non-infected wounds (B) and from infected wounds (C). A plate incubated with sodium phosphate buffer (A) compared to the non-infected wound fluid reveals the natural color obtained from the biological sample.

The infection detection system based on carrier immobilized aminomethoxyphenol revealed its suitability for the fast detection of elevated MPO activities in biological systems. A color development was observed after 5 min reaction time, which was a great improvement compared to a previously published detection system based on carrier immobilized Fast blue that achieved a color development after 30 min incubation [5].

4.3.1. Reaction Mechanism of 5-Amino-2-Methoxyphenol Oxidation by MPO

To prove the consumption of alkoxy-silane-functionalized aminomethoxyphenol, the MPO-responsive material was incubated with MPO in buffers of pH 4 and pH 7. HPLC analysis of

the MPO-mediated oxidation indicated a fast decrease of substrate concentration within 1 h and around 50% substrate consumption after 15 min reaction time. No significant differences in the reaction kinetics were observed upon incubation at neutral and acidic pH (Fig. 5). Control samples lacking MPO prove that phenol oxidation was exclusively obtained from enzymatically produced hypochlorite while H_2O_2 did not show any oxidation activity on the functionalized substrate. The increase in absorbance of the reaction mixture in solution after 30 min incubation was photometrically monitored and showed the development of an absorbance maximum around 510 nm confirming formation of the red color.

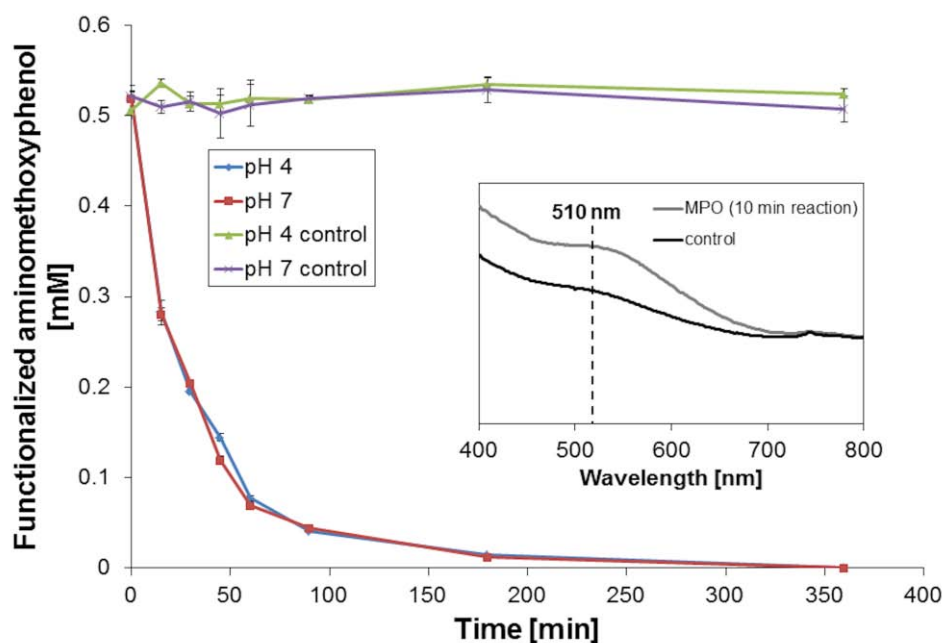


Figure 5: HPLC analysis of MPO-mediated conversion of alkoxy silane functionalized aminomethoxyphenol in buffer solution at different pH values. After 15 min incubation, around 50% of the substrate was consumed with complete conversion observed after 6 h of incubation. Control samples lacked MPO. The absorbance scan in a range of 400 nm to 800 nm indicated an increased signal over a wide range.

Studies on the well-known MPO substrate guaiacol reported oligomerization upon MPO oxidation [11,12]. Despite the detailed investigation of the substrate specificities of MPO, less information is available about their reaction products. However, the reactivity and stability of the reaction products have a great impact on the suitability of an enzyme substrate for the incorporation into diagnostic tools like point-of-care (PoC) devices. In this study LC-ESI TOF measurements and NMR measurements were performed, giving insight into the MPO-mediated oxidation and its reaction products.

To detect the reaction products obtained after the MPO-mediated oxidation of non-functionalized 5-amino-2-methoxyphenol, the reaction was monitored online via NMR by

performing the reaction in NMR tubes. After short incubation time, new singlets were observed in the aromatic region at 6.50 ppm and 6.72 ppm indicating the start of a starting polymerization process (Fig. 6). A dimerization that formed a new bond in the para position resulted in a downfield shift of the proton in the meta position whereas the signal of the ortho-substituted proton was shifted upfield. Additional HSQC and HMBC experiments further proved a significant dimerization to the bisphenol after only 10 min of reaction time.

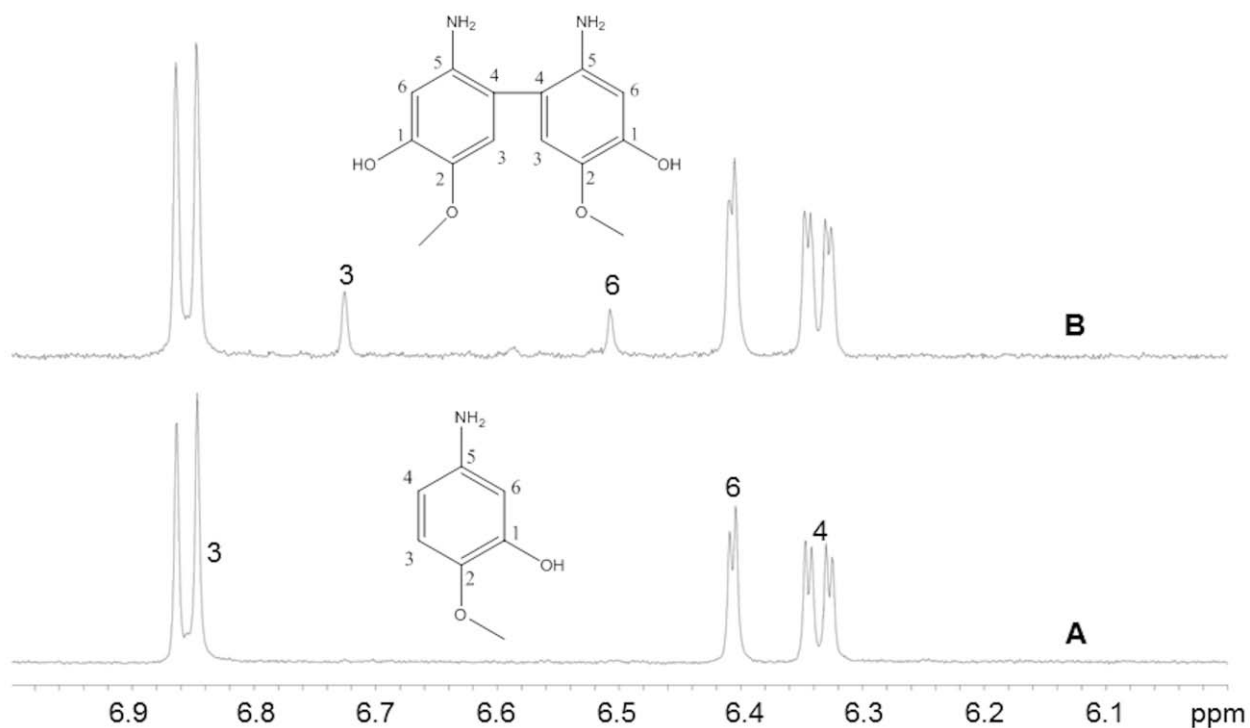


Figure 6: ¹H-NMR spectra of the MPO-catalyzed oxidation of a 10 mmol solution of non-functionalized 5-amino-2-methoxyphenol with 10 mmol H₂O₂ in 100 mmol phosphatebuffer in D₂O: (A) before the addition of myeloperoxidase; (B) 10 min after the addition of 10 U myeloperoxidase.

Subsequent LC-MS measurements of the functionalized substrate indicated the emergence of molecular masses of 299.1, again confirming the bisphenol formation. Another mass of 275.1 can be attributed to a quinone formed from the bisphenol with highest intensity after 30 min incubation (Fig. 7). The dimeric product emerged at the same time point as observed with NMR analysis although LC-MS experiments were performed with the alkoxy silane-modified substrate. Interestingly, since NMR measurements were carried out with the non-functionalized substrate, spacer attachment obviously did not impair the reaction rate and subsequent polymerization. Oxidation of the functionalized AMP resulted in immediate cleavage of the urea bond connecting the phenol with the spacer.

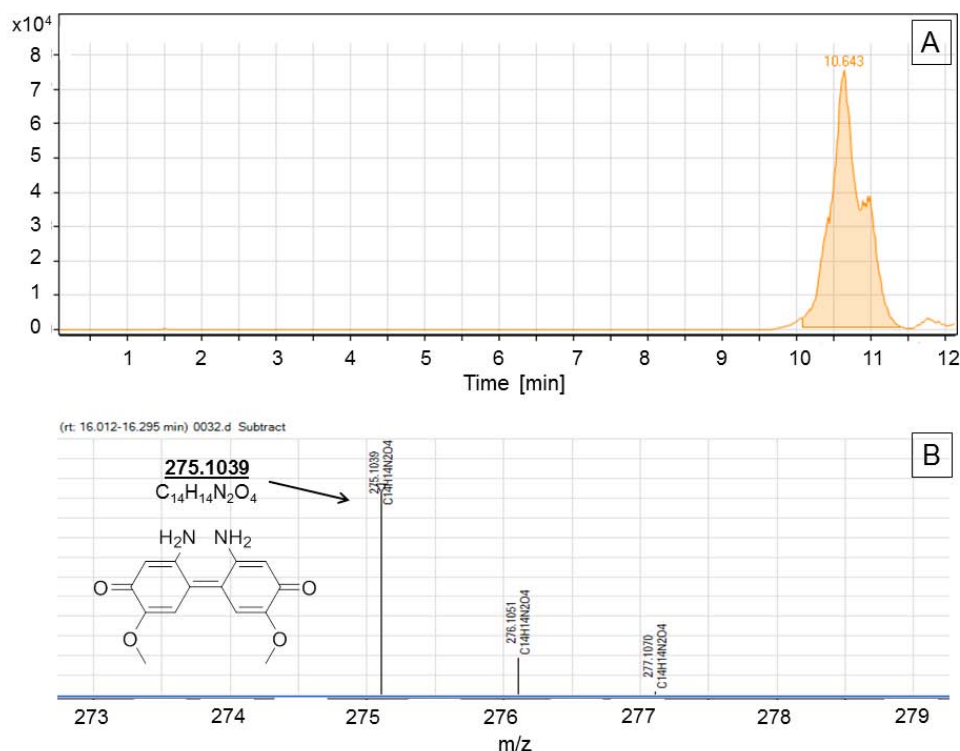


Figure 7: LC-ESI TOF analysis of MPO-mediated oxidation of functionalized aminomethoxyphenol after 30 min incubation. (A) Extracted ion chromatogram (EIC) of the dimer as main reaction product after 30 min incubation. (B) Mass spectrum showing the mass of the aminomethoxyphenol dimer.

Accumulation and further consumption of the formed dimeric reaction products was compared via LC-ESI TOF measurements (Fig. 8). A complete consumption of the substrate was observed within 60 min reaction time whereas constant production of the respective reaction products was determined. The bisphenol could only be detected in low amount, probably resulting from its low stability, which directly resulted in quinone formation. Accumulation of the quinone reaction product was observed within 30 min reaction time whereas no quinone could be detected anymore after 60 min reaction time, indicating further polymerization of this reaction product.

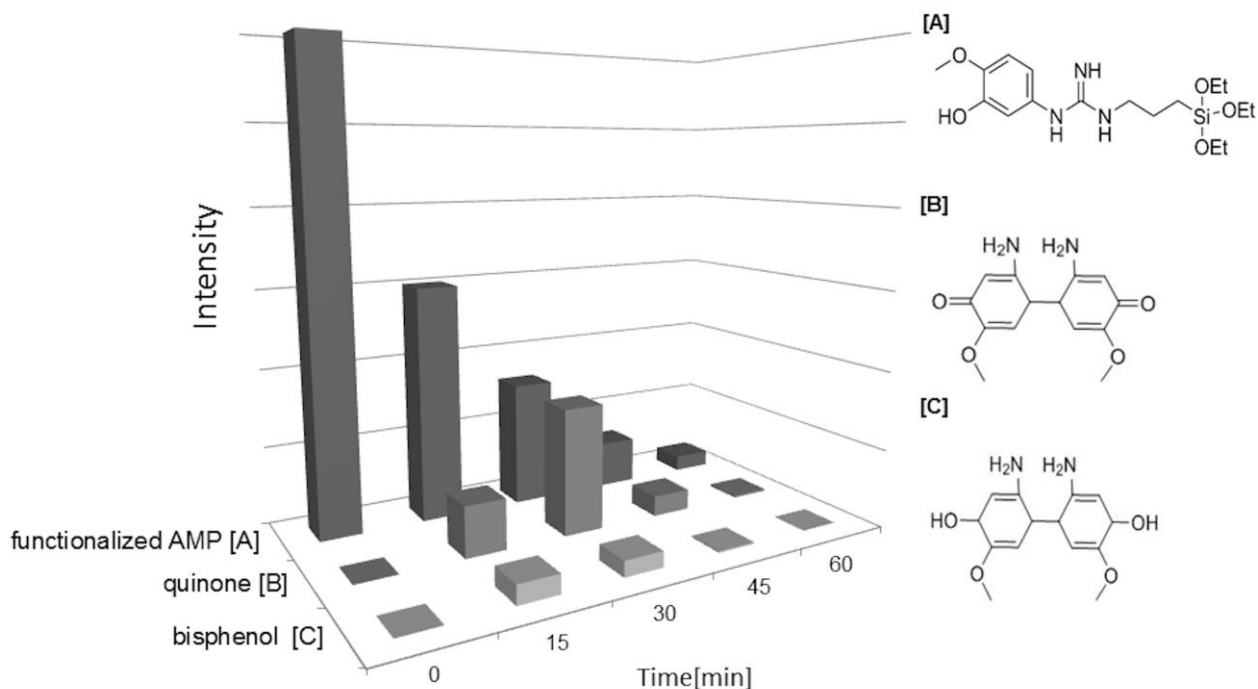


Figure 8: LC-ESI TOF analysis of MPO-mediated oxidation of functionalized AMP.

The obtained data suggested a reaction mechanism based on radical polymerization (Fig. 9). The unstable oxygen radical upon MPO-mediated oxidation resulted in delocalization of the radical and subsequently led to dimerization. This reaction mechanism was supported by literature suggesting a similar mechanism for peroxidase-mediated guaiacol polymerization [12].

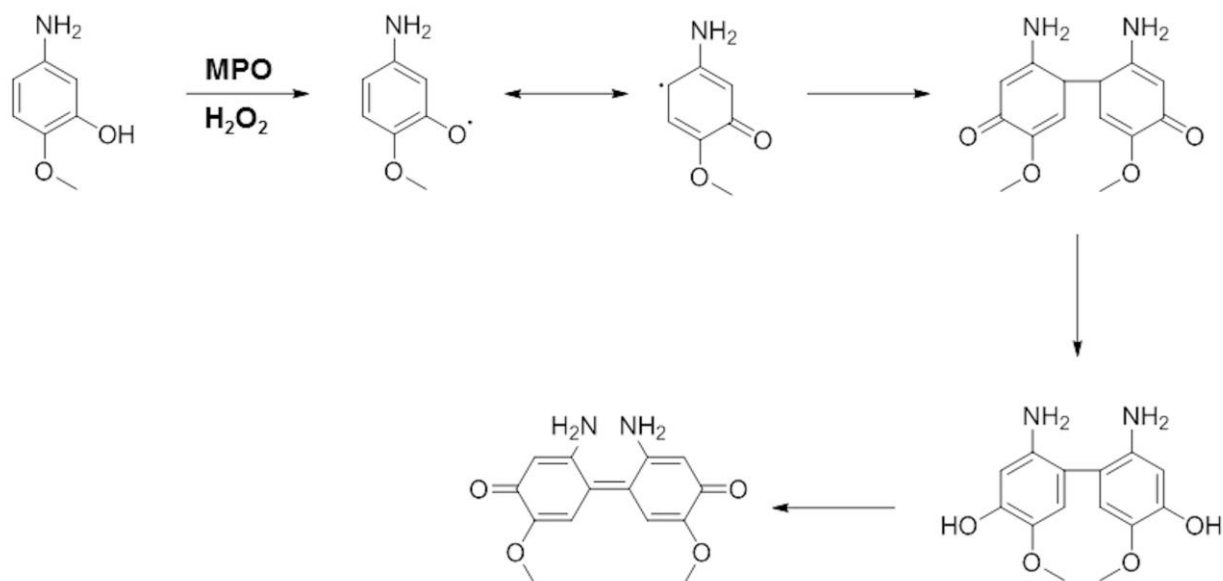


Figure 9: Proposed reaction mechanism of MPO-mediated aminomethoxyphenol oxidation. Delocalization of the oxygen radical in the ring system leads preferably to dimerization resulting in a redish quinone.

Further monitoring of the reaction progress via NMR and LC-MS indicated the accumulation of various other oligomeric products with simultaneous consumption of the formed dimeric products at longer incubation times. NMR measurements after 6 h incubation time resulted in multiple signals arising in the range of 6.2-7.0 ppm that could be assigned to complex derivatives of aminomethoxyphenol including substitutions on the primary amine and hydroxyl group.

Dimer accumulation within the 30 min incubation time in combination with the fast color change observed in the biotransformation experiments on silica plates implies that the dimer is responsible for the color formation. No further increase of color intensity of the functionalized silica plates was observed after 30 min incubation, which could be explained by consecutive oxidation of dimers and the formation of products with increased degree of polymerization. This progressive polymerization was further confirmed by NMR measurements after 6 h incubation indicating substitution on amines and hydroxides. The accumulation of the color-giving reaction product after a short time and its subsequent consumption recommends the prepared MPO detection system as suitable for a fast detection of wound infection based on elevated MPO activity. Undesired cross reactions of the main reaction products are now more predictable due to enhanced knowledge of the reaction progress and the chemistry of the reaction products, which furthermore facilitates future applications.

4.4. Conclusion

In this study, 5-amino-2-methoxyphenol was demonstrated as a specific substrate for the detection of infection based on elevated MPO activity. The substrate was functionalized with alkoxysilanes facilitating its immobilization on various carrier systems. The functionalized aminomethoxyphenol was immobilized on silica plates and further approved for the fast visual detection of MPO in buffer and artificial wound fluid via a significant color change within the first minutes of incubation. HPLC measurements further revealed the high consumption rate of this substrate and LC-MS analysis and NMR measurements uncovered the dimer of aminomethoxyphenol as the coloring reaction product. The successful implementation and comprehensive characterization of the MPO-mediated reaction progression illustrated the suitability of the novel substrate for infection detection.

Conflicts of Interest

The authors declare no conflict of interest.

Acknowledgements

This study was performed within the European Project Infact. Financial support from the European FP7-programme under grant agreement no. 604278 and the Austrian Centre of Industrial Biotechnology (ACIB) is gratefully acknowledged.

4.5. References

- [1] Tegl G, Schiffer D, Sigl E, Heinzle A, Guebitz GM. Biomarkers for infection: enzymes, microbes, and metabolites. *Appl Microbiol Biotechnol* 2015;99:4595–614..
- [2] Schiffer D, Blokhuis-Arkes M, van der Palen J, Sigl E, Heinzle A, Guebitz GM. Assessment of infection in chronic wounds based on the monitoring of elastase, lysozyme and myeloperoxidase activities. *Br J Dermatol* 2015.
- [3] Nauseef WM. Myeloperoxidase in human neutrophil host defence. *Cell Microbiol* 2014;16:1146–55..
- [4] Hasmann A, Marold A, Wiesbauer H, Schoeftner R, Gewessler U, Kandelbauer A, et al. Analysis of myeloperoxidase activity in wound fluids as a marker of infection. *Ann Clin Biochem* 2013;50:245–54.
- [5] Schiffer D, Tegl G, Vielnascher R, Weber H, Schoeftner R, Wiesbauer H, et al. Fast Blue RR—Siloxane Derivatized Materials Indicate Wound Infection Due to a Deep Blue Color Development. *Materials (Basel)* 2015;8:6633–9.
- [6] Hajnsek M, Schiffer D, Harrich D, Koller D, Verient V, Palen J V.D., et al. An electrochemical sensor for fast detection of wound infection based on myeloperoxidase activity. *Sensors Actuators B Chem* 2015;209:265–74.
- [7] Rollett A, Schroeder M, Schneider KP, Fischer R, Kaufmann F, Schöftner R, et al. Covalent immobilisation of protease and laccase substrates onto siloxanes. *Chemosphere* 2010;80:922–8.
- [8] Hasmann A, Wehrschoetz-Sigl E, Marold A, Wiesbauer H, Schoeftner R, Gewessler U, et al. Analysis of myeloperoxidase activity in wound fluids as a marker of infection. *Ann Clin Biochem* 2013;50:245–54.
- [9] Furtmüller PG, Obinger C, Hsuanyu Y, Dunford HB. Mechanism of reaction of myeloperoxidase with hydrogen peroxide and chloride ion. *Eur J Biochem* 2000;267:5858–64.
- [10] Kapralov A, Vlasova II, Feng W, Maeda A, Walson K, Tyurin VA, et al. Peroxidase activity of hemoglobin-haptoglobin complexes: covalent aggregation and oxidative

stress in plasma and macrophages. *J Biol Chem* 2009;284:30395–407.

[11] Doerge DR, Divi RL, Churchwell MI. Identification of the Colored Guaiacol Oxidation Product Produced by Peroxidases. *Anal Biochem* 1997;17:10–7.

[12] Hwang S, Lee C, Ahn I. Product identification of guaiacol oxidation catalyzed by manganese peroxidase. *J Ind Engeneering Chem* 2008;14:487–92.

5 Antimicrobial cellobiose dehydrogenase-chitosan particles

Published in: ACS Applied Materials and Interfaces 2016, 8, 967-973

Gregor Tegl, Barbara Thallinger, Bianca Beer, Christoph Sygmund, Roland Ludwig, Alexandra Herrero-Rollett, Gibson S. Nyanhongo and Georg M. Guebitz

Abstract

Increasing prevalence of chronic wounds and microbial infection constitute a severe health challenge. The situation is further complicated by emerging multidrug resistance making the treatment of infections increasingly difficult. Here, a novel antimicrobial system based on *in-situ* release of hydrogen peroxide (H_2O_2) by cellobiose dehydrogenase (CDH) immobilized on chitosan (CTS) particles is described. Covalent immobilization using carbodiimide coupling lead to a higher amount of protein immobilized on CTS (104 μg CDH/mg CTS) when compared to non-covalent immobilization, which, however, showed highest recovery of CDH activity (0.01 U/mg CTS). The CDH-CTS *in-situ* generated H_2O_2 completely inhibited growth of *E. coli* and *S. aureus* over a period of 24 h. This resilient antimicrobial system represents a novel strategy for preventing infection with potential application in counteracting microbial colonization of chronic wounds.

5.1. Introduction

Chronic wounds fail to precede the healing process, retrieve their functional integrity and constitute a major health issue. Increasing multidrug resistance is further complicating the successful treatment and management of chronic wounds. To date, approximately 2% of the population in developed countries will at some point develop chronic wounds and the number is set to increase in the near future as ageing population increases. Growing health care costs combined with costly wound treatment strategies due to complex and long lasting treatment procedures, which represent a high financial burden. Statistical observations of this health issue still is inexact, because chronic wounds are rarely stated as an individual disease but are much more seen as consequence of previous diseases. This leads to the underestimation of an important and dangerous health issue of the modern population [1,2]. Current standard wound management procedures comprise the monitoring of infection, cleaning, dressing and treatment with antiseptics and/or antibiotics. Although systemic antibiotic therapies still predominate, topical antimicrobial treatments have superior advantages. In particular the enhanced possibility to influence the wound healing process on site constitutes a major advantage. A variety of antimicrobial agents are implemented today

especially silver, being the most popular one that was already used in the earliest forms of wound care. However, studies show cytotoxic effect of silver on intact skin tissues, alternative novel wound dressings were implemented and gradually gain acceptance among clinicians [3–6].

Topical wound treatments enable the application of high concentrations of antimicrobials. However, when applied at once, these can cause irritations over an extended time frame like hypersensitivity, alter the cutaneous flora or the wound healing process [7,8].

Chitosan (CTS), a biopolymer consisting of randomly distributed units of $\beta(1,4)$ -linked N-acetyl-D-glucosamine and D-glucosamine, is frequently described for wound applications. CTS is obtained by alkaline hydrolysis of chitin from exoskeletons of crustaceans and fungi. Due to its primary amine groups and consequent cationic character in solution, chitosan exhibits antimicrobial properties through electrostatic interactions with the cell surface of bacteria. Numerous beneficial properties of CTS like biocompatibility and various bioactivities are reported. Its great functionality regarding modification and processability combined with the antimicrobial activity render this polymer an attractive carrier for biomedical applications [9,10]. Nevertheless, despite some antimicrobial activity CTS alone does not completely prevent microbial growth.

An antimicrobial enzyme attracting increasing attention in the recent years is cellobiose dehydrogenase (CDH). This flavocytochrome based protein commonly found in wood degrading fungi is known to oxidize a wide variety of mono- and oligosaccharides, with its best substrates being cellobiose and lactose. The resulting electrons can reduce molecular oxygen resulting in the formation of hydrogen peroxide (H_2O_2), a strong oxidative agent commonly used for the disinfection of surfaces [11,12]. CDH thereby uses with cellobiose a substrate that is not consumed by bacteria providing a great advantage for the application in antimicrobial systems. The antimicrobial effectivity of this enzyme against various organisms has recently been demonstrated. Moreover, CDH was immobilized on polydimethylsiloxanes in order to create novel antimicrobial surfaces for urinary catheters [13–15]. Hence, this enzyme could likewise have potential for the application in antimicrobial wound dressings [16].

In this study, *in-situ* production of H_2O_2 on chitosan particles frequently used in wound dressings was investigated as an alternative topical treatment circumventing overdosing of antimicrobial molecules in conventional treatment strategies.

5.2. Material and Methods

5.2.1. Materials and Microorganisms

All chemicals used were of analytical grade. Media components and cellobiose were purchased from Carl Roth (Karlsruhe, Germany) while all other chemicals were purchased from Sigma-Aldrich (Steinheim, Germany). Chitosan from shrimp shells (Sigma-Aldrich, Steinheim, Germany) was used throughout the presented work with a number average molecular weight of 200 kDa and a degree of acetylation of 13%. The recombinant *Myriococcum thermophilum* cellobiose dehydrogenase (rMtCDH) was optimized for increased oxygen reactivity by a single mutation (N748G) and was produced in *Pichia pastoris* as previously described [12]. *Staphylococcus aureus* strain ATCC 25923 and *Escherichia coli* strain XL1 used throughout the experiments were acquired from the culture collection of the Institute of Environmental Biotechnology from Graz University of Technology.

5.2.2. Purification of Chitosan

The chitosan was purified to remove residual proteins and glucans prior to modifications and substrate preparation. Therefore, chitosan (20 g) was dispersed in double distilled water (ddH₂O) prior to acidification with acetic acid to obtain a 1% chitosan solution in 0.05% acetic acid. The solution was stirred overnight. Insoluble particles were removed via vacuum filtration using a 30 µm filter. Subsequently, the pH was adjusted to 8.0 for precipitation of chitosan. The precipitate was washed with ddH₂O and ethanol until pH 7.0. Pure chitosan was lyophilized for further use.

5.2.3. Immobilization of CDH on Chitosan

For all immobilization strategies, a 20 mM potassium phosphate buffer, pH 7.0) was used. CDH (32 U, 0.16 U/mg) was applied per gram of chitosan in the immobilization reactions.

Adsorption

Chitosan was suspended in buffer (3% w/v) and allowed to swell. Afterwards 2 mL of CDH solution (20 g/L) was added and the reaction mixture was incubated for 24 h at 10°C before the isolation of chitosan by centrifugation. The obtained precipitate was washed with deionized water with agitation until CDH could not be detected anymore in the washing solution. The particles were subsequently freeze dried.

Covalent immobilization using glutaraldehyde

Chitosan was suspended in buffer (3% w/v) containing 2% (v/v) glutaraldehyde and stirred for 10 min at 10°C. Subsequently, 2 mL of CDH solution (20 g/L) was added and the reaction mixture was incubated for 24 h at 10°C before the isolation of chitosan by centrifugation. The obtained precipitate was washed with deionized water with agitation until CDH could not be detected anymore in the washing solution. The particles were subsequently freeze dried.

Covalent immobilization using the EDC/NHS system

CDH was mixed with 1-ethyl-3-(3-dimethylaminopropyl)carbodiimide (EDC) (200 mole equivalents) and stirred for 20 min at 10°C. A chitosan suspension in buffer (3% w/v) was mixed with the CDH solution and subsequently NHS (200 mole equivalents) was added. The reaction mixture was incubated for 24 h at 10°C before the isolation of chitosan by centrifugation. The obtained precipitate was washed with deionized water with agitation until CDH could not be detected anymore in the washing solution. The particles were subsequently freeze dried.

5.2.4. Analyses of Enzyme Immobilized on Chitosan

Selective determination of the total protein content and immobilization efficiency

The protein content of CDH was analyzed photometrically by measuring the absorbance of the oxidized heme cofactor in the enzyme. Briefly, oxygen was bubbled through the respective solution for 1 min to ensure an oxidized heme cofactor that was subsequently detected at 420 nm. The concentration of CDH was calculated using the molar extinction coefficient of heme ($100 \text{ mM}^{-1} \text{ cm}^{-1}$). The protein and activity recovery of CDH on chitosan was analyzed based on the assessment of CDH remaining in the reaction supernatant and all washing solutions.

Determination of CDH activity

CDH activity was measured as function of the H_2O_2 production using the Amplex Red assay [6]. Briefly, 10 μL of enzyme (20 g/L) was added to 157.5 μL 250 mM phosphate buffer, pH 7.4 as well as 0.5 μL horse radish peroxidase (0.1 U/mL) and 2 μL Amplex Red (10 mM). Shortly before starting the measurement, 30 μL of a 200 mM cellobiose solution was added. The production of H_2O_2 was monitored detecting the Amplex Red oxidation product at an excitation and emission wavelength at 550 nm and 585 nm, respectively. One unit of CDH activity is defined as 1 μmol of H_2O_2 produced per minute under the described conditions.

Activity in CDH-CTS particles

For the detection of CDH activity in the particles, the above mentioned assay was used, but 2 mg of CDH loaded chitosan particles were pre-weighed in a 96 well plate prior to the addition of the remaining reagents.

Swelling characteristics

The swelling properties of the respective CTS particles were determined by allowing them to swell in 250 mM sodium phosphate buffer, pH 7.4 for 2 h. Subsequently the swollen particles were removed from the swelling medium and excess of water was carefully absorbed with a paper filter. The swelling ratio (S_i) was calculated using following formula: $S_i = (w_i - w_0) / w_0$, where w_i is the weight of the swollen particle and w_0 is the weight of the dried particle.

Determination of size and zeta potential

The zeta potential was analyzed in the buffer previously described at 25°C in a Malvern zetasizer NS. A value for viscosity was considered as 0.89 cP and a refractive index of 1.334. The particle size distribution was determined via laser diffraction on a Beckman particle sizer (Margency, France) dispersed in deionized water. Each sample was measured in triplicate.

Temperature stability

Two mg of CDH loaded chitosan particles were incubated in 1 mL of a 250 mM sodium phosphate buffer, pH 7.4 at 20 – 80°C. Aliquots of the supernatant were removed after centrifugation and analyzed towards their hydrogen peroxide content using the Amplex Red assay.

5.2.5. Antimicrobial activity

Minimal inhibitory concentration

The antimicrobial activity of different concentrations of the three CDH-chitosan formulations was assessed against *S. aureus* and *E. coli*. Amounts ranging from 0.1 to 50 mg of the produced particles were weighed into 25 ml Erlenmeyer culture flasks followed by the addition of 7.49 ml of Mueller Hinton (MH) broth and 2.5 ml of cellobiose to reach a final concentration of 50 mM in solution. Microbial growth was started by adding a defined amount of overnight culture of *E. coli* and *S. aureus* with starting OD600 of 0.1 (equal to 10⁵ CFU/ml). Bacterial growth was monitored for 24 h by removing 250 µl of the culture supernatant every 2 h. The samples were used to determine the OD600 at a plate reader as well as the amount of viable cells present in solution using the drop plate method [17]. Briefly, 20 µl of the supernatant were diluted with 180 µl of MH broth in a 96 well plate until a dilution of 10⁻¹ was reached. Then, 10 µl of each dilution were pipetted onto a plate

containing MH agar. After 24 hours of incubation, colonies were counted at suitable dilutions and used for the calculation of the respective CFU/ml for each time point. The experiment was performed in triplicates. At the same time intervals the leaching behavior of CDH from chitosan was studied in the culture medium. At each sampling point 10 μ l was taken from the culture supernatant and the enzymatic activity was measured as previously described. As alternative substrate addition, chitosan loaded with cellobiose was used. Chitosan (200 mg) was incubated overnight in 7 mL of a 200 mM cellobiose solution and afterwards removed from the solution by centrifugation and freeze dried.

5.3. Results and Discussion

Immobilization of CDH on chitosan

Using enzymes for the production of antimicrobial systems implies the need of an effective immobilization strategy protecting the respective enzyme from being degraded by proteolytic enzymes [18]. In this study, a novel CDH-chitosan antimicrobial system was investigated. CDH was immobilized using different strategies including glutaraldehyde, carbodiimide coupling and non-covalent adsorption. The highest amount of CDH of 124 μ g/mg immobilized on CTS was measured when EDC/NHS was used in 200 times molar excess (compared to CDH) for coupling (Figure 1). The reaction was thereby enhanced by the use of NHS activating the acylisourea bond generated by EDC with carboxyl groups of the enzyme in a pre-incubation time of 20 min.

Interestingly, the lowest CDH total protein content and the lowest CDH activity was detected for the glutaraldehyde cross-linked CDH-CTS (Figure 1). Performing the reaction at pH 7.0 including a pre-incubation of chitosan with glutaraldehyde was a major reason for the lower yield in comparison to the other methods since amine cross linkers usually work best at basic pH values. Moreover, due to the high reactivity of glutaraldehyde towards primary amines, a high degree of intramolecular cross-linking within chitosan was most likely obtained which was confirmed by the high amount of unbound enzyme released during washing of the particles. Despite the low protein content with this approach, a high degree of intramolecular cross-linking strongly increases the strength of the particle, which could render it a stable candidate for the incorporation in topical wound care products.

The adsorption method constitutes the easiest immobilization strategy since no additional reagents and pre-incubation times are required. Following this approach an adequate protein recovery of 52% was obtained. The wash out of unbound enzyme was comparable with that of the glutaraldehyde cross-linked particle. Due to the non-covalent immobilization of CDH, a high degree of leaching was expected in comparison to the methods applying cross linkers.

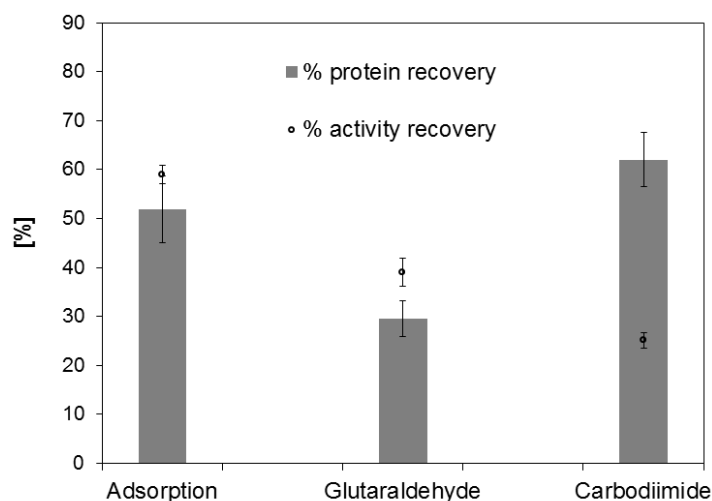


Fig. 1: Immobilization of CDH on chitosan via adsorption and covalent coupling using glutaraldehyde or carbodiimide chemistry (EDC/NHS). The grey columns indicate the protein recoveries found after immobilization and the black circles depict the CDH activity recovery on the particles after immobilization.

A factor strongly influencing the reaction kinetic is the degree of swelling of CDH-CTS. Within the first 2 h, no influence of the CDH immobilization strategy on the degree of swelling of the CDH-CTS particles was observed. This was quite unexpected since chemical modification, e.g., glutaraldehyde cross-linking, is known to alter the swelling properties of chitosan [19].

The particles were further characterized regarding their particle size using laser diffraction and resulted in average particles sizes of 272 μm for adsorption, 620 μm for carbodiimide immobilization and 78 μm for glutaraldehyde coupling. All particles showed expectedly high polydispersity in size due to the heterogeneity of the used chitosan. The surface charge was determined via the zeta potential being 27 mV for the adsorption particle and 30 mV for the EDC treated particle. Positive values for these particles were obtained indicating a cationic surface charge, which was in accordance with the literature [20] and the chemical nature of chitosan. Considerable low zeta potential of -5 mV was obtained for the glutaraldehyde particle, most probably caused by the crosslinker strategy.

Tab. 1: Degree of swelling of CDH functionalized chitosan particles depending on the enzyme immobilization strategy.

Enzyme immobilization strategy	Degree of Swelling
Adsorption	3.53 ± 1.75

Covalent: glutaraldehyde	3.10 ± 0.69
Covalent: carbodiimide	3.61 ± 1.71

ATR-FTIR analysis indicated successful covalent immobilization of CDH on chitosan. The cross-linking of primary amines using glutaraldehyde results in the formation of Schiff-base linkages allowing detection of the emerging C-N bonds at 1412 cm^{-1} (Fig 2.). Only a low signal intensity of this peak was observed for immobilization using glutaraldehyde confirming the low amount of enzyme bound. In contrast, immobilization using the carbodiimide EDC resulted in a significant intensity increase of the peaks related to amide bonds. In a first reaction step, EDC forms an unstable acylisourea intermediate with carboxyl groups of the enzyme. Subsequently this intermediate reacts with primary amines yielding in amide bonding. This reaction works best at acidic pH values of around 4.0 – 5.0, but is less efficient at physiological pH. Enhancing the reaction efficiency at pH values of around 7.0, succinimides are efficiently improving the coupling yield. Within this work N-hydroxysuccinimide (NHS) was used forming NHS ester with the EDC intermediate that finally reacts with primary amines. Figure 2 (B) shows a significant increase of the amide signals in the FTIR considering the amide carbonyl stretching band at 1640 cm^{-1} and the amide N-H stretching band at 1540 cm^{-1} . The considerable signal intensities further confirm the good immobilization efficiency using this coupling strategy.

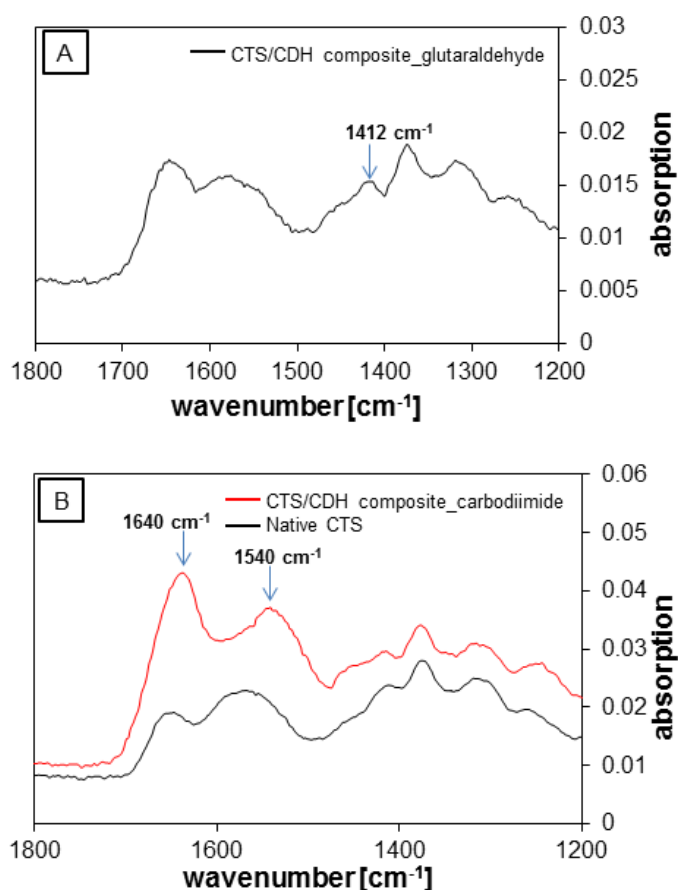


Fig. 2: ATR-FTIR analysis of the CDH-CTS produced by covalent immobilization of the enzyme. **(A)** CDH-CTS produced using glutaraldehyde as cross linker showed a peak at 1412 cm^{-1} indicating the emerging C-N bond of the Schiff base linkage. **(B)** Coupling of CDH to CTS using EDC/NHS as carbodiimide resulted in amide bonding of the enzyme indicated by peaks at 1640 cm^{-1} and 1540 cm^{-1} .

Activity of CDH-CTS particles

The crucial factor of enzyme immobilization constitutes the maintenance of the enzymatic activity and structural stability [18]. The immobilization methods chosen in this study comprise covalent cross-linking and physical entrapment by adsorption. Due to the primary amine groups of chitosan, chemical immobilization using bifunctional cross linker represents an efficient strategy. In the same manner, excessive hydrogen bonding of the amine groups with the enzyme favors a decent non-covalent immobilization [10].

The enzyme activities in terms of H_2O_2 production of the produced particles were determined using the Amplex Red activity assay. The highest CDH activity was observed for CDH-CTS using the adsorption method with $99.45\ \mu\text{M}^{-1}\ \text{min}^{-1}\ \text{H}_2\text{O}_2$. Together with the good protein recovery, the result was expected since non-covalent immobilization usually does not affect structure and function of the enzyme compared to chemical crosslinking [21]. A lower H_2O_2

production was observed for the carbodiimide coupled CDH-CTS ($50.43 \mu\text{M}^{-1} \text{min}^{-1}$) as a consequence of the lower activity recovery. An excess of EDC/NHS was used that probably resulted in multiple attachment of the enzyme to the chitosan matrix and thus led to sterical hindrance. The lowest CDH activity was observed immobilizing the enzyme with glutaraldehyde with $35.15 \mu\text{M}^{-1} \text{min}^{-1}$. Low protein recovery combined with an activity recovery of 39%, which is commonly obtained using glutaraldehyde, explains the impeded H_2O_2 production (Figure 1). Although differences in the CDH activities were observed, all particles showed a considerable production of H_2O_2 that is known to suppress bacterial growth of both, gram-negative and gram-positive bacteria [22]. Further experiments were conducted assessing the increase of H_2O_2 within a time frame of 8 h upon incubation of the EDC coupled particle in buffer. Constant levels of H_2O_2 around $600 \mu\text{M}$ were measured within this time suggesting a steady state in this concentration range under given conditions. Within 10 min of incubation time the maximum concentration was nearly reached, furthermore indicating the fast reaction kinetics also of the immobilized CDH.

The production of H_2O_2 could result in pH changes, which would influence the swelling behavior of chitosan that shows increased swelling at acidic pH. Influences of the H_2O_2 concentration up to 50 mM in buffer were thus studied and found to not significantly alter the pH. Due to the considerable high concentrations of H_2O_2 produced by the CDH-CTS particles combined with study on pH, influences of produced H_2O_2 on CDH activity could be excluded.

Temperature stability

Antimicrobial systems based on biological matter like enzymes have to be reliably active under various conditions including a broad temperature range. Immobilized enzymes can exhibit higher temperature stability than their free counterparts. Major parameters influencing these values are the physicochemical properties of the carrier matrix [23].

All particles showed H_2O_2 production over a wide range of temperatures from $20 - 60^\circ\text{C}$ with a sharp drop at higher temperatures (Fig. 3). The amount of CDH-CTS taken for this experiment was adjusted applying equal amounts of CDH. Best results were obtained for the carbodiimide treated particle showing the highest production of H_2O_2 up to a temperature of 60°C and even slight activity at 70°C . Compared to the free enzyme, the carbodiimide functionalized CDH was around twice as active and exhibited highest H_2O_2 production at 40°C . The lowest production of H_2O_2 was observed for glutaraldehyde coupled CDH being even less active than free CDH within the investigated temperature range. The adsorbed CDH on chitosan revealed increased activity in comparison to the free CDH, which confirms the stabilizing effect of the hydrophilic carrier matrix due to H-bonding interactions. The results of the carbodiimide functionalized CDH suggests multiple coupling of the enzyme consequently lowering the activity recovery (Figure 3) but increasing temperature resistance.

Glutaraldehyde coupling of CDH on CTS did not improve temperature resistance and thus renders less efficient also considering the results of activity and protein recovery.

The engineered CDH used in this study originates from *Myriococcum thermophilum*, a fungus growing on self-heating compost with temperatures ranging 30 – 50°C. Consequently the enzyme exhibits considerable thermo stability and shows activity up to 60°C [24]. Activity maxima at physiological conditions obtained within this study reveal the potential of these particles for medical applications.

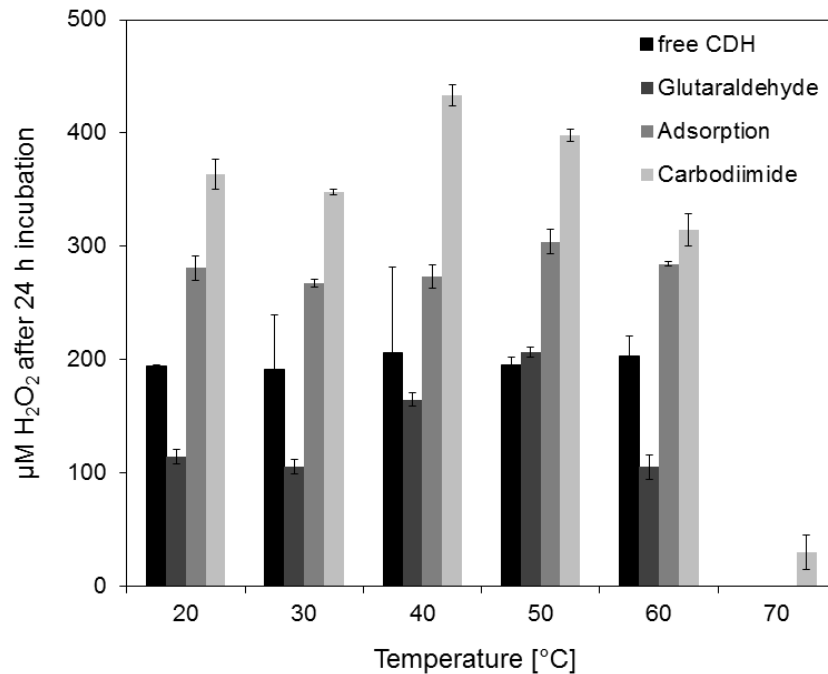


Fig. 3: Temperature stability of immobilized CDH after 24 h incubation at the respective temperature.

5.3.1. Antimicrobial activity and leaching behavior of CDH-chitosan particles

In a first step the antimicrobial activity of the three different types of CDH-CTS particles was assessed against *E. coli* and *S. aureus* (Figure 4).

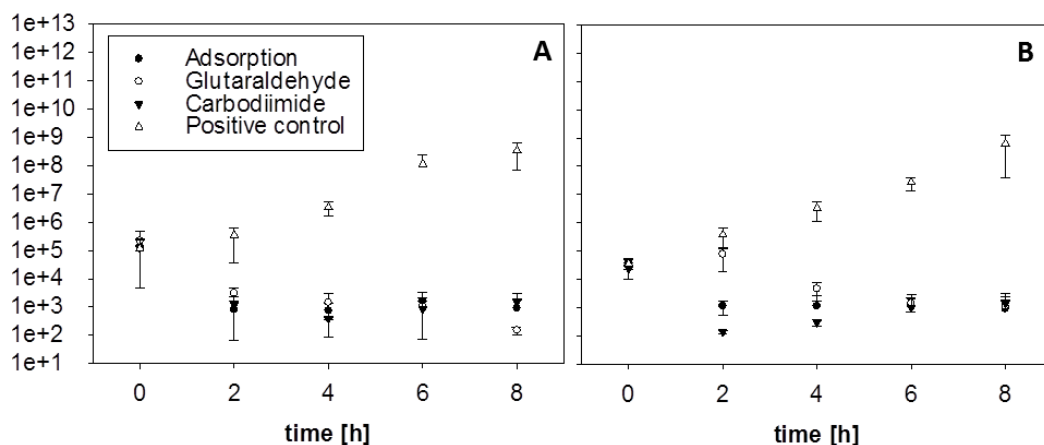


Fig 4: Inhibition effect of different types of CDH-CTS particles (20 mg) on growth of *E. coli* (A) and *S. aureus* (B) in medium, quantified as colony forming units (CFU/ml). The inhibiting particles were compared to *E. coli* cells (A) and *S. aureus* cells (B) growing in the absence of CDH-CTS particles.

All three CDH functionalized chitosan preparations showed a strong inhibition on the growth of *E. coli* and *S. aureus* based on CFU/ml based measurements (Figure 5A and B). Already within the first two hours of incubation a strong antimicrobial effect was seen resulting in approx. 100 times lower amount of *E. coli* and *S. aureus* cells when compared to cells growing in the absence of chitosan as control. There was no further growth seen after 24 h of incubation for the incubation mixtures containing the three different CDH-CTS particles (data not shown). The data suggests that the amount of H_2O_2 produced by the different particles under the given conditions is sufficient to act in a bactericidal manner and that the substrate concentration (cellobiose) added is high enough to maintain the antimicrobial activity of the enzyme for 24 h. Control samples using chitosan without CDH were also compared to the particles bearing CDH, but did not show any inhibitory effect resulting bacterial growth curves identical with the indicated positive controls. Hydrogen peroxide is a strong oxidative agent that has been widely used as an antiseptic and for the disinfection of surfaces in concentrations up to 3% [25]. Issues concerning cytotoxicity and the low stability of H_2O_2 have been raised but as previous studies of the CDH/cellobiose system have shown, the antimicrobial effective concentrations of H_2O_2 do not adversely affect the growth of various mammalian cell lines [13]. The *in situ* production of H_2O_2 by CDH solves the issue of low stability in solution and makes it less harmful for surrounding tissue cells. Studies have also shown that CDH is not only active against laboratory strains but also against clinical isolates such as multi resistant *Staphylococcus aureus* and *Acinetobacter baumannii*. Additionally a killing effect could also be observed when the system was applied to already formed biofilms [14]. No significant difference could be noted between the different preparation methods of

the particles. The chitosan used for preparing the particles was also tested but did not show any antimicrobial activity on its own (data not shown).

In the same experiment, the leaching behavior of the particles was assessed by measuring the CDH activity in the culture medium after separation from the particles at the given time points. As shown in Figure 5, both the type of particle as well as the composition of the culture medium, depending on the inoculated organism, had an influence on the leaching behavior.

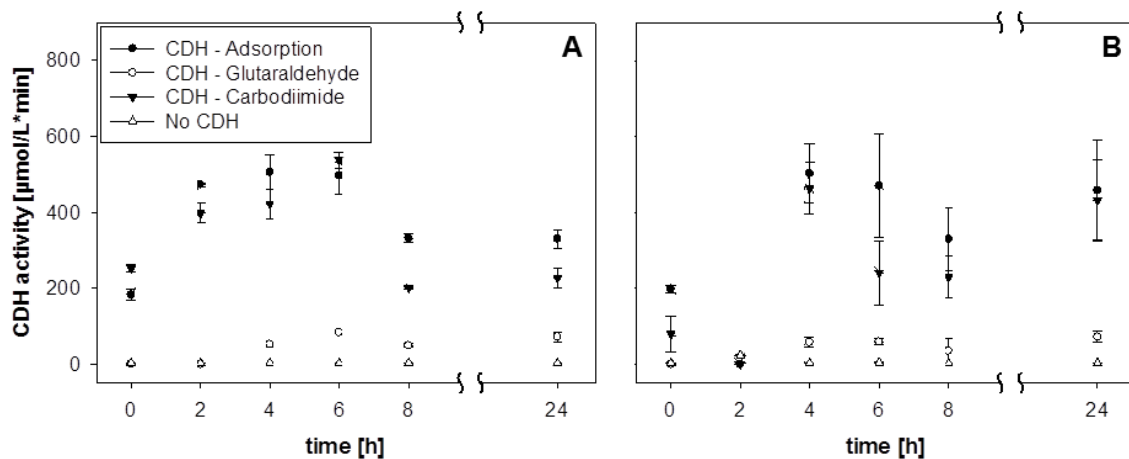


Fig 5: Leaching of CDH from CDH-CTS particles in the presence of **(A)** *E. coli* or **(B)** *S. aureus* over a time course of 24 h measured in terms of CDH activity in solution. Control reaction was performed with CTS particles lacking CDH

The amount of leaching observed followed the same pattern drawn by the swelling properties and the measured enzyme activity of the different particles. The glutaraldehyde particle with a high degree of intramolecular cross-linking showed the lowest amount of leaching due to the high capture ability. The carbodiimide and adsorption particles on the other hand showed strong leaching from the beginning on, peaking after 6 h followed by a drastic decrease probably due to the fact that equilibrium was reached and chitosan started to resorb the enzyme from solution. It was expected that the particles prepared based on adsorption would leach the highest amount of CDH into solution as the enzyme is non-covalently attached to chitosan. A possible explanation for the high enzyme activity detected in the supernatant in the case of the carbodiimide particle is that chitosan-CDH fragments were solubilized and could therefore be detected.

As the amount of CDH-chitosan particle used should be kept at a minimum, the next experiment aimed at elucidating the minimal inhibitory concentration of the particle prepared using the EDC/NHS method needed to inhibit the growth of *E. coli* and *S. aureus* by 50 and 100% (Figure 6).

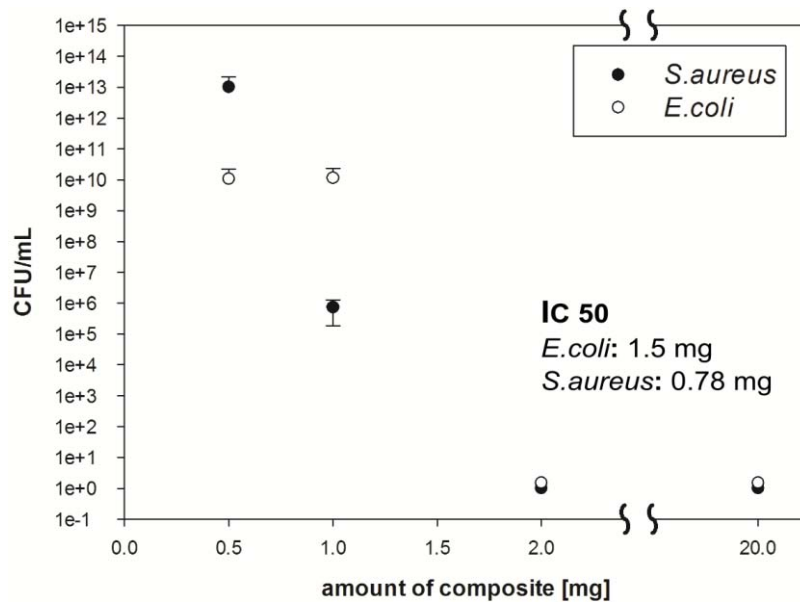


Fig 6: Determination of minimal inhibitory concentration and inhibiting concentration 50 of EDC/NHS cross linked CDH-chitosan particles against *E. coli* and *S. aureus* grown in liquid cultures in the presence of 50 mM cellobiose

S. aureus was found to be more susceptible to the antimicrobial system, because already 0.78 mg of the CDH-chitosan particles (loaded with 97 μ g CDH) were sufficient to reduce the growth by 50% (IC50). In order to achieve the same degree of inhibition with *E. coli*, 1.5 mg of the particles were necessary. The growth of both organisms was completely inhibited (MIC) when 2 mg of particles were added to the culture medium. These results are in agreement with previous results obtained by our group that showed the inhibition of this *S. aureus* strain at lower H_2O_2 concentrations than *E. coli* and further revealed antimicrobial effects against various pathogenic bacteria [14]. For a possible application of this system these results mean that only small amounts of the particle have to be incorporated into the treatment system.

The current system uses cellobiose as a co-substrate for CDH to produce hydrogen peroxide. Consequently, in a next step cellobiose chitosan particles were produced and tested in a formulation with carbodiimide CDH-chitosan particles regarding bacterial growth inhibition (Figure 7)

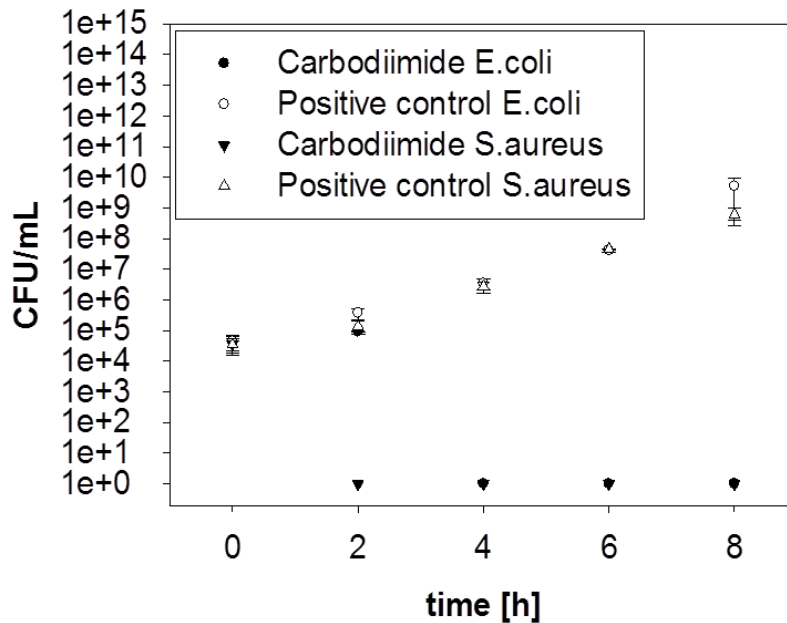


Fig 7: Incubation of 10 mg EDC/NHS cross linked CDH-chitosan-cellobiose particles with *E. coli* and *S. aureus* assessing the count of viable cells over time. Complete inhibition was obtained already after 2 h incubation for all particles systems.

The results clearly show that incorporated cellobiose maintains the effect of the CDH-chitosan system as the particles were still able to completely inhibit the growth of both *E. coli* and *S. aureus*. The only difference that can be noted is that in the case of *E. coli* the system needs a little bit more time to establish its full antimicrobial potential as it took 4 h to kill all the viable cells present in solution. Obviously, there is some transport limitation for “immobilized” cellobiose within the particle to reach CDH when compared to cellobiose added to the solution. Nevertheless, the application of the CDH-chitosan-cellobiose particles is quite simple. Once the particles get into contact with moisture, i.e. when being applied on infected wounds, cellobiose starts to leach in regions of CDH functionalized CTS leading to the production of antimicrobial hydrogen peroxide.

5.4. Conclusion

In this study, the antimicrobial enzyme CDH was successfully immobilized on chitosan and the resulting particles *in-situ* generated of H_2O_2 thereby inhibiting bacterial growth of both, gram-negative and gram-positive bacteria. The different immobilization strategies used resulted in particles with varying properties regarding enzyme activity and leaching rendering this antimicrobial system flexible for multiple medicinal applications. Promising values for the MIC and IC_{50} were obtained. Future experiments should focus on the integration of these antimicrobial particles into products like wound bandages.

Acknowledgements

The research leading to these results has received funding from the European Union Seventh Framework Programme (FP7/2007-2013) under grant agreement no. 604278 and the Austrian Centre of Industrial Biotechnology (ACIB). All authors declare no potential conflicts of interest.

5.5. References

- [1] Sen, C. K.; Gordillo, G. M.; Roy, S.; Kirsner, R.; Lambert, L.; Hunt, T. K.; Gottrup, F.; Gurtner, G. C.; Longaker, M. T. Human Skin Wounds: A Major and Snowballing Threat to Public Health and the Economy. *Wound Rep Reg.* 2009, 17 (6), 763–771.
- [2] Gardner, S. E.; Frantz, R. a; Doebbeling, B. N. The Validity of the Clinical Signs and Symptoms Used to Identify Localized Chronic Wound Infection. *Wound Rep Reg.* 2001, 9 (3), 178–186.
- [3] Dreifke, M. B.; Jayasuriya, A. a.; Jayasuriya, A. C. Current Wound Healing Procedures and Potential Care. *Mater. Sci. Eng., C* 2015, 48, 651–662.
- [4] Murphy, P. S.; Evans, G. R. D. Advances in Wound Healing: A Review of Current Wound Healing Products. *Plast. Surg. Int.* 2012, 2012, 1–8.
- [5] Schultz, G. S.; Sibbald, R. G.; Falanga, V.; Ayello, E. a.; Dowsett, C.; Harding, K.; Romanelli, M.; Stacey, M. C.; Teot, L.; Vanscheidt, W. Wound Bed Preparation: A Systematic Approach to Wound Management. *Wound Rep Reg.* 2003, 11, 1-28.
- [6] Poon, V. K. M.; Burd, A. In Vitro Cytotoxicity of Silver: Implication for Clinical Wound Care. *Burns* 2004, 30 (2), 140–147.
- [7] Lipsky, B. a; Hoey, C. Topical Antimicrobial Therapy for Treating Chronic Wounds. *Clin. Infect. Dis.* 2009, 49 (10), 1541–1549.
- [8] Cooper, R. A review of the evidence for the use of topical antimicrobial agents in wound care <http://www.worldwidewounds.com/2004/february/Cooper/Topical-Antimicrobial-Agents.html> (accessed Jan 16, 2015).

- [9] Benhabiles, M. S.; Salah, R.; Lounici, H.; Drouiche, N.; Goosen, M. F. a.; Mameri, N. Antibacterial Activity of Chitin, Chitosan and Its Oligomers Prepared from Shrimp Shell Waste. *Food Hydrocolloids*. 2012, 29 (1), 48–56.
- [10] Krajewska, B. Application of Chitin- and Chitosan-Based Materials for Enzyme Immobilizations: A Review. *Enzyme Microb. Technol.* 2004, 35, 126–139.
- [11] Pricelius, S.; Ludwig, R.; Lant, N.; Haltrich, D.; Guebitz, G. M. Substrate Specificity of *Myriococcum Thermophilum* Cellobiose Dehydrogenase on Mono-, Oligo-, and Polysaccharides Related to in Situ Production of H₂O₂. *Appl. Microbiol. Biotechnol.* 2009, 85, 75–83.
- [12] Flitsch, A.; Prasetyo, E. N.; Sygmund, C.; Ludwig, R.; Nyanhongo, G. S.; Guebitz, G. M. Cellulose Oxidation and Bleaching Processes Based on Recombinant *Myriococcum Thermophilum* Cellobiose Dehydrogenase. *Enzyme Microb. Technol.* 2013, 52 (1), 60–67.
- [13] Thallinger, B, Brandauer, M, Burger, P, Sygmund, C, Ludwig, R, Ivanova, K, Kun, J, Scaini, D, B.; M, Tzanov, T, Nyanhongo, GS, G. Cellobiose Dehydrogenase Functionalized Urinary Catheter as Novel Antibiofilm System. *J Biomed Mater Res B* 2015:00B:000-000.
- [14] Thallinger, B.; Argirova, M.; Lesseva, M.; Ludwig, R.; Sygmund, C.; Schlick, A.; Nyanhongo, G. S.; Guebitz, G. M. Preventing Microbial Colonisation of Catheters: Antimicrobial and Antibiofilm Activities of Cellobiose Dehydrogenase. *Int. J. Antimicrob. Agents* 2014, 44 (5), 402–408.
- [15] Lipovsky, A.; Thallinger, B.; Perelshtein, I.; Ludwig, R.; Sygmund, C.; Nyanhongo, G. S.; Guebitz, G. M.; Gedanken, A. Ultrasound Coating of Polydimethylsiloxanes with Antimicrobial Enzymes. *J. Mater. Chem. B* 2015, 3, 7014-7019.
- [16] Thallinger, B.; Prasetyo, E. N.; Nyanhongo, G. S.; Guebitz, G. M. Antimicrobial Enzymes: An Emerging Strategy to Fight Microbes and Microbial Biofilms. *Biotechnol. J.* 2013, 8 (1), 97–109.
- [17] Herigstad, B.; Hamilton, M.; Heersink, J. How to Optimize the Drop Plate Method for Enumerating Bacteria. *J. Microbiol. Methods* 2001, 44, 121–129.

- [18] Hanefeld, U.; Gardossi, L.; Magner, E. Understanding Enzyme Immobilisation. *Chem. Soc. Rev.* 2009, 38 (2), 453–468.
- [19] Goycoolea, F. M.; Heras, A.; Aranaz, I.; Galed, G.; Fernández-Valle, M. E.; Argüelles-Monal, W. Effect of Chemical Crosslinking on the Swelling and Shrinking Properties of Thermal and pH-Responsive Chitosan Hydrogels. *Macromol. Biosci.* 2003, 3 (10), 612–619.
- [20] Hoven, V.; Tangpasuthadol, V.; Angkitpaiboon, Y.; Vallapa, N.; Kiatkamjornwong, S. Surface-Charged Chitosan: Preparation and Protein Adsorption. *Carbohydr. Polym.* 2007, 68 (1), 44–53.
- [21] Alloue, W. A. M.; Destain, J.; El Medjoub, T.; Ghalfi, H.; Kabran, P.; Thonart, P. Comparison of *Yarrowia Lipolytica* Lipase Immobilization Yield of Entrapment, Adsorption, and Covalent Bond Techniques. *Appl. Biochem. Biotechnol.* 2008, 150 (1), 51–63.
- [22] Alt, E.; Leipold, F.; Milatovic, D.; Lehmann, G.; Heinz, S.; Schömig, A. Hydrogen Peroxide for Prevention of Bacterial Growth on Polymer Biomaterials. *Ann. Thorac. Surg.* 1999, 68 (6), 2123–2128.
- [23] Datta, S.; Christena, L. R.; Rajaram, Y. R. S. Enzyme Immobilization: An Overview on Techniques and Support Materials. *3 Biotech* 2013, 3 (1), 1–9.
- [24] Zamocky, M.; Ludwig, R.; Peterbauer, C.; Hallberg, B.; Divne, C.; Nicholls, P.; Haltrich, D. Cellobiose Dehydrogenase – A Flavocytochrome from Wood-Degrading, Phytopathogenic and Saprotrophic Fungi. *Curr. Protein Pept. Sci.* 2006, 7 (3), 255–280.
- [25] Imlay, J. A. Pathways of Oxidative Damage. *Annu. Rev. Microbiol.* 2003, 57, 395–418

6 Cellobiohydrolases Produce Different Oligosaccharides from Chitosan

Published in: *Biomacromolecules* 2016, 17, 2284–2292

Gregor Tegl, Christoph Öhlknecht, Robert Vielnascher, Alexandra Rollett, Andreas Hofinger-Horvath, Paul Kosma, Georg M. Guebitz

Abstract

Chito-oligosaccharides (COS) are bioactive molecules with interesting characteristics. However, their exploitation is still restricted due to limited amounts accessible with current production strategies. Here, we present a strategy for the production of COS based on hydrolysis of chitosan by using readily available glycosidases. Cellobiohydrolases (EC 3.2.1.91) were compared to chitosanases (EC 3.2.1.132) regarding their ability for COS production and the resulting fractions were analyzed by MS and NMR. The oligosaccharides had a degree of polymerization between 3 and 6 units and the degree of acetylation (DA) varied depending on the applied enzyme. Different cellobiohydrolases produced COS with varying DA and based on comprehensive NMR analysis the preferred cleavage sites of the respective enzymes that show chitosanase and chitinase activity was elucidated. The study reveals the high potential of readily available cellulolytic enzymes besides chitosanases for the production of COS with distinct structure facilitating access to this bioactive compound class.

6.1. Introduction

Consisting of glucosamine and N-acetyl glucosamine units of varying ratios, unique functionalities and bioactive properties were observed already at the early stage research on chitosan. The polymer is to date used for multiple applications. However, further investigations and especially applications of chitosan in various areas like medicine and food science are limited due to poor solubility under physiological conditions[1–4]. A simple solution improving solubility is found in the decrease of the degree of polymerization (DP) by the aid of chemicals or enzymes resulting in lower molecular weight chitosan (LMWC) and chito-oligosaccharides (COS)[5]. The properties of these hydrolysis products were characterized in detail indicating their potential for applications in various research areas like food, nutrition and medicine. To date a variety of functionalities of COS are described, like improving food quality as well as several health benefits including antimicrobial activity and

even antitumor properties [6]. However, in many studies on bioactivities, heterogeneous mixtures of COS were used with incomplete analysis of chemical properties and composition. Yet, mixtures of LMWC and COS, obtained after hydrolysis of chitosan, differ in their DP and degree of N-acetylation (DA), which strongly affect their biological activity. Consequently, the impact of these parameters on various COS properties often remained unclear. In the past decade, COS were primarily produced by using enzymes rather than chemical hydrolysis to avoid traces of chemicals in products limiting application in medicine [7]. To date, a variety of enzymes is described possessing chitosan cleaving activity including a number of glycoside hydrolases and even monooxygenases [7,8]. Several chitosanases are listed in the CAZY database and differ in their site of cleavage that is influenced by the pattern of acetylation (P_A). On the other hand, for larger scale production of COS more readily available cellulases could have potential. However, their chitosan hydrolysis products were often poorly analyzed.

Cellobiohydrolases (CBHs) are important components of cellulose degrading enzyme systems especially secreted by fungi [9]. Classified as exo-glucanases, CBHs liberate cellobiose units from reducing and non-reducing ends of cellulose [10]. In contrast, for the hydrolysis of chitosan by a CBH from *Trichoderma reesei* an endo-type hydrolysis was reported [11]. Despite the importance of the impact of the chitosan DA and P_A on hydrolysis [12] and distinct activities of different resulting COS, the hydrolysis mechanism of chitosan by CBHs compared to chitosanases or lysozyme has not yet been systematically studied.

Consequently, in this study oligomeric reaction products resulting from chitosan hydrolysis by cellobiohydrolases and chitosanases were analysed in detail to elucidate the mode of action of these distinct enzymes. This will make enzyme based tools available for the production of well-defined chito-oligosaccharides for various applications.

6.2. Materials and Methods

6.2.1. Materials

Two different chitosanases from *Streptomyces sp.* termed StrCSN1 (Sigma-Aldrich C9830) and StrCSN2 (Sigma-Aldrich C0794), the cellobiohydrolase I from *Hypocrea jecorina* termed HJCBH (Sigma-Aldrich E6412) and lysozyme from chicken egg white and chitosan were purchased from Sigma-Aldrich.

Cellobiohydrolase I from *Trichoderma longibrachiatum* (TrCBH) was purchased from Megazyme (Bray, Co. Wicklow, Ireland). The StrCSN1 was dissolved in 50% glycerol and stored at -20°C. Chitosan from shrimp shells (number average molecular weight of 200 kDa, degree of acetylation (DA) of 13%) was used for all experiments. For lysozyme, the same

chitosan was used as substrate, but with a DA of 48%. The chito-oligosaccharide standards (chitobiose and chitopentaose) were purchased from Carbosynth Ltd. (West Berkshire, UK) and D-glucosamine-HCl was purchased from Sigma-Aldrich. Pullulan reference standards for size exclusion chromatography (SEC) were purchased from Sigma-Aldrich. All chemicals were purchased from Sigma-Aldrich and used without further purification.

6.2.2. Purifications of Chitosan

Residual impurities (glucans and proteins) were removed dissolving the chitosan in 1% acetic acid to a final chitosan concentration of 1% and subsequently removing remaining solids by centrifugation. Thereafter, chitosan was precipitated adjusting the pH to 8.0, the precipitate was washed with 90% EtOH, 70% EtOH and 50% EtOH in consecutive washing steps and freeze-dried.

6.2.3. Characterization of enzyme activities on chitosan

Elaboration of hydrolysis conditions

In hydrolysis experiments the different enzymes were dosed in a concentration leading to complete conversion of 0.5% (w/v) chitosan solution into COS. To determine this concentration, chitosan was dissolved in sodium acetate buffer (pH 5, 0.1 M) resulting in a 0.5% solution that was subsequently incubated for 96 h at 37°C with the respective enzymes of varying molarity. The optimum enzyme concentration was defined as the minimum enzyme concentration necessary to quantitatively convert the chitosan into water soluble COS. The reaction progress was monitored by thin layer chromatography (TLC). All experiments were performed in triplicates.

The following molarities (MW given in brackets) were obtained for the respective enzymes:

- Chitosanase *StrCSN1*: 14.5 nM (34 000 Da*)
- Chitosanase *StrCSN2*.: 55 nM (30 000 Da)
- Cellobiohydrolase I from *Hypocrea Jecorina*: 0.5 mM (53 000 Da)
- Cellobiohydrolase I from *Trichoderma longibrachiatum*: 0.55 µM (65 000 Da)
- Lysozyme from chicken egg white: 2.75 µM (14 600 Da)

*[13]

The temperature and pH optima of the enzymes for hydrolysis of chitosan were determined using the enzyme concentrations mentioned above while the decrease in molecular weight was analyzed by size exclusion chromatography. Temperature profiles were obtained from 20°C to 80°C using a 0.5% chitosan solution in sodium acetate buffer (pH 5, 0.1 M) as substrate stock. The reaction tubes were incubated at 100 rpm for 24 h. Similarly the pH

optimum was determined incubating the enzymes at the determined optimal temperature of each of the respective enzymes. Due to the known narrow pH stability of the used enzymes, pH optima were obtained in a range of pH 4 to 6.

6.2.4. Characterization of oligomeric hydrolysis products

Determination of the reducing sugar content

The reducing sugar content was determined using the 3,5-dinitrosalicylic acid (DNS) assay of Miller ¹⁴. Briefly, the sample solution was mixed 1:1 (v/v) with the DNS solution and the mixture was incubated in a water bath at 100°C for 5 min. The reaction was stopped directly by pouring the samples in an ice bath. Precipitating polysaccharides were removed by centrifugation and thereafter the absorbance at 540 nm was determined. As calibration standard, D-glucosamine was used.

Thin layer chromatography (TLC)

After the enzymatic hydrolysis of chitosan, an aliquot of the reaction supernatant was deposited on a TLC plate (silica gel FC 60, Merck) and separated using a mixture of 2-propanol, pyridine, acetic acid and water (7:6:6:9 v/v/v/v) as mobile phase. Spots were visualized by coating the plate after migration with a 0.2% ninhydrin solution in ethanol and subsequent heating at 100°C.

Size exclusion chromatography (SEC)

The molecular mass of the chitosan hydrolysis products was analyzed by analytical size exclusion chromatography using an Agilent 1100 Series Chromatography system and an Agilent 1200 G1362 refractive index detector. A TSKgel G5000PW_{XL} column was used for analysis (Tosoh Bioscience, Montgomeryville, PA, USA) and pullulan standards (Fluka, Buchs, Switzerland) were used as reference material. An acetic acetate buffer consisting of 0.15 M acetic acid, 0.1 M sodium acetate and 0.4 mM sodium azide was used as mobile phase. Prior to injection, the samples were filtered through an Express™Plus filter with 0.22 µm pore size (47 mm diameter, Millipore).

MALDI-TOF Mass Spectrometry

Once the optimal conditions for chitosan hydrolysis were found, chitosan was incubated with enzyme up to 96 h and resulting oligomeric products were analyzed by MALDI-TOF MS and LC ESI-TOF MS. All samples were desalted prior to the measurements increasing the signal-to-noise ratio. MALDI-TOF MS was performed using a Bruker Autoflex Speed instrument, equipped with a 1000 Hz Smartbeam™-II laser. The samples were applied with 2,5,-

dihydroxybenzoic acid as matrix and spectra were acquired in positive reflection mode. Glycan spectra were processed using Bruker Flex Analysis 3.3 and the SNAP algorithm. Glycans were annotated according to component monosaccharide masses and mass increments between peaks by the help of Glycoworkbench 2.0. All samples were desalted using PD-10 desalting columns (GE Healthcare, USA) prior to measurements.

LC – ESI TOF measurements

HPLC was performed using a LC coupled with DAD monitoring at 254 nm (Agilent G4212B, Palo Alto, CA, USA) on a Hypercarb column with a particle size of 5 μ M (thermo scientific, USA). For LC ESI-TOF experiments, the LC system was coupled to a Dual ESI G6230B TOF (Agilent, Palo Alto, CA, USA). Electrospray ionization (operating in positive ion mode) was performed using a nebulizer with a set dry gas flow to 8 L/min and a pressure of 40 psi at 300°C. The fragmenter voltage was set to 200 V, the skimmer at 100 V, the octopole to a voltage of 750 V and the reference masses were 121.0509 m/z and 922.0098 m/z. Ions from 50 m/z to 3000 m/z were acquired with the Agilent MassHunter Workstation (Version B06.01, Palo Alto, CA, USA). A statistical calculation in accordance to German industrial standard 32645 for the detection limit, detectability limit, and limit of determination was performed. Significance was tested with p-values less than 0.05.

NMR Spectroscopy

Produced chito oligosaccharides COS were desalted using a series of PD10 column (GE Healthcare) with water as mobile phase. The collected fractions were analyzed by TLC and respective fractions were lyophilized prior to NMR analysis. NMR spectra of the oligosaccharide samples were acquired for D₂O solutions at 300 K on a Bruker Avance III 600 instrument (600.2 MHz for ¹H, 150.9 MHz for ¹³C). ¹H spectra were measured with suppression of the HOD signal and referenced using DSS as standard ($\delta = 0$); ¹³C spectra were referenced using 1,4-dioxane as external standard ($\delta = 67.40$). Data were acquired and processed using standard Bruker software TopSpin 3.0. The TOCSY experiments were performed acquiring 2k x 256 data points and using 80, 100 or 120 ms mixing time. For ROESY spectra, the roesy-spinlock pulse was set at 30 msec. Multiplicity edited HSQC spectra were recorded with 1k x 128 data points. Double-quantum filtered HMBC experiments were recorded with long-range *J*(C,H) values of 8 Hz, respectively, and 4k x 128 data points.

6.3. Results and Discussion

Knowledge about the relation of chitosan oligomer (COS) characteristics like DP, DA and PA and various bioactivities of COS is highly important for various applications [7]. However, such information is only available for COS obtained via hydrolysis by chitosanases and lysozyme while considerably less is known about substrate specificities of cellobiohydrolases (CBH) on chitosan. Yet, especially the latter enzymes are readily available and might lead to COS with novel properties. Hence, enzymatic production of COS by CBH was compared mechanistically to lysozyme and chitosanase.

6.3.1. Temperature and pH Optima of the Enzymes with Chitosan as Substrate

The temperature optimum for chitosan degradation was determined for all enzymes (figure 1) up to a temperature of 60°C in order to avoid auto hydrolysis of chitosan at elevated temperatures. The chitosanases from *Streptomyces* sp. had their temperature optima at 37°C (*StrCSN1*) and 50°C (*StrCSN2*), respectively. In contrast, both CBHs and lysozyme had their temperature optima at 60°C, which was in accordance with literature on enzymatic cellulose degradation[15]. No significant differences in temperature optima of the CBHs were observed for chitosan hydrolysis when compared to cellulose degradation. A temperature optimum of 60°C was previously reported for half N-acetylated chitosan by lysozyme by Zhang et al[16] and was in agreement with results in this study.

The pH optima of the chitosanases were in accordance to literature of related chitosanases showing pH optima in a range of 5.5 – 6.0 [17,18]. Both CBHs exhibited highest chitosanase activity at pH 5.5, which slightly differs from the optima published on cellulose hydrolysis of pH 5.0 and below. Chitosan hydrolysis was performed in a homogeneous aqueous system whereas enzymatic hydrolysis of water insoluble cellulose (containing crystalline regions) is a heterogeneous reaction which may explain differences in pH optima [19]. It is also supposed that the cationic charge of the primary amine alters the binding modalities of the enzymes and thus favors enzyme binding at higher pH. Lysozyme showed highest activity at pH 6. However only slightly lower degradation rates were observed between pH 4-5, which was in accordance to literature [16,20] (table 1).

Table 1: Temperature and pH optima for hydrolysis of chitosan by chitosanases, lysozyme and CBHs after 24 h incubation based on analysis of reaction products by SEC.

Enzyme	pH optimum	Temperature Optimum [°C]
Chitosanase <i>StrCSN1</i>	5.5	37
Chitosanase <i>StrCSN2</i>	6	50
CBH <i>H. jecorina</i>	5.5	60
CBH <i>T.longibrachiatum</i>	5.5	60
Lysozyme from hen egg white	6	60

6.3.2. Analysis of Produced Chito-oligosaccharides

Figure 1 further reveals the decrease of molecular weight illustrated as the inverse of the number average molecular weight (Mn) after 24 h (figure 1A). After 48 h of incubation equal degradation rates were obtained for all enzymes (data not shown). However, results after short incubation times indicate different hydrolysis rates of the respective enzymes towards the substrate. The chitosanases applied in this experiment showed expectably higher hydrolysis rates towards chitosan than the CBHs and lysozyme. SEC analysis of chitosan hydrolysis shows an endo-type of hydrolysis for all enzymes tested (figure 1B) indicated by the fast decrease of molecular weight. While this was expected and is documented for lysozyme and chitosanases, CBHs typically show progressive exo-activity on (water insoluble) cellulose [21]. However, the mode of action may change depending on substrate solubility which was already observed by Ike et al that found chitosanase activity of a CBH from *Trichoderma reesei* [11].

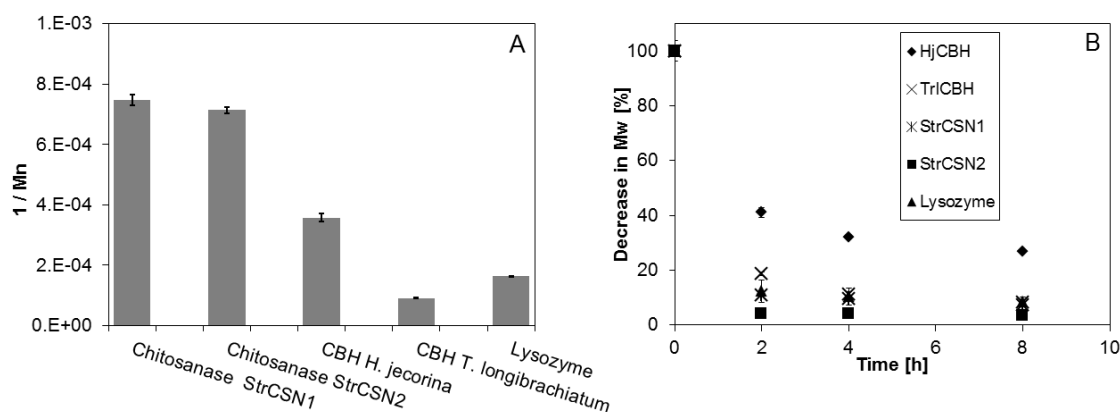


Figure 1: Hydrolysis rate of the different enzymes illustrated as the inverse of the number average molecular weight (Mn) determined by SEC after 24 h incubation (A) and SEC analysis of the enzyme hydrolysis rates within 8 h incubation (B) indicating endo-activity of all enzymes. All enzymes were applied in the amounts stated in the methods section.

The obtained chito oligosaccharides were analyzed by MALDI-TOF MS and LC ESI-TOF MS. Lysozyme liberated partially acetylated COS ranging from DP 3 to DP 6 from chitosan according to MALDI-TOF analysis (fig.2) which was in accordance to literature [22]. The high DA of the COS released is most likely due to the binding specificity of lysozyme to hexameric regions bearing four N-acetyl glucosamines (GlcNAc) in the applied chitosan with DA 48% [23]. In contrast, chitosanases mainly liberated oligomers with lower DA consisting of one GlcNAc. Comparing the spectra of the COS released by the investigated chitosanases, similar COS were obtained ranging from DP 3 to DP 6, a pattern that was also observed for other chitosanases [24]. LC ESI-TOF analysis was used to record time profiles of COS released (figure 3). Lysozyme was not considered for further analysis because of the comprehensive information about lysozyme interaction with N-acetyl chitosan that is available in literature [25–27]. Chitosan hydrolysis with *StrCSN1* led to a constant accumulation of the oligomers identified via MALDI-TOF whereas no significant further degradation was observed. The reaction pattern indicated endo-type hydrolysis, which was further confirmed by SEC measurements detecting a fast decrease of molecular weight of 94% within 8 h incubation.

Applying *StrCSN2* a similar oligomer pattern was found with LC ESI-TOF compared to MALDI-TOF measurements. However, a substantial accumulation mainly of low DP oligomers was observed via LC ESI-TOF including chitobiose (figure 3D). The substantial decrease of $(\text{GlcN})_3(\text{GlcNAc})_1$ after 24 h incubation in combination with the accumulation of non-acetylated and acetylated chitobiose reveals the potential of this chitosanase to also cleave short-chain COS.

Interestingly, *HjCBH* mediated hydrolysis yielded COS in the range of DP 3 to DP 6 of varying DA whereas *TrCBH* exclusively produced non-acetylated and mono-acetylated COS. The accumulation of COS with different DA indicated different cleavage specificities of the two CBHs on chitosan. Time profiles of *HjCBH* mediated hydrolysis taken by using LC ESI-TOF measurements showed both, the accumulation of oligomers lacking acetyl groups as well as the occurrence of highly acetylated oligomers. These results suggest that the binding and cleavage sites of *HjCBH* prefer a medium DA of chitosan and COS.

Interestingly, for this CBH degradation of fully acetylated COS from DP 2 to DP 4 was observed demonstrating some chitinase activity on short chain oligomers (figure 3B). The hydrolysis of the acetylated COS with DP 3 and DP 4 explained the intensity increase of $(\text{GlcNAc})_2$ and GlcNAc over time. After complete hydrolysis of $(\text{GlcNAc})_4$ to $(\text{GlcNAc})_2$ further cleavage of the GlcNAc dimer into its monomers was observed. Possible conversion and disappearance of the fully acetylated COS via transglycosylation (TG) from the product mixture was investigated by incubating a $(\text{GlcNAc})_2$ standard with *HjCBH*. The formation of the respective TG-product $(\text{GlcNAc})_4$ and higher COS was not observed but slight degradation of the $(\text{GlcNAc})_2$ to GlcNAc was observed, suggesting the ability of *HjCBH* to degrade acetylated COS like $(\text{GlcNAc})_2$. While further degradation of cellobiose to glucose was not reported so far for this enzyme, it reveals weak chitinase activity for the acetylated chitobiose.

Time course measurements of *TrCBH* mediated COS production confirmed the MALDI-TOF results. Mainly non-acetylated oligomers ranging from DP 2 to DP 7 were accumulated with minor fractions of mono acetylated oligomers found. The results reveal that *TrCBH* is an endo acting enzyme on chitosan, which was furthermore confirmed by SEC showing a substantial decrease of the molecular weight in short time.

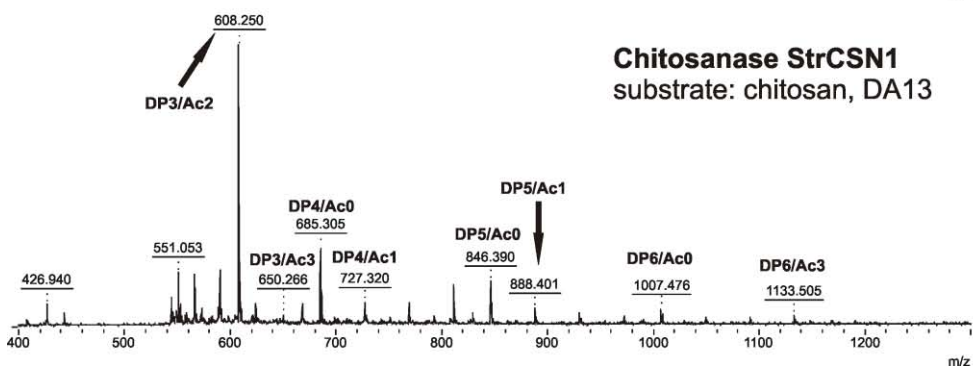
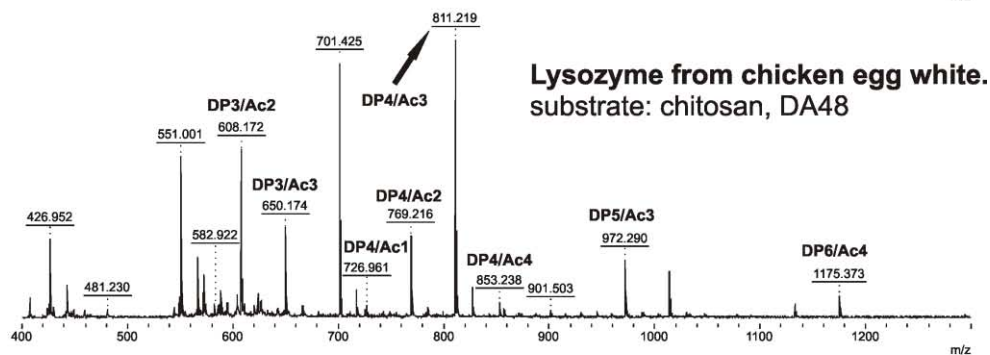
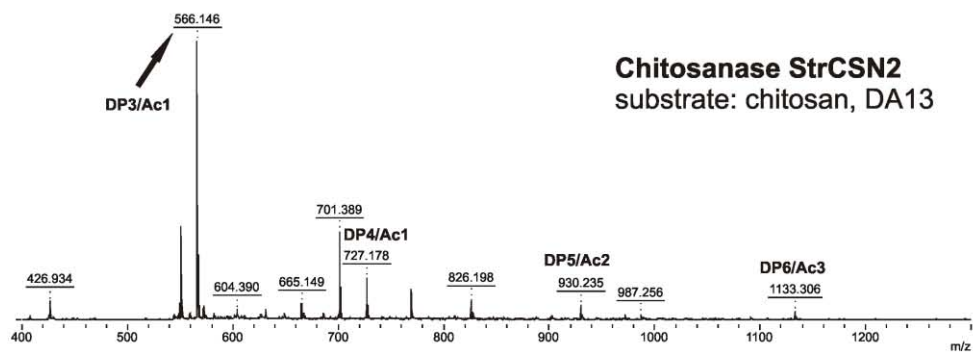
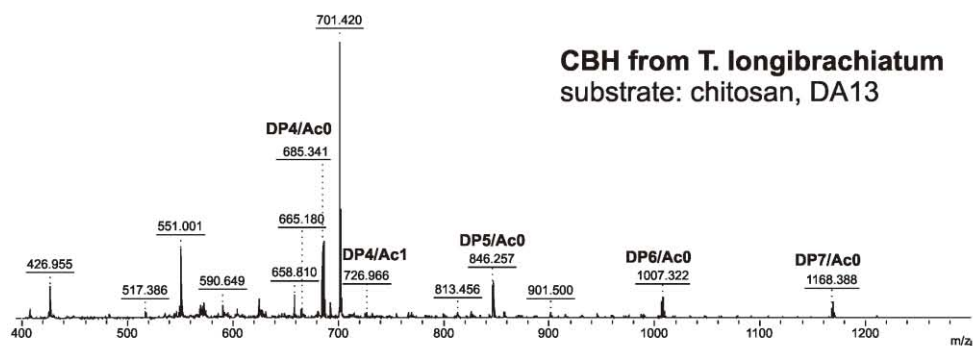
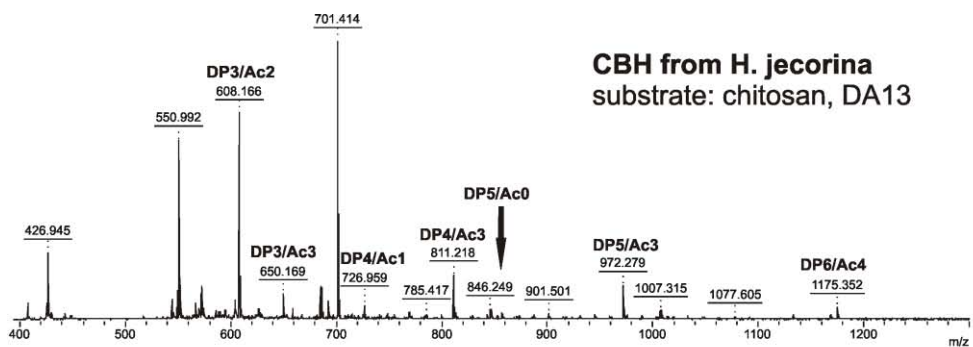


Figure 2: MALDI-TOF analysis of oligomeric hydrolysis products from chitosan after 96 h incubation with lysozyme, different chitosanases and CBHs. Chitosan with a DA of 13% was used for all enzymes except lysozyme, whose preferred chitosan substrate was determined to have a DA of 48%.

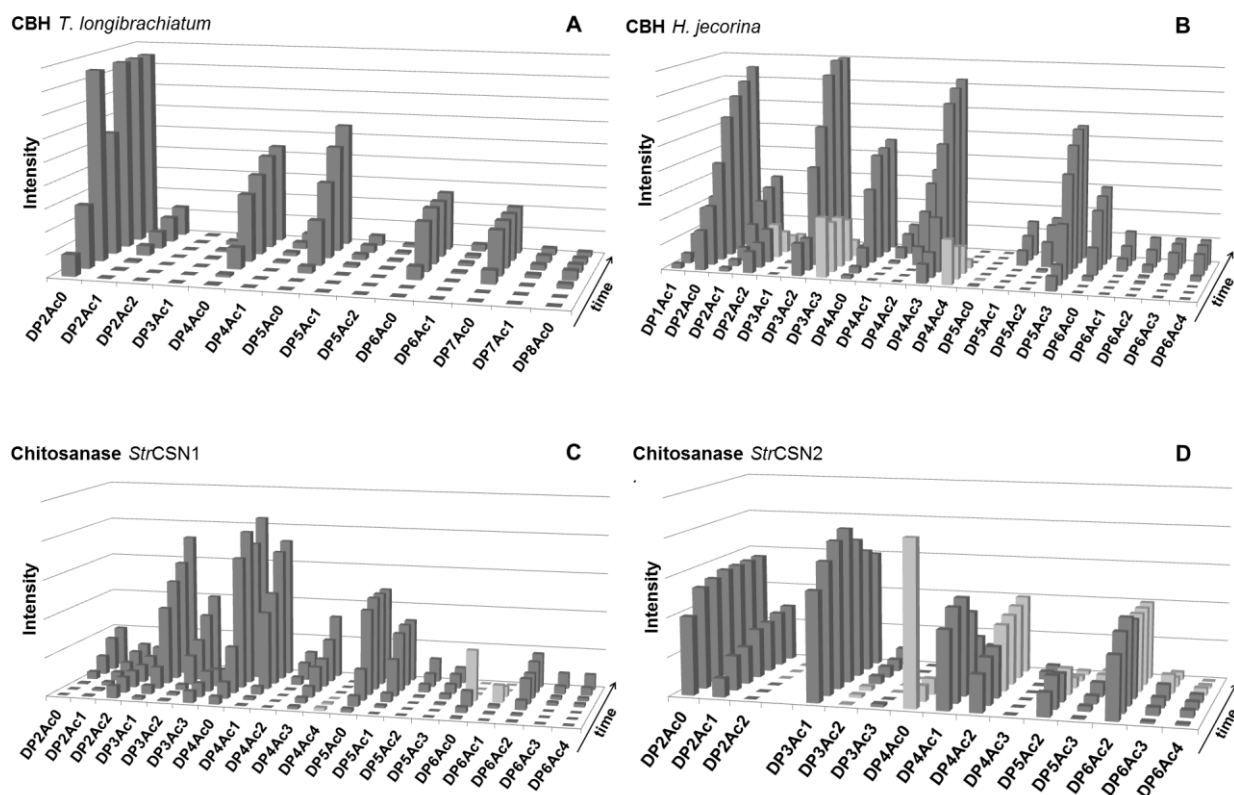


Figure 3: LC ESI TOF MS analysis of oligomers liberated during chitosan hydrolysis of 96 h of incubation with. Time points were taken at 2 h, 4 h, 8 h, 24 h, 48 h, 72 h and 96 h. Accumulating oligomers are depicted in dark grey, oligomers degraded during enzyme incubation are depicted in light grey. COS not listed in the graph were not produced by the respective enzymes.

6.3.3. Characterization of the Preferred Enzyme Cleavage Sites

The COS mixtures were further analyzed by NMR to characterize the cleavage sites of the respective enzymes. Although the samples were heterogeneous, relevant NMR data could be obtained leading to the assignment of end groups, which were further supported by comparison to published data [28–30]. Literature on structural studies of chitooligosaccharides by NMR was available and consulted for spectra analysis.

The overall degree of N-acetylation was calculated based on the respective signal intensities of H-2 protons of the GlcN residues, which were shifted to higher field, relative to the N-

acetyl CH₃-groups. Thus GlcN: GlcNAc ratios of 2.7:1, 4.7:1, 1.8:1 and 3.3:1 were calculated for the product mixtures from *TrlCBH*, *StrCSN1*, *StrCSN2* and *HjCBH*, respectively. As representative example the spectra of the hydrolysate obtained from chitosan hydrolysis with *TrlCBH* are shown. The 600 MHz ¹H NMR spectrum (figure 4) contained *inter alia* signals in the anomeric region corresponding to protons of the reducing GlcN end (H-1 α at 5.40, H-1 β at 4.90 ppm), of internal GlcN residues between 4.78 - 4.70 ppm as well as anomeric protons from GlcNAc units at 4.58-4.50 ppm. In addition to the anomeric signals of reducing GlcN units, very minor anomeric ¹H/¹³C signals of reducing GlcNAc moieties were also seen at 5.15/91.1 ppm (α -GlcNAc) and 4.74/96.8 ppm (β -GlcNAc), respectively. The main portion of the pyranosyl ring protons was observed in the range of 4.02-3.48 ppm, followed by a triplet signal at 3.44 ppm and signals of H-2 protons of GlcN units between 3.30 and 2.95 ppm. Acetyl signals were seen at 2.02-1.99 ppm and an acetate signal at 1.87 ppm. HSQC, HMBC and HSQC-TOCSY experiments allowed establishing the assignments of the reducing end units and of the distal terminus (figure 5). Notably, the triplet signal at 3.44 ppm showed correlations to a ¹³C NMR signal at 70.42 ppm and to H-5 proton / C-5 carbon signals at 3.50/77.15 ppm, which is indicative of an unsubstituted C-4 position. Eventually TOCSY correlations of the triplet to the high-field shifted region of the GlcN H-2 signals (3.10-2.95 ppm) identified this unit as a terminal GlcN moiety. GlcNAc residues were identified through an HMBC-correlation of a low-field shifted H-2 signal (3.72-3.74 ppm) to the amide carbonyl signal at 175.64 ppm and to the anomeric carbon at 102.11 ppm. In addition, an HMBC correlation was found from the carbon signal at 79.4 ppm to the GlcNAc anomeric proton, in agreement with an internal GlcNAc-GlcN linkage. Hence, this data would be compatible with the presence of tetrasaccharides GlcN-GlcNAc-GlcN-GlcN and/or GlcN-GlcN-GlcNAc-GlcN as major component(s) among other oligomers ²⁴[31–34].

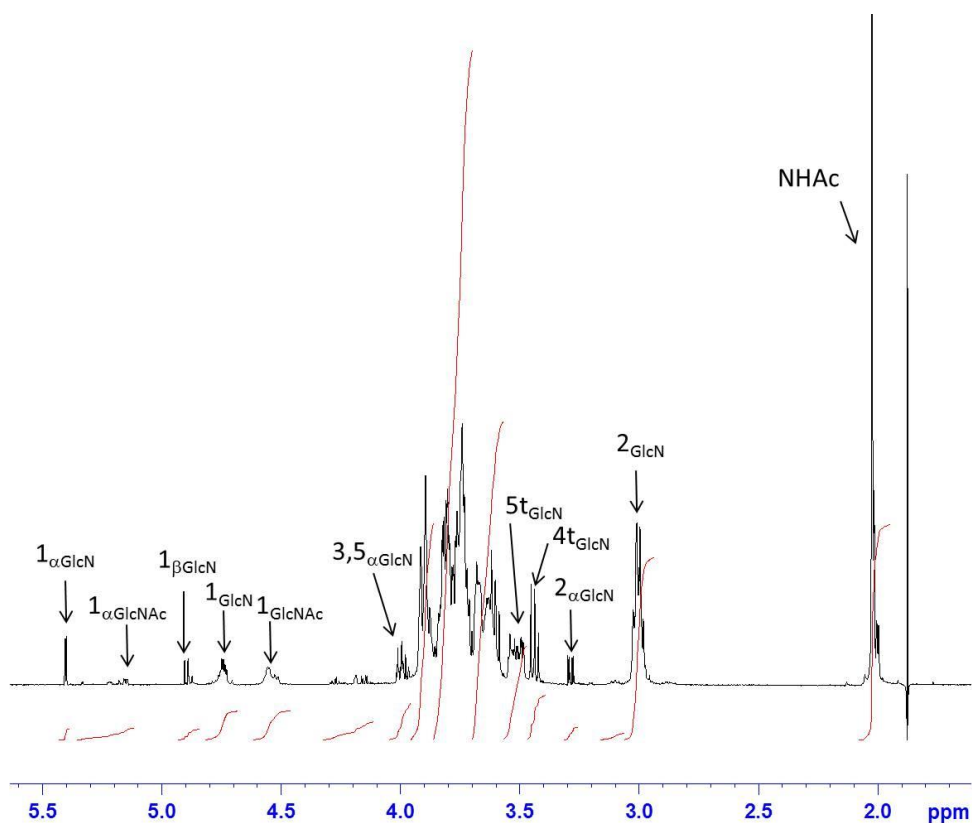


Figure 4: 600 MHz ^1H NMR spectrum and main assignments of COS obtained after chitosan hydrolysis by *TrICBH* (*t denotes the non-reducing terminus)

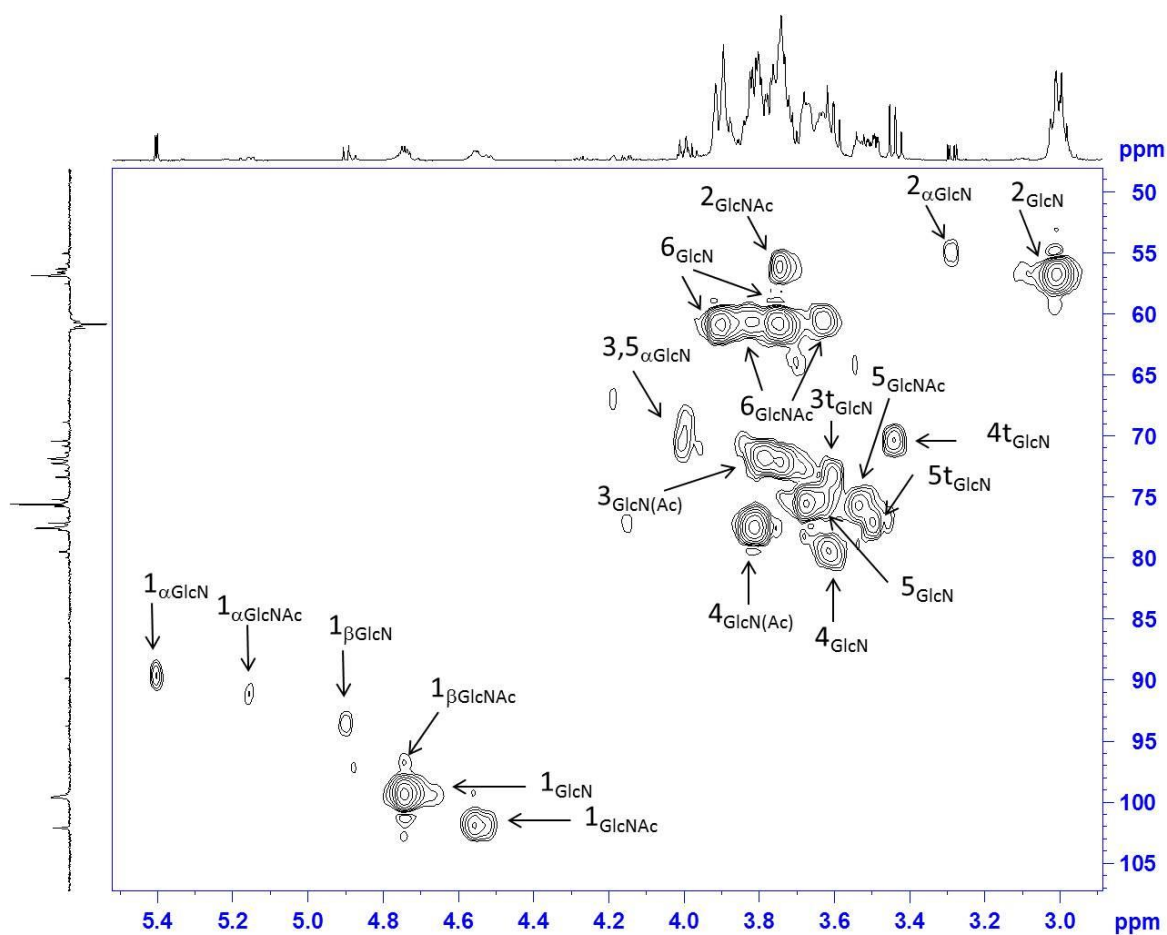


Figure 5: Expansion plot of the HSQC-spectrum of COS obtained after chitosan hydrolysis by *Tr*/CBH

COS generated by *Str*CSN1 had similar spectral features as the *Tr*/CBH sample with respect to the identification of the reducing end mainly as a non-acetylated GlcN residue, which again was based on the COSY-correlation of both anomeric protons at the reducing end to the high-field shifted H-2 protons. In addition, anomeric $^1\text{H}/^{13}\text{C}$ signals of reducing GlcNAc residues were also seen, but in lower intensity at 5.15/91.0 ppm for (α -GlcNAc) and 4.66/95.7 ppm (β -GlcNAc), respectively. Again, a separated triplet signal was observed at 3.43/70.4 ppm for H-4/C-4 located at the non-reducing end. In contrast to the previous sample, however, TOCSY correlations of this signal could be tracked back to the anomeric $^1\text{H}/^{13}\text{C}$ signals of β -GlcNAc units at 4.56-4.51/102.1 and 102.3 ppm which indicates that the oligomers are terminated by a GlcNAc residue. The assignment of a terminating GlcNAc residue was also in good agreement with comparable NMR data from the literature [35–38]. NMR data of the sample obtained from treatment with *Str*CSN2 were comparable to those of the *Str*CSN1 hydrolysate with a reducing GlcN unit and a higher proportion of reducing GlcNAc units (figure 6). The latter signals were observed at 5.16/91.4 ppm for α -GlcNAc and 4.69/95.6 ppm for β -GlcNAc, respectively. This assignment was confirmed by a connectivity of H-1 α to H/C-2 of the reducing GlcNAc at 3.88/55.0 ppm. Terminal GlcNAc residues were again being assigned on the basis of TOCSY correlations of the high-field shifted H-4 signal to the GlcNAc anomeric protons. Additional correlations of H-4 – albeit with lower intensity – were also seen to the anomeric GlcN protons. Integral values of the anomeric protons were of increased intensity relative to the H-2 GlcN proton signals indicating the presence of smaller oligomers. In conjunction with an average ~2:1 ratio of GlcN to GlcNAc, the trisaccharides GlcNAc-GlcN-GlcN, GlcN-GlcNAc-GlcN or GlcN-GlcN-GlcNAc might constitute some of the components of the mixture.

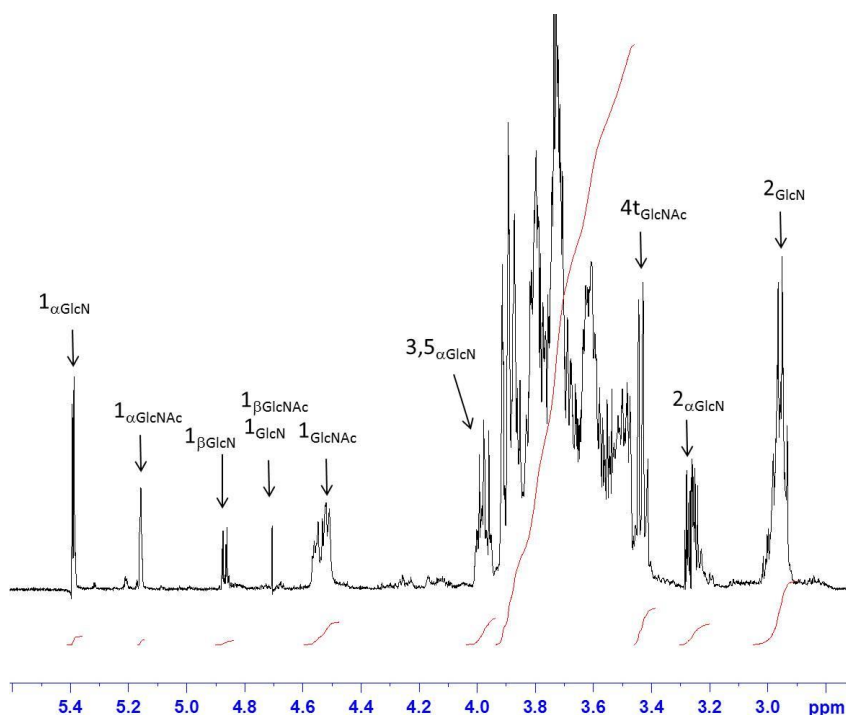


Figure: 6: Section of the 600 MHz ^1H NMR spectrum and main assignments of COS obtained after chitosan hydrolysis by *StrCSN2* (*t denotes the non-reducing terminus).

The spectrum of the product mixture obtained by treatment with *HjCBH* suffered from severe line broadening but indicated the presence of higher chitosan oligomers with GlcN/GlcNAc substitution

Figure 7 illustrates a comparison of ^1H NMR spectra of the hydrolyzed chitosan samples of the investigated chitosanases and cellobiohydrolases. Differences in signals intensities and shifts between the samples can mainly be detected between 4.4-5.5 ppm and underline the varying ratios of reducing and non-reducing GlcN/GlcNAc.

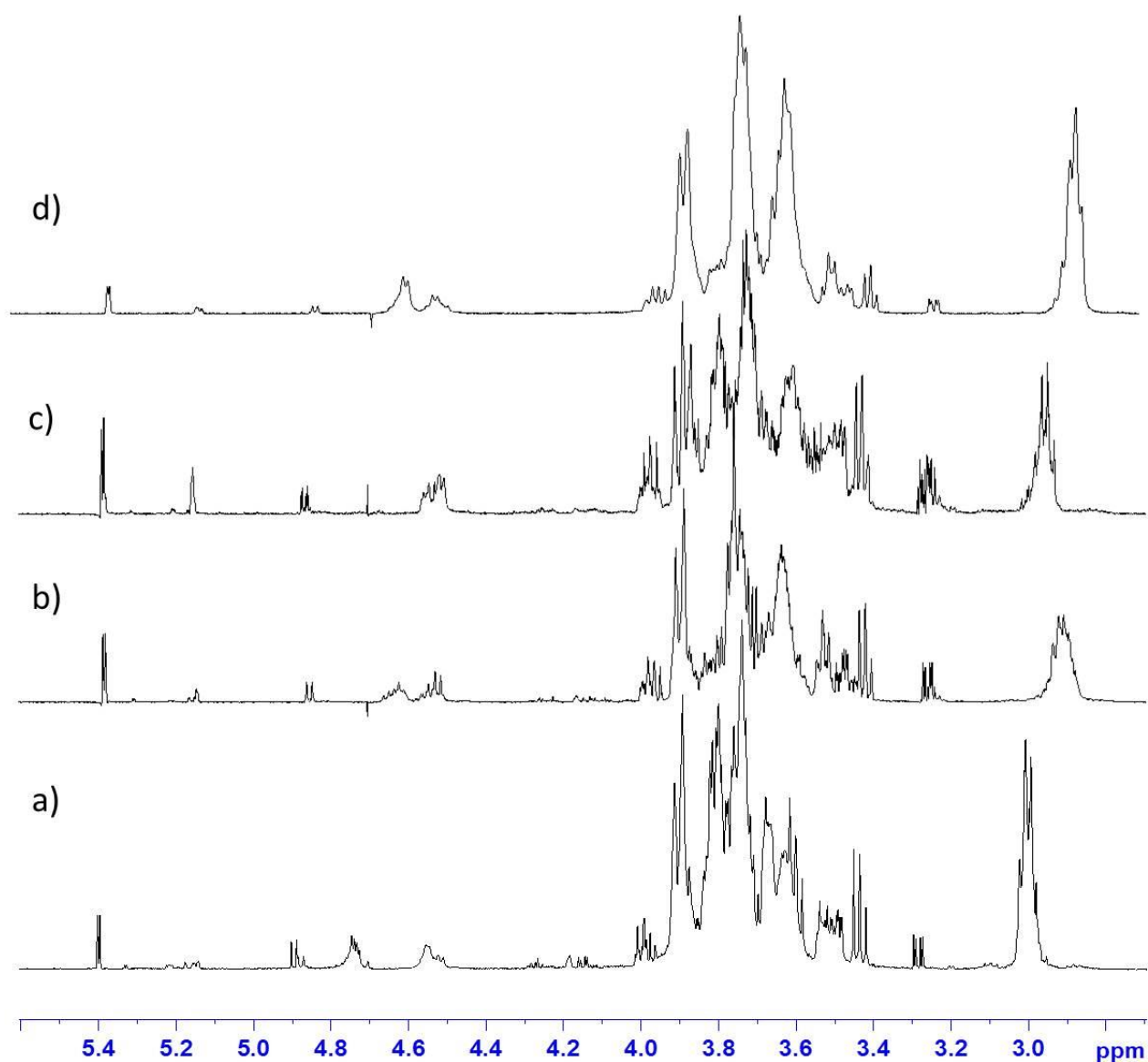


Figure: 7: Comparison of the 600 MHz ^1H NMR spectra of the hydrolyzed chitosan samples from all enzymes. a) *HjCBH* b) *StrCSN2* c) *StrCSN1* d) *TrlCBH*.

A comparison of the used chitosanases and CBHs illustrates the differences in the mode of action of these enzymes. The chitosanases do not exclusively show chitosanase activity but also chitinase activity due to non-selective cleavage sites that also include GlcNAc residues, on the reducing and non-reducing end, respectively. The ratios determined by NMR were confirmed by MS analyses that show an accumulation of COS with a high DA (figure 3 C+D). SDS-PAGE proved the purity of the used enzymes, thus the occurrence of additional enzymes in the purchased enzyme solution is unlikely. Whether these chitosanases require GlcNAc residues for substrate binding or not remains unclear. However both, NMR and MS

analysis, suggest GlcNAc residues to be involved in enzyme binding during chitosan hydrolysis.

The used CBHs were to the best of our knowledge the first time applied for the production of COS and show significant differences regarding their mode of action on chitosan. *HjCBH* mediated hydrolysis resulted in an oligosaccharide pool mainly consisting of highly N-acetylated COS according to both NMR and MS analysis. Although NMR analysis could not definitely determine the cleavage site of *HjCBH*, MS data suggests GlcNAc residues present on the reducing and/or non-reducing end due to the high DA of the detected COS. Compared to *HjCBH*, *TrlCBH* produced COS without acetyl groups and one acetyl group, respectively. NMR results confirmed that non-reducing and reducing ends are solely consisting of GlcN residues (cleavage site). Minor amounts of GlcNAc residues were detected that could be assigned to the internal fraction in the found COS. Although a similar mode of action of the two CBHs is described for exo-type cellulose degradation, significant differences in substrate specificities were observed for endo-type chitosan hydrolysis. This enables a flexible production of the desired COS by the choice of the respective enzyme.

On the basis of the NMR-analysis of the reaction mixtures the following preferred cleavage sites can be proposed:

- *TrlCBH*: $\text{GlcN} \perp \text{GlcN}$
- *StrCSN1*: $\text{GlcN} \perp \text{GlcNAc}$
- *StrCSN2*: $\text{GlcN}(\text{Ac}) \perp \text{GlcN}(\text{Ac})$

Due to the reduced quality of the NMR spectra of COS obtained by *HjCBH*, a distinct cleavage site cannot be proposed. However the high DA observed by MS and NMR supposes occurring GlcNAc residues in the cleavage site. The conclusions about the cleavage sites based on the terminal sugars give valuable information about the subsite preferences of the respective enzymes. However additional cleavage sites cannot be excluded from the derived data and deserve further investigations [39].

6.4. Conclusion

This study demonstrated the potential of cellobiohydrolases (CBH) for the production of chito-oligosaccharides (COS). The investigated CBHs hydrolyzed chitosan to COS of similar DP compared to chitosanases but significant differences were observed in the DA. While *HjCBH* mediated chitosan hydrolysis yielded COS with high DA, *TrlCBH* mainly produced COS without acetyl groups, which reveals the great potential of this enzyme class producing COS of varying physicochemical properties. Detailed knowledge about the difference in

catalytic action of the enzymes could elucidate further enzymes suitable for the production of COS with distinct properties.

The used chitosanases, CBHs and lysozyme were characterized and compared towards their temperature and pH optima, and their oligomeric products were comprehensively analyzed using different MS techniques and NMR. The different enzymes produced varying pools of COS differing in the DP and DA, which underlines the suitability of these commercial enzymes to produce bioactive COS with different properties. Detailed NMR analysis revealed the cleavage site of the investigated enzymes and supposes diverging enzyme binding sites among the chosen candidates. Further work is necessary to unveil the underlying catalytic mechanisms of the described CBHs that are responsible for their different modes of action. The enhanced knowledge facilitates the use of cheap and commercial enzymes for the production of bioactive COS, which are a substance class of high interest that can so far not be produced in desired amounts.

Funding Sources

The authors appreciate funding from the European FP7-programme under grant agreement no. 604278 and the Austrian Centre of Industrial Biotechnology (ACIB).

Conflict of Interest Disclosure

The authors declare no competing financial interest.

6.5. References

- [1] Chou T-C, Fu E, Wu C-J, Yeh J-H. Chitosan enhances platelet adhesion and aggregation. *Biochem Biophys Res Commun* 2003;302:480–3.
- [2] Domard A. A perspective on 30 years research on chitin and chitosan. *Carbohydr Polym* 2011;84:696–703.
- [3] Rhoades J, Gibson G, Formentin K, Beer M, Rastall R. Inhibition of the adhesion of enteropathogenic *Escherichia coli* strains to HT-29 cells in culture by chito-oligosaccharides. *Carbohydr Polym* 2006;64:57–9.
- [4] Usami Y, Okamoto Y, Takayama T, Shigemasa Y, Minami S. Effect of N-acetyl-D-glucosamine and D-glucosamine oligomers on canine polymorphonuclear cells in vitro. *Carbohydr Polym* 1998;36:137–41.
- [5] Fernandes JC, Tavaría FK, Soares JC, Ramos ÓS, João Monteiro M, Pintado ME, et al. Antimicrobial effects of chitosans and chito-oligosaccharides, upon *Staphylococcus*

- aureus and *Escherichia coli*, in food model systems. *Food Microbiol* 2008;25:922–8.
- [6] Jeon Y-J, Shahidi F, Kim S-K. Preparation of Chitin and Chitosan oligomers and their applications in physiological functional foods. *Food Rev Int* 2000;16:159–76.
- [7] Aam BB, Heggset EB, Norberg AL, Sørli M, Vårum KM, Eijsink VGH. Production of chitooligosaccharides and their potential applications in medicine. *Mar Drugs* 2010;8:1482–517.
- [8] Vaaje-Kolstad G, Horn SJ, Sørli M, Eijsink VGH. The chitinolytic machinery of *Serratia marcescens* - A model system for enzymatic degradation of recalcitrant polysaccharides. *FEBS J* 2013;280:3028–49.
- [9] Sandgren M, Wu M, Karkehabadi S, Mitchinson C, Kelemen BR, Larenas E a., et al. The structure of a bacterial cellobiohydrolase: The catalytic core of the thermobifida fusca family GH6 cellobiohydrolase Cel6B. *J Mol Biol* 2013;425:622–35.
- [10] Liu YS, Baker JO, Zeng Y, Himmel ME, Haas T, Ding SY. Cellobiohydrolase hydrolyzes crystalline cellulose on hydrophobic faces. *J Biol Chem* 2011;286:11195–201.
- [11] Ike M, Ko Y, Yokoyama K, Sumitani JI, Kawaguchi T, Ogasawara W, et al. Cellobiohydrolase I (Cel7A) from *Trichoderma reesei* has chitosanase activity. *J Mol Catal B Enzym* 2007;47:159–63.
- [12] Han T, Nwe N, Furuike T, Tokura S, Tamura H. Methods of N -acetylated chitosan scaffolds and its in vitro biodegradation by lysozyme. *J Biomed Sci Eng* 2012;5:15–23.
- [13] Tanabe T, Morinaga K, Fukamizo T, Mitsutomi M. Novel chitosanase from *Streptomyces griseus* HUT 6037 with transglycosylation activity. *Biosci Biotechnol Biochem* 2003;67:354–64. doi:10.1271/bbb.67.354.
- [14] Miller GL. Use of Dinitrosalicylic Acid Reagent for Determination of Reducing Sugar. *Anal Biochem* 1959;31:426–8.
- [15] Andreus J, Azevedo H, Cavaco-Paulo a. Effects of temperature on the cellulose binding ability of cellulase enzymes. *J Mol Catal - B Enzym* 1999;7:233–9.
- [16] Zhang Y, Wang Z, Zhang J, Chen C, Wu Q, Zhang L, et al. Quantitative determination of chitinolytic activity of lysozyme using half-deacetylated chitosan as a substrate. *Carbohydr Polym* 2011;85:554–9.

- [17] Tanabe T, Morinaga K, Fukamizo T, Mitsutomi M. Novel Chitosanase from *Streptomyces griseus* HUT 6037 with Transglycosylation Activity. *Biosci Biotechnol Biochem* 2014;67:354–64.
- [18] Jiang X, Chen D, Chen L, Yang G, Zou S. Purification, characterization, and action mode of a chitosanase from *Streptomyces roseolus* induced by chitin. *Carbohydr Res* 2012;355:40–4.
- [19] Volkov P V, Rozhkova AM, Gusakov A V, Sinitsyn AP. Homologous cloning, purification and characterization of highly active cellobiohydrolase I (Cel7A) from *Penicillium canescens*. *Protein Expr Purif* 2014;103:1–7.
- [20] Nordtveit RJ, Varum KM, Smidsrod O. Degradation of partially N-acetylated chitosans with hen egg white and human lysozyme. *Carbohydr Polym* 1996;29:163–7.
- [21] Kurasin M, Väljamäe P. Processivity of cellobiohydrolases is limited by the substrate. *J Biol Chem* 2011;286:169–77.
- [22] Mengíbar M, Ganan M, Miralles B, Carrascosa a. V., Martínez-Rodríguez a. J, Peter MG, et al. Antibacterial activity of products of depolymerization of chitosans with lysozyme and chitosanase against *Campylobacter jejuni*. *Carbohydr Polym* 2011;84:844–8.
- [23] Stokke BT, Varum KM, Holme HK, Hjerde RJN, Smidsrsd O. Sequence specificities for lysozyme depolymerization of partially N-acetylated chitosans. *Can J Chem* 1995;1981:1972–81.
- [24] Cheng CY, Li Y. An *Aspergillus* chitosanase with potential for large-scale preparation of chitosan oligosaccharides. *Biotechnol Appl Biochem* 2000;203:197–203.
- [25] Kristiansen a, Vårum KM, Grasdalen H. The interactions between highly de-N-acetylated chitosans and lysozyme from chicken egg white studied by 1H-NMR spectroscopy. *Eur J Biochem* 1998;251:335–42.
- [26] Stan Tsai C. Molecular modelling studies of lysozyme catalysed hydrolysis of synthetic substrates. *Int J Biochem Cell Biol* 1997;29:325–34.
- [27] Stokke BT, Varum KM, Holme HK, Hjerde RJN, Smidsrod O. Sequence specificities for lysozyme depolymerization of partially N-acetylated chitosans. *Can J Chem Can Chim* 1995;73:1972–81.
- [28] Sugiyama H, Hisamichi K, Sakai K, Usui T, Ishiyama JI, Kudo H, et al. The

- conformational study of chitin and chitosan oligomers in solution. *Bioorganic Med Chem* 2001;9:211–6.
- [29] Fukamizo T, Honda Y, Goto S, Boucher I, Brzezinski R. Reaction mechanism of chitosanase from *Streptomyces* sp. N174. *Biochem J* 1995;311:377–83.
- [30] Makino A, Kurosaki K, Ohmae M, Kobayashi S. Chitinase-catalyzed synthesis of alternately N-deacetylated chitin: A chitin-chitosan hybrid polysaccharide. *Biomacromolecules* 2006;7:950–7.
- [31] Lavertu M, Xia Z, Serreqi a. N, Berrada M, Rodrigues a., Wang D, et al. A validated ¹H NMR method for the determination of the degree of deacetylation of chitosan. *J Pharm Biomed Anal* 2003;32:1149–58.
- [32] Kasaai MR. Determination of the degree of N-acetylation for chitin and chitosan by various NMR spectroscopy techniques: A review. *Carbohydr Polym* 2010;79:801–10.
- [33] Vårum KM, Anthonsen MW, Grasdalen H, Smidsrød O. Determination of the degree of N-acetylation and the distribution of N-acetyl groups in partially N-deacetylated chitins (chitosans) by high-field n.m.r. spectroscopy. *Carbohydr Res* 1991;211:17–23.
- [34] Weinhold MX, Sauvageau JCM, Kumirska J, Thöming J. Studies on acetylation patterns of different chitosan preparations. *Carbohydr Polym* 2009;78:678–84.
- [35] Germer A, Mügge C, Peter MG, Rottmann A, Kleinpeter E. Solution- and bound-state conformational study of N,N',N"-triacetyl chitotriose and other analogous potential inhibitors of hevamine: application of trNOESY and STD NMR spectroscopy. *Chemistry* 2003;9:1964–73.
- [36] Aboitiz N, Cañada FJ, Husakova L, Kuzma M, Kren V, Jiménez-Barbero J. Enzymatic synthesis of complex glycosaminotrioses and study of their molecular recognition by hevein domains. *Org Biomol Chem* 2004;2:1987–94.
- [37] Kawada T, Yoneda Y. Selection of protecting groups and synthesis of a β -1,4-GlcNAc- β -1,4-GlcN unit. *Monatshefte Für Chemie - Chem Mon* 2009;140:1245–50.
- [38] Vårum KM, Anthonsen MW, Grasdalen H, Smidsrød O. ¹³C-n.m.r. studies of the acetylation sequences in partially N-deacetylated chitins (chitosans). *Carbohydr Res* 1991;217:19–27.
- [39] Viens P, Lacombe-Harvey M-È, Brzezinski R. Chitosanases from Family 46 of Glycoside Hydrolases: From Proteins to Phenotypes. *Mar Drugs* 2015;13:6566–87.

7 General Conclusion

This work of this thesis was conducted within the INFACCT project of the seventh framework program of the European Union, which aimed at the development of functional materials for fast diagnosis of wound infection. Early detection of an emerging infection enables the timely initiation of treatment and consequently lowers the severity of the disease. The target of the project was the production of diagnostic materials for the three immune system-derived infection biomarkers lysozyme (LYS), myeloperoxidase (MPO) and elastase (ELA), which show highly elevated activities in infected wounds. As the development stage is progressed, these materials should be incorporated in diagnostic wound dressings, which inform the therapist and the patient about the wound status.

Within the scope of the thesis, infection responsive materials were designed and investigated, based on LYS and MPO as diagnosing enzymes. The most suitable and distinct option for the assessment of elevated enzymes activities, also easily interpretable by the untrained patients, is the visualization via a clear color change. Thus, the concept was to synthesize an infection responsive material, insoluble under physiological conditions that releases a dye or dyed fragments in response to the mentioned enzymes.

Only few LYS responsive materials are known, to date just peptidoglycan and chitosan, where LYS catalyzes the hydrolysis of the β -1,4-glycosidic linkages. The utilization of peptidoglycan in products for medical applications is critical because of its bacterial origin. Chitosan is commonly extracted from crustaceans but can also be acquired from non-animal sources like fungi without containing critical proteinogenic impurities and was thus chosen as LYS responsive material. The susceptibility of native chitosan towards LYS mediated hydrolysis is low and required selective N-acetylation of chitosan to a degree of N-acetylation of around 50% for optimal LYS responsivity. Choosing a chitosan with high molecular weight, N-acetyl chitosan with poor solubility under physiological conditions was produced. Starting from the synthesized N-acetyl chitosan, two strategies were followed to obtain a color release, the covalent attachment of Reactive Black 5 as well as the non-covalent incorporation of Toluidine O Blue in N-acetyl chitosan-starch co-precipitate. Both strategies resulted in LYS responsive materials showing a color response after 2 h of incubation with LYS in buffer. The suitability of these substrates was further proven by applying human wound fluids from infected wounds and resulted in clear indication of infection after 2.5 h incubation. The two concepts could be successfully converted to functional materials for LYS mediated infection detection and constitute promising substrates for the possible incorporation in point-of-care diagnostics.

The detection of wound infection using just one biomarker is valid but the response of the immune system to bacterial contamination naturally depends on the type of wound and moreover differs from patient to patient. A strategy ensuring a reliable detection system is the simultaneous assessment of several biomarkers, which provides a definite prediction of the wound status. The need for the assessment of more than one enzyme gave rise to the development of a diagnostic material for myeloperoxidase. Like many peroxidases, myeloperoxidase shows a high promiscuity regarding possible electron acceptors and also includes various phenolic compounds. Most phenols undergo oligomerization upon treatment with oxidases via a radical reaction which often results in colored quinones. Within this thesis aminomethoxyphenol was utilized for MPO mediated infection detection via immobilization on silica carrier materials. The phenol was chosen for this study because of its functional groups, which facilitate chemical immobilization. Frequently used MPO substrates like guaiacol are volatile and do not bear functional groups, which makes further functionalization impracticable. The phenol was functionalized with an alkoxysiloxane spacer, which enabled covalent immobilization and resulted in modified silica plates suitable for infection detection. The detection system was again successfully proven using human wound fluid from infected wounds and MPO oxidation of the substrate led to the appearance of red spot on the plates within 5 min incubation time. Due to other wound fluids components showing peroxidase activity like haeme, selectivity tests were performed, which proved the diagnostic substrate insensitive towards competing haeme and horseradish peroxidase. The work also covered a look behind the MPO mediated oxidation of aminomethoxyphenol, which could determine the main reaction products and the underlying reaction mechanism. A dimerization of aminomethoxyphenol could be identified via radical polymerization, which resulted in the respective quinone that was responsible for the red color. Detailed investigations of the exact mode-of-action of such systems are crucial to gain knowledge about the underlying processes. If the reaction chain is known, eventual side reactions, which happen frequently measuring in complex media like wound fluids, can be predicted and avoided or retrospectively backtracked. The combination of well working infection detection systems together with the knowledge about the underlying mode of actions constitutes a solid set up for further utilization in point-of-care devices. To date implemented MPO detection system indicating wound infection are mainly based on MPO mediated color changes but also electrochemical sensors are described in the literature. The main obstacle of the most detection systems is the required external supply of H_2O_2 , which still complicates the utilization of these detection systems and impedes a fast and easy usage.

The importance of an early detection of wound infection accompanies with the treatment strategies that can be set in a timely manner before an infection is evident. Another parameter of high importance, which is in public dialogue, is the use of antimicrobials in therapy. The emergence of bacterial resistances is a long-known problem and had always been the engine for the development of new antimicrobial agents. Despite the progress in this research area including the steady development of new antibiotics and antimicrobial peptides, bacteria seem to grow with the obstacles human put in their way. The high demand of new and effective antimicrobial treatments led to an increased interest in the native antimicrobial activity of natural products as well as to the reemergence and refinement of therapies that already have been used for a long time. A frequently antimicrobial substance that is in used over decades is hydrogen peroxide (H_2O_2). It is beside iodine still one of the most popular substances for topical wound disinfection. The high effectiveness of H_2O_2 is constrained by its moderate cytotoxicity, which impedes the continuous use as antimicrobial. The natural instability of H_2O_2 in solution is another problem, which greatly complicates the storage. Since H_2O_2 treatment is topical, high concentration are applied at once to ensure the antimicrobial effect, however this high dose is the main reason for the observed cytotoxic effect. A remedy could be the continuous production of moderate concentrations of H_2O_2 , which do not harm intact tissue but show the antimicrobial effects against bacterial contaminants. Such an *in situ* generation system of H_2O_2 could be realized in wound dressings for topical wound treatment and a general proof-of-concept was realized within this thesis. This concept comprised the antimicrobial enzyme cellobiose dehydrogenase (CDH), which is capable of reducing O_2 to H_2O_2 in the course of the oxidation of cellobiose. Within this study a recombinant CDH was used, which was optimized for the electron transfer to O_2 to produce H_2O_2 in high concentrations. CDH was immobilized in chitosan, a process that is also required for the use of enzymes in functional materials like wound dressings. Different immobilization strategies were compared and analyzed regarding their effects on CDH activity and applicability and finally resulted in CDH-chitosan particles capable to completely inhibit the growth of *E. coli* and *S. aureus*. The covalent immobilization of CDH expectably resulted in a decrease of activity compared to non-covalent adsorption, however resulted in low IC_{50} values of 1.5 mg (*E. coli*) and 0.78 mg (*S. aureus*). The H_2O_2 concentration was found to reach a steady state of around 600 μ M after short time and could be kept constant for 24 h. Compared to actually applied solutions of H_2O_2 (880 mM) in hospitals, a tremendous decrease of the required concentration was achieved, which is according to literature below the cytotoxicity level of H_2O_2 for intact tissue. Additionally, superior stability of the immobilized CDH was observed over a wide temperature range, which further proved this enzyme an alternative strategy for antimicrobial wound treatment.

Chitosan was used for the previously described work because of the various properties that favor its use in medical applications. Besides biocompatibility, the native antimicrobial function greatly contributes to the high interest on this biomaterial. The major drawback of chitosan is the restricted solubility under physiological conditions, which complicates its use for multiple applications. Solubility can be improved by the reduction of the molecular weight and results in case of chitosan hydrolysis in chito-oligosaccharides (COSs). Great potential for multiple medical applications was found in COSs and a broad spectrum of bioactivities is described for this substance class including antimicrobial and antitumor activities. Only heterogeneous mixtures of COSs are obtained with current production strategies, which complicate their analysis and so far prevented the exploitation of structure-function relationships. This led to the curiosity that a high interest in these substances emerged but the structural impact on the diverse biological activities is still unresolved.

Within the thesis two commercial cellobiohydrolases (CBHs) were found capable of producing COSs from chitosan and were unveiled as potential low cost source for large-scale production. A CBH from *Hypocrea jecorina* and one from *Trichoderma longibrachiatum* produced different sets of COSs regarding the degree of N-acetylation. Comprehensive analysis with MS and NMR was conducted and could elucidate the preferred cleavage site of the enzymes and brought light into the mode-of-action of cellulolytic enzymes for the production of COSs. Chitosan-unspecific enzymes like cellobiohydrolases could be a potential and readily available catalyst to facilitate access to an important bioactive material. The thorough structural analysis of produced COSs, no matter from which source obtained, must be the prerequisite for the research on COS production. Without proper analysis, structure-functions relationships cannot be made, but these properties are the key player bringing COS into applied research and to potential medical applications.

The thesis illustrates that engineering enzyme-substrate interactions are a powerful tool in basic and applied research and can lead to biomedical applications, ranging from diagnosis to treatment. Bioactive materials are ubiquitous, the key player in nature and most often enzyme-responsive. The steadily increasing knowledge about the mode-of-action of enzymes and their reactions with biomaterials renders them important biocatalysts, which will find broad use in many applications in future.

8 Appendix

8.1. Scientific publications

1. Schiffer D, **Tegl G**, Vielnascher R, Weber H, Schoeftner R, Wiesbauer H, et al. Fast Blue RR—Siloxane Derivatized Materials Indicate Wound Infection Due to a Deep Blue Color Development. *Materials* **2015**;8:6633–9. DOI:10.3390/ma8105329.
2. **Tegl G**, Schiffer D, Sigl E, Heinzle A, Guebitz GM. Biomarkers for infection: enzymes, microbes, and metabolites. *Appl Microbiol Biotechnol* **2015**;99:4595–614. DOI:10.1007/s00253-015-6637-7.
3. Schiffer D, **Tegl G**, Heinzle A, Sigl E, Metcalf D, Bowler P, et al. Enzyme-responsive polymers for microbial infection detection. *Expert Rev Mol Diagn* **2015**;15:1–7. DOI:10.1586/14737159.2015.1061935.
4. **Tegl G**, Thallinger B, Beer B, Sygmund C, Ludwig R, Rollett A, et al. Antimicrobial cellobiose dehydrogenase-chitosan particles. *ACS Appl Mater Interfaces* **2016**;8:967–73. DOI:10.1021/acsami.5b10801.
5. **Tegl G**, Rollett A, Dopplinger J, Gamerith C, Guebitz GM. Chitosan based substrates for wound infection detection based on increased lysozyme activity. *Carbohydr Polym* **2016**;151:260–7. DOI:10.1016/j.carbpol.2016.05.069.
6. Schiffer D, **Tegl G**, Vielnascher R, Weber H, Herrero-Rollett A, Sigl E, et al. Myeloperoxidase-responsive materials for infection detection based on immobilized aminomethoxyphenol. *Biotechnol Bioeng* **2016**;9999:1–8. DOI:10.1002/bit.26025.
7. **Tegl G**, Öhlknecht C, Vielnascher R, Rollett A, Hofinger-Horvath A, Kosma P, et al. Cellobiohydrolases Produce Different Oligosaccharides from Chitosan. *Biomacromolecules* **2016**;17:2284–92. DOI:10.1021/acs.biomac.6b00547.

8.2. Oral presentations

1. **Tegl G**, Heinzle A, Sigl E, Schneider KP, Rollett A, Guebitz GM. Enzyme-responsive polysaccharide based materials for medical applications. *Austrian Carbohydrate Seminar 2014*, Vienna, Austria, February **2014**
2. **Tegl G**, Thallinger B, Beer B, Guebitz GM. CDH/Chitosan formulations: enhanced antimicrobial properties. *Austrian Carbohydrate Seminar 2015*, Graz, Austria, February **2015**
3. **Tegl G**, Thallinger B, Beer B, Guebitz GM. Immobilization of Cellobiose Dehydrogenase on chitosan particles: an antimicrobial system for medical applications. *13th International Conference on Chitin and Chitosan 2015 (ICCC13th)*, Münster, Germany, September **2015**

4. **Tegl G**, Thallinger B, Beer B, Guebitz GM. Cellobiose Dehydrogenase immobilized on chitosan: a novel strategy for antimicrobial wound treatment. *International Polysaccharide Conference 2015 (4th EPNOE)*, Warsaw, Poland, October **2015**
5. **Tegl G**, Thallinger B, Beer B, Nyanhongo GS, Guebitz GM. Chitosan composites encapsulating Cellobiose Dehydrogenase: an antimicrobial system for wound applications, *The international chemical Congress of Pacific Basin Societies 2015 (Pacifichem 2015)*, Honolulu, Hawaii, USA, December **2015**
6. **Tegl G**, Thallinger B, Beer B, Nyanhongo GS, Guebitz GM. Recombinant *Myriococcus thermophilum* Cellobiose Dehydrogenase possessing increased oxygen reactivity: application in antimicrobial composites, *The international chemical Congress of Pacific Basin Societies 2015 (Pacifichem 2015)*, Honolulu, Hawaii, USA, December **2015**
7. **Tegl G**, Thallinger B, Beer B, Nyanhongo GS, Guebitz GM. Strategies for the incorporation of Cellobiose Dehydrogenase into chitosan formulations: antimicrobial systems for medical applications, *The international chemical Congress of Pacific Basin Societies 2015 (Pacifichem 2015)*, Honolulu, Hawaii, USA, December **2015**
8. **Tegl G**, Thallinger B, Rollett A, Sygmund C, Ludwig R, Guebitz GM. Infection prevention and infection detection by the aid of chitosan. *Austrian Carbohydrate Seminar 2016*, Vienna, Austria, February **2016**

8.3. Acknowledgements

I was not writing acknowledgements in my bachelor and master thesis and always told the people that I will just write them in my PhD thesis, my last study stage in biotechnology. You can guess that there is a bunch of people now that I want to thank, because they have been playing important parts along my studies. Without their support over the years, I would not just write the last part of my PhD thesis. So thanks to:

My supervisor Prof. Georg Guebitz, who gave me the opportunity to work on an exciting topic. Thanks for all the support along the years, for the freedom you gave me to realize my ideas and for the many opportunities to attend conferences all around the world. All the mentioned things and many more were the trigger that I learned many things about science and life in the past three years

Prof. Paul Kosma for his great support along my studies. I learned so much about carbohydrates and accompanying topics from you in the past years and I still do in every further discussion. I acknowledge the steady support from the bachelor thesis until now, that's not self-evident and highly appreciated.

Bernhard Müller, Christian Stanetty and Hannes Mikula, who supported me throughout the bachelor and master thesis and thereby made major contributions for my later carrier.

Alex Herrero-Rollet, for the great support, especially during the first months of my PhD thesis, which paved the way to successfully perform my experiments and realize my ideas.

Ale Pellis, my friend and crazy scientist. We had much fun along the years, traveled around the world and pushed each other with great scientific and other discussions. I am looking forward to our future trips and more.

Dani, Barbara Th., Orti, Caro, Robert, Quique and all the other members of the BET group for the great time we had and will have and their support throughout the years.

Elke and Petra, thanks for your patience all the years, you directed me the way through all the bureaucratic issues.

My last big thanks you go to my family. My parents and grandparents provided me the support and enabling me a life where I could explore the secrets of life and study in an unburdened way. This is a luxury situation not everybody has, I am very thankful for that.

Thank you Katrin for sharing your life with me and thank you for your support through the years that brings my sometimes overmotivated enthusiasm in line. Without you, life would be much less exciting.

8.4. Statutory declaration

I declare that I have authored this thesis independently, that I have not used other than the declared sources/resources, and that I have explicitly marked all material which has been quoted either literally or by content from the used source.

date

signature